Physics Letters B 786 (2018) 59–86

Contents lists available at ScienceDirect

Physics Letters B

www.elsevier.com/locate/physletb

Observation of $H \to b\bar{b}$ decays and VH production with the ATLAS detector

The ATLAS Collaboration *

ARTICLE INFO

Article history:
Received 25 August 2018
Accepted 6 September 2018
Available online 14 September 2018
Editor: M. Doser

ABSTRACT

A search for the decay of the Standard Model Higgs boson into a $b\bar{b}$ pair when produced in association with a W or Z boson is performed with the ATLAS detector. The data, corresponding to an integrated luminosity of 79.8 fb^{-1} were collected in proton–proton collisions during Run 2 of the Large Hadron Collider at a centre-of-mass energy of 13 TeV. For a Higgs boson mass of 125 GeV, an excess of events over the expected background from other Standard Model processes is found with an observed (expected) significance of 4.9 (4.3) standard deviations. A combination with the results from other searches in Run 1 and in Run 2 for the Higgs boson in the $b\bar{b}$ decay mode is performed, which yields an observed (expected) significance of 5.4 (5.5) standard deviations, thus providing direct observation of the Higgs boson decay into b-quarks. The ratio of the measured event yield for a Higgs boson decaying into $b\bar{b}$ to the Standard Model expectation is $1.01 \pm 0.12(\text{stat.})^{+0.16}_{-0.15}(\text{syst.})$. Additionally, a combination of Run 2 results searching for the Higgs boson produced in association with a vector boson yields an observed (expected) significance of 5.3 (4.8) standard deviations.

1. Introduction

The Higgs boson [1–4] was discovered in 2012 by the ATLAS and CMS Collaborations [5,6] with a mass of approximately 125 GeV from the analysis of proton–proton (pp) collisions produced by the Large Hadron Collider (LHC) [7]. Since then, the analysis of data collected at centre-of-mass energies of 7 TeV, 8 TeV and 13 TeV in Runs 1 and 2 of the LHC has led to the observation of many of the production modes and decay channels predicted by the Standard Model (SM). The bosonic decay channels are well established and have entered an era of precision measurements [8–18]. The decay into τ-lepton pairs was first observed in the combination of the ATLAS and CMS analyses [19,20]. The main Higgs boson production modes, gluon–gluon fusion (ggF) and vector-boson fusion (VBF), were already measured following the analysis of the Run 1 data, and recently the coupling of the Higgs boson to top quarks was directly observed by the ATLAS and CMS Collaborations [21,22] through the observation of the associated production of a Higgs boson and a top-quark pair ($t\bar{t}H$).

The dominant decay of the SM Higgs boson is into pairs of b-quarks, with an expected branching fraction of approximately 58% for a mass of $m_H = 125$ GeV [23]. However, large backgrounds from multi-jet production make a search in the dominant gluon–gluon fusion production mode very challenging at hadron colliders. The most sensitive production modes for detecting $H \to b\bar{b}$ decays are the associated production of a Higgs boson and a W or Z boson [24] (VH), where the leptonic decay of the vector boson enables efficient triggering and a significant reduction of the multi-jet background. As well as probing the dominant decay of the Higgs boson, this measurement allows the overall Higgs boson decay width [25,26] to be constrained and provides the best sensitivity to the ZH and WH production modes, which are (for instance) important elements in the interpretation of Higgs boson measurements in effective field theories [27].

Searches in this channel at the Tevatron by the CDF and D0 Collaborations showed an excess of events with a significance of 2.8 standard deviations for a Higgs boson with a mass of 125 GeV [28]. Analysing the 2015 and 2016 data and combining with the Run 1 results [29,30], both the ATLAS and CMS Collaborations reported evidence for Higgs boson production and decay in this channel, with observed (expected) significances of 3.6 (4.0) and 3.8 (3.8) standard deviations, respectively [32,33]. Searches for $H \to b\bar{b}$ decays have also been conducted in the VBF [34–36] and $t\bar{t}H$ [37–42] channels, and with high transverse momentum Higgs bosons [43], but with markedly lower sensitivities.

This Letter reports an update to the search for the SM Higgs boson decaying into a $b\bar{b}$ pair in the VH production mode with the ATLAS detector in Run 2 of the LHC presented in Ref. [32]. This update uses 79.8 fb^{-1} of pp collision data collected at a centre-

* *E-mail address:* atlas.publications@cern.ch.

https://doi.org/10.1016/j.physletb.2018.09.013

of-mass energy of 13 TeV, to be compared with 36.1 fb^{-1} for the previous result. In addition, an updated version of the ATLAS reconstruction code and improved object calibrations are used, the impact of the luminosity and modelling systematic uncertainties are reduced from updated measurements and estimates, and larger samples of simulated events are used to model the background processes. Events are selected in 0-, 1- and 2-lepton channels, based on the number of charged leptons, ℓ (electrons or muons), to explore the $ZH \to \nu\nu b\bar{b}$, $WH \to \ell\nu b\bar{b}$ and $ZH \to \ell\ell b\bar{b}$ signatures, respectively. The dominant background processes after the event selection are V + jets, $t\bar{t}$, single-top and diboson process. Multivariate discriminants, built from variables that describe the kinematics of the selected events, are used to maximise the sensitivity to the Higgs boson signal. Their output distributions are combined using a binned maximum-likelihood fit, referred to as the global likelihood fit, which allows the signal yield and the background normalisations to be extracted. The signal extraction method is cross-checked with the dijet-mass analysis, where the signal yield is extracted using the mass of the dijet system as the main fit observable, and validated using the diboson analysis, where the nominal multivariate analysis is modified to extract the VZ, $Z \to b\bar{b}$ diboson process. The result of the multivariate analysis is then combined with that of the previously published analysis of Run 1 data [30], with other searches for $b\bar{b}$ decays of the Higgs boson and with other searches in the VH production mode. The latter two combinations lead to the observation of both the $b\bar{b}$ decay of the Higgs boson and VH production. An observation of the $b\bar{b}$ decay of the Higgs boson by the CMS Collaboration [31] was submitted for publication at the same time as this Letter.

2. The ATLAS detector

ATLAS [44] is a general-purpose particle detector covering nearly the entire solid angle[1] around the collision point. An inner tracking detector, located within a 2 T axial magnetic field generated by a thin superconducting solenoid, is used to measure the trajectories and momenta of charged particles. The inner layers consist of high-granularity silicon pixel detectors covering a pseudorapidity range $|\eta| < 2.5$, and include an innermost layer [45,46] that was added to the detector between Run 1 and Run 2. Silicon microstrip detectors covering $|\eta| < 2.5$ are located beyond the pixel detectors. Outside the microstrip detectors and covering $|\eta| < 2.0$, there are straw-tube tracking detectors, which also provide measurements of transition radiation that are used in electron identification. A calorimeter system surrounds the inner tracking detector, covering the pseudorapidity range $|\eta| < 4.9$. Within the region $|\eta| < 3.2$, electromagnetic calorimetry is provided by barrel ($|\eta| < 1.475$) and endcap ($1.375 < |\eta| < 3.2$) high-granularity lead/liquid-argon (LAr) sampling calorimeters, with an additional thin LAr presampler covering $|\eta| < 1.8$ to correct for energy loss in material upstream of the calorimeters. Hadronic calorimetry is provided by a steel/scintillator-tile calorimeter within $|\eta| < 1.7$, and copper/LAr endcap calorimeters extend the coverage to $|\eta| = 3.2$. The solid angle coverage for $|\eta|$ between 3.2 and 4.9 is completed with copper/LAr and tungsten/LAr calorimeter modules optimised for electromagnetic and hadronic measurements, respectively. The outermost part of the detector is the muon spectrometer, which measures the curved trajectories of muons in the magnetic field of three large air-core superconducting toroidal magnets. High-precision tracking is performed within the range $|\eta| < 2.7$ and there are chambers for fast triggering within the range $|\eta| < 2.4$. A two-level trigger system [47] is used to reduce the recorded data rate. The first level is a hardware implementation aiming to reduce the rate to around 100 kHz, while the software-based high-level trigger provides the remaining rate reduction to approximately 1 kHz.

3. Object and event selection

The event topologies characteristic of VH, $H \to b\bar{b}$ processes considered contain zero, one or two charged leptons, and two 'b-jets' containing particles from b-hadron decays. The object and event selections follow those of Ref. [32] to a large extent.

3.1. Object reconstruction

Tracks measured in the inner detector are used to reconstruct interaction vertices [48], of which the one with the highest sum of squared transverse momenta of associated tracks is selected as the primary vertex.

Electrons are reconstructed from topological clusters of energy deposits in the calorimeter [49] and matched to a track in the inner detector. Following Refs. [32,50], *loose* electrons are required to have $p_{\mathrm{T}} > 7$ GeV and $|\eta| < 2.47$, to have small impact parameters,[2] to fulfil a loose track isolation requirement, and to meet a 'LooseLH' quality criterion computed from shower shape and track quality variables [51]. In the 1-lepton channel, *tight* electrons are selected using a 'TightLH' likelihood requirement and a stricter calorimeter-based isolation.

Muons are required to be within the acceptance of the muon spectrometer $|\eta| < 2.7$, to have $p_{\mathrm{T}} > 7$ GeV, and to have small impact parameters. *Loose* muons are selected using a 'loose' quality criterion [52] and a loose track isolation. In the 1-lepton channel, *tight* muons fulfil the 'medium' quality criterion and a stricter track isolation.

Hadronically decaying τ-leptons [53,54] are required to have $p_{\mathrm{T}} > 20$ GeV and $|\eta| < 2.5$, to be outside of the transition region between the barrel and end-cap electromagnetic calorimeters $1.37 < |\eta| < 1.52$, and to meet a 'medium' quality criterion [54]. They are only used in the analysis to avoid τ-leptons being misidentified as jets.

Jets are reconstructed from topological clusters [55] using the anti-k_t algorithm [56] with radius parameter $R = 0.4$. A jet vertex tagger [57] is used to remove jets associated with vertices other than the primary one for jet $p_{\mathrm{T}} < 60$ GeV and $|\eta| < 2.4$. Jet cleaning criteria are used to identify jets arising from non-collision backgrounds or noise in the calorimeters [58] and events containing such jets are removed. Jets are required to have $p_{\mathrm{T}} > 20$ GeV in the central region ($|\eta| < 2.5$), and $p_{\mathrm{T}} > 30$ GeV outside ($2.5 < |\eta| < 4.5$) of the tracker acceptance. In the central region, they are tagged as containing b-hadrons using a multivariate discriminant [59] (MV2), with the selection tuned to produce an average efficiency of 70% for b-jets in simulated $t\bar{t}$ events, which corresponds to light-flavour (u-, d-, s-quark and gluon) and c-jet misidentification efficiencies of 0.3% and 12.5% respectively.

Simulated jets are labelled as b-, c- or light-flavour jets according to which hadrons with $p_{\mathrm{T}} > 5$ GeV are found within a cone

[1] ATLAS uses a right-handed coordinate system with its origin at the nominal interaction point (IP) in the centre of the detector and the z-axis coinciding with the axis of the beam pipe. The x-axis points from the IP towards the centre of the LHC ring, and the y-axis points upward. Cylindrical coordinates (r, ϕ) are used in the transverse plane, ϕ being the azimuthal angle around the z-axis. The pseudorapidity is defined in terms of the polar angle θ as $\eta = -\ln\tan(\theta/2)$. The distance in (η, ϕ) coordinates, $\Delta R = \sqrt{(\Delta\phi)^2 + (\Delta\eta)^2}$, is also used to define cone sizes. Transverse momentum and energy are defined as $p_{\mathrm{T}} = p\sin\theta$ and $E_{\mathrm{T}} = E\sin\theta$, respectively.

[2] Transverse and longitudinal impact parameters are defined relative to the primary vertex position, where the beam line is used to approximate the primary vertex position in the transverse plane.

of size $\Delta R = 0.3$ around their axis. Simulated $V+$jets events are categorised depending on the labels of the jets that form the Higgs boson candidate: $V+ll$ when they are both light-flavour jets, $V+cl$ when there is one c-jet and one light-flavour jet, and $V+$HF (heavy flavour) in all other cases, mainly two b-jets. Owing to the large rejection of light-flavour jets achieved by the MV2 discriminant, simulated $V+ll$, $V+cl$ and WW events are not subjected to the b-tagging requirement due to the resulting low number of simulated events, but instead they are weighted by the probability that their jets pass the b-tagging selection [32].

In addition to the standard jet energy scale calibration [60], b-tagged jets receive additional flavour-specific corrections to improve their energy measurement (scale and resolution): if any muons are found within $\Delta R = 0.4$, the four-momentum of the closest muon is added to that of the jet, and a residual correction is applied to equalise the response to jets with leptonic or hadronic decays of heavy-flavour hadrons. In the 2-lepton channel, a per-event kinematic likelihood uses the full reconstruction of the event kinematics to improve the estimate of the energy of the b-jets. The corrections improve the resolution of the dijet mass by up to 40% [32].

The missing transverse momentum $\boldsymbol{E}_{\mathrm{T}}^{\mathrm{miss}}$ is reconstructed as the negative vector sum of the momenta of leptons, hadronically decaying τ-leptons and jets, and of a 'soft term' built from additional tracks matched to the primary vertex [61]. The magnitude of $\boldsymbol{E}_{\mathrm{T}}^{\mathrm{miss}}$ is referred to as $E_{\mathrm{T}}^{\mathrm{miss}}$. An overlap removal procedure is applied to avoid any double-counting between the reconstructed leptons, including the hadronically decaying τ-leptons, and jets.

3.2. Event selection and categorisation

Events are categorised into the 0-, 1- and 2-lepton channels depending on the number of selected electrons and muons, to target the $ZH \to \nu\nu b\bar{b}$, $WH \to \ell\nu b\bar{b}$ and $ZH \to \ell\ell b\bar{b}$ signatures, respectively. In all channels, events are required to have exactly two b-tagged jets, which form the Higgs boson candidate. At least one b-tagged jet is required to have p_{T} greater than 45 GeV. Events are further split into 2-jet or 3-jet categories depending on whether additional, untagged jets are present. In the 0- and 1-lepton channels, only one such jet is allowed, as the $t\bar{t}$ background is much larger in events with four jets or more. In the 2-lepton channel any number of jets is accepted in the 3-jet category.

The reconstructed transverse momentum p_{T}^{V} of the vector boson corresponds to $E_{\mathrm{T}}^{\mathrm{miss}}$ in the 0-lepton channel, to the vectorial sum of $\boldsymbol{E}_{\mathrm{T}}^{\mathrm{miss}}$ and the charged-lepton transverse momentum in the 1-lepton channel, and to the transverse momentum of the 2-lepton system in the 2-lepton channel. As the signal-to-background ratio increases for large Higgs boson transverse momenta [62,63], the analysis focuses on a high-p_{T}^{V} region defined as $p_{\mathrm{T}}^{V} > 150$ GeV. In the 2-lepton channel, the sensitivity is increased by the addition of a medium-p_{T}^{V} region with $75\,\mathrm{GeV} < p_{\mathrm{T}}^{V} < 150\,\mathrm{GeV}$.

Two versions of the analysis are carried out, one using a multivariate approach and the other using the dijet mass as the final discriminant. The event selection shown in Table 1 is applied to both versions, with further selections applied for the dijet-mass analysis. The two versions of the analysis also have different event categorisations, with further details outlined below.

0-lepton channel The online selection uses $E_{\mathrm{T}}^{\mathrm{miss}}$ triggers with thresholds that varied from 70 GeV to 110 GeV between the 2015 and 2017 data-taking periods. Their efficiency was measured in $W+$jets, $Z+$jets and $t\bar{t}$ events in data using single-muon triggers, resulting in correction factors that are applied to the simulated events, ranging from 1.05 at the offline $E_{\mathrm{T}}^{\mathrm{miss}}$ threshold of 150 GeV to a negligible deviation from unity at an $E_{\mathrm{T}}^{\mathrm{miss}}$ above 200 GeV. A requirement on the scalar sum of the transverse momenta H_{T} of the jets removes a small part of the phase space where the trigger efficiency depends mildly on the number of jets in the event. Events with any *loose* lepton are rejected. High $E_{\mathrm{T}}^{\mathrm{miss}}$ in multi-jet events typically arises from mismeasured jets in the calorimeters. Such events are efficiently removed by requirements on the angular separation of the $\boldsymbol{E}_{\mathrm{T}}^{\mathrm{miss}}$, jets, and $\boldsymbol{p}_{\mathrm{T}}^{\mathrm{miss}}$ (the missing transverse momentum calculated using only tracks reconstructed in the inner tracking detector and matched to the primary vertex).

1-lepton channel In the electron sub-channel, events are required to satisfy a logical OR of single-electron triggers with identification and isolation criteria looser than those used in the offline analysis, and p_{T} thresholds that started at 24 GeV in 2015 and increased to 26 GeV in 2016 and 2017. The muon sub-channel uses the same $E_{\mathrm{T}}^{\mathrm{miss}}$ triggers and correction factors as the 0-lepton channel, as these triggers effectively select on p_{T}^{V} given that muons are not included in the online $E_{\mathrm{T}}^{\mathrm{miss}}$ calculation and they perform more efficiently than the single-muon triggers in the analysis phase space. Events are required to have exactly one high-p_{T} *tight* electron or muon, and no additional *loose* leptons. In the electron sub-channel an additional selection of $E_{\mathrm{T}}^{\mathrm{miss}} > 30$ GeV is applied to reduce the background from multi-jet production. Events are categorised into the signal region (SR) or into a control region enriched in $W+$HF events ($W+$HF CR) using selections on the invariant mass of the two b-tagged jets (m_{bb}), and on the reconstructed mass of a semi-leptonically decaying top-quark candidate (m_{top}). The latter is calculated as the invariant mass of the lepton, the reconstructed neutrino[3] and the b-tagged jet that yields the lowest mass value. The resulting purity of the $W+$HF control region is around 75%.

2-lepton channel The online selection in the electron sub-channel is the same as in the 1-lepton channel. In the muon sub-channel, a similar OR of single-muon triggers is used, with lowest p_{T} thresholds increasing with luminosity and ranging from 20 GeV to 26 GeV. Events must have exactly two *loose* leptons, one of which must have $p_{\mathrm{T}} > 27$ GeV, and the invariant mass of the lepton pair must be compatible with that of the Z boson. Events with same-flavour leptons enter the signal region, while events with one muon and one electron define an $e\mu$ control region which is over 99% pure in $t\bar{t}$ and single-top-quark events.

The acceptances in the three channels after the event selection, as well as the predicted cross-sections times branching fractions for $(W/Z)H$ with $W \to \ell\nu$, $Z \to \ell\ell$, $Z \to \nu\nu$, and $H \to b\bar{b}$ are given in Table 2. The non-negligible acceptance for the $qq \to WH$ process in the 0-lepton channel is mostly due to events with an unidentified hadronically decaying τ-lepton produced in the W decay, while the larger acceptance for the $gg \to ZH$ process compared with $qq \to ZH$ is due to the harder p_{T}^{V} spectrum of the gluon-induced process.

3.3. Multivariate analysis

Boosted decision trees (BDT) are trained in eight signal regions, corresponding to two jet categories for the three lepton channels in the high-p_{T}^{V} region, in addition to the two jet categories for the 2-lepton medium-p_{T}^{V} region. The BDT outputs are used as the final discriminating variables in the analysis. Two sets of BDTs are constructed with the same input variables and parameters. The nominal one (BDT_{VH}) is designed to separate Higgs boson events from the sum of expected backgrounds, while the second one (BDT_{VZ})

[3] The transverse component of the neutrino momentum is identified with $\boldsymbol{E}_{\mathrm{T}}^{\mathrm{miss}}$, and the longitudinal component is obtained by constraining the lepton–neutrino system to the W mass.

Table 1
Summary of the event selection and categorisation in the 0-, 1- and 2-lepton channels.

Selection	0-lepton	1-lepton		2-lepton
		e sub-channel	μ sub-channel	
Trigger	$E_{\mathrm{T}}^{\mathrm{miss}}$	Single lepton	$E_{\mathrm{T}}^{\mathrm{miss}}$	Single lepton
Leptons	0 *loose* leptons with $p_{\mathrm{T}} > 7$ GeV	1 *tight* electron $p_{\mathrm{T}} > 27$ GeV	1 *tight* muon $p_{\mathrm{T}} > 25$ GeV	2 *loose* leptons with $p_{\mathrm{T}} > 7$ GeV ≥ 1 lepton with $p_{\mathrm{T}} > 27$ GeV
$E_{\mathrm{T}}^{\mathrm{miss}}$	> 150 GeV	> 30 GeV	–	–
$m_{\ell\ell}$	–	–		81 GeV $< m_{\ell\ell} <$ 101 GeV
Jets	Exactly 2 / Exactly 3 jets			Exactly 2 / ≥ 3 jets
Jet p_{T}	> 20 GeV for $\lvert\eta\rvert < 2.5$, > 30 GeV for $2.5 < \lvert\eta\rvert < 4.5$			
b-jets	Exactly 2 b-tagged jets			
Leading b-tagged jet p_{T}	> 45 GeV			
H_{T}	120 GeV (2 jets), >150 GeV (3 jets)	–		–
$\min[\Delta\phi(\boldsymbol{E}_{\mathrm{T}}^{\mathrm{miss}}, \textbf{jets})]$	$> 20°$ (2 jets), $> 30°$ (3 jets)	–		–
$\Delta\phi(\boldsymbol{E}_{\mathrm{T}}^{\mathrm{miss}}, \boldsymbol{bb})$	$> 120°$	–		–
$\Delta\phi(\boldsymbol{b_1}, \boldsymbol{b_2})$	$< 140°$	–		–
$\Delta\phi(\boldsymbol{E}_{\mathrm{T}}^{\mathrm{miss}}, \boldsymbol{p}_{\mathrm{T}}^{\mathrm{miss}})$	$< 90°$	–		–
p_{T}^{V} regions	> 150 GeV			75 GeV $< p_{\mathrm{T}}^{V} <$ 150 GeV, > 150 GeV
Signal regions	–	$m_{bb} \geq 75$ GeV or $m_{\mathrm{top}} \leq 225$ GeV		Same-flavour leptons Opposite-sign charges ($\mu\mu$ sub-channel)
Control regions	–	$m_{bb} < 75$ GeV and $m_{\mathrm{top}} > 225$ GeV		Different-flavour leptons Opposite-sign charges

Table 2
The cross-section (σ) times branching fraction ($\mathcal{B}$) and acceptance for the three channels at $\sqrt{s} = 13$ TeV. The qq- and gg-initiated ZH processes are shown separately. The branching fractions are calculated considering only decays into muons and electrons for $Z \to \ell\ell$, decays into all three lepton flavours for $W \to \ell\nu$ and decays into all neutrino flavours for $Z \to \nu\nu$. The acceptance is calculated as the fraction of events remaining in the combined signal and control regions after the full event selection.

Process	$\sigma \times \mathcal{B}$ [fb]	Acceptance [%]		
		0-lepton	1-lepton	2-lepton
$qq \to ZH \to \ell\ell b\bar{b}$	29.9	<0.1	0.1	6.0
$gg \to ZH \to \ell\ell b\bar{b}$	4.8	<0.1	0.2	13.5
$qq \to WH \to \ell\nu b\bar{b}$	269.0	0.2	1.0	–
$qq \to ZH \to \nu\nu b\bar{b}$	89.1	1.9	–	–
$gg \to ZH \to \nu\nu b\bar{b}$	14.3	3.5	–	–

Table 3
Summary of the event selection criteria in the 0-, 1- and 2-lepton channels for the dijet-mass analysis, applied in addition to those described in Table 1 for the multivariate analysis.

Channel			
Selection	0-lepton	1-lepton	2-lepton
m_{T}^{W}	–	< 120 GeV	–
$E_{\mathrm{T}}^{\mathrm{miss}}/\sqrt{S_{\mathrm{T}}}$	–	–	$< 3.5\sqrt{\mathrm{GeV}}$
p_{T}^{V} regions			
p_{T}^{V}	75–150 GeV (2-lepton only)	150–200 GeV	> 200 GeV
$\Delta R(\boldsymbol{b}_1, \boldsymbol{b}_2)$	<3.0	<1.8	<1.2

is used to validate the analysis by the extraction of the diboson VZ, $Z \to b\bar{b}$ process from the sum of all other SM processes.

The same input variables, BDT settings and BDT output binning transformation as those detailed in Ref. [32] are used, with one exception in the 2-lepton channel where the $E_{\mathrm{T}}^{\mathrm{miss}}$ is replaced with $E_{\mathrm{T}}^{\mathrm{miss}}/\sqrt{S_{\mathrm{T}}}$ (where S_{T} is the scalar sum of transverse momenta of the charged leptons and jets in the event). Eight to thirteen input variables describing the kinematics of the events are used depending on the channels, of which m_{bb}, p_{T}^{V} and $\Delta R(\boldsymbol{b_1}, \boldsymbol{b_2})$ (where b_1 and b_2 refer to the two b-tagged jets) are the most discriminating.

3.4. Dijet-mass analysis

A cross-check of the main multivariate analysis is performed by using the invariant mass of the two b-tagged jets as the discriminating variable. Additional selections displayed in Table 3 increase the purity of the signal regions and are necessary to improve the sensitivity of this method.

The high-p_{T}^{V} region is split into two regions 150 GeV $< p_{\mathrm{T}}^{V} <$ 200 GeV and $p_{\mathrm{T}}^{V} > 200$ GeV, with further requirements placed upon $\Delta R(\boldsymbol{b_1}, \boldsymbol{b_2})$. Selections on the transverse mass of the W boson (m_{T}^{W}) and on $E_{\mathrm{T}}^{\mathrm{miss}}/\sqrt{S_{\mathrm{T}}}$ reduce the $t\bar{t}$ background in the 1- and 2-lepton channels, respectively.

In the 1-lepton channel the m_{bb} distribution is able to sufficiently constrain the W + HF background, thus it is not necessary to separate events into a dedicated W + HF CR.

4. Data, simulated samples and multi-jet background

The data used in this analysis were collected at a centre-of-mass energy of 13 TeV during the 2015–2017 running periods. Events are selected for analysis only if they are of good quality and if all the relevant detector components are known to have been in good operating condition, which corresponds to a total integrated luminosity of 79.8 ± 1.6 fb^{-1} [64,65]. The recorded events contain an average of 32 inelastic pp collisions.

Monte Carlo (MC) simulated events are used to model the backgrounds from SM processes and VH, $H \to b\bar{b}$ signal processes. All simulated processes are normalised using the most accurate theoretical cross-section predictions currently available and were generated at least to next-to-leading-order (NLO) accuracy. All samples of simulated events were passed through the ATLAS detector simulation [66] based on GEANT 4 [67] and were reconstructed with the standard ATLAS reconstruction software. The effects of multiple interactions in the same and nearby bunch crossings (pile-up) were modelled by overlaying minimum-bias events, simulated using the soft QCD processes of Pythia 8.186 [68] with the A2 [69] set of tuned parameters (tune) and MSTW2008LO [70] parton distribution functions (PDF). For all samples of simulated events, except for

Table 4
The generators used for the simulation of the signal and background processes. If not specified, the order of the cross-section calculation refers to the expansion in the strong coupling constant (α_S). The acronyms ME, PS and UE stand for matrix element, parton shower and underlying event, respectively. ($\star$) The events were generated using the first PDF in the NNPDF3.0NLO set and subsequently reweighted to the PDF4LHC15NLO set [73] using the internal algorithm in POWHEG-BOX v2. (†) The NNLO(QCD)+NLO(EW) cross-section calculation for the $pp \to ZH$ process already includes the $gg \to ZH$ contribution. The $qq \to ZH$ process is normalised using the cross-section for the $pp \to ZH$ process, after subtracting the $gg \to ZH$ contribution. An additional scale factor is applied to the $qq \to VH$ processes as a function of the transverse momentum of the vector boson, to account for electroweak (EW) corrections at NLO. This makes use of the VH differential cross-section computed with HAWK [74,75].

Process	ME generator	ME PDF	PS and hadronisation	UE model tune	Cross-section order
Signal, mass set to 125 GeV and $b\bar{b}$ branching fraction to 58%					
$qq \to WH$ $\to \ell\nu b\bar{b}$	POWHEG-BOX v2 [76] + GOSAM [79] + MINLO [80,81]	NNPDF3.0NLO$^{(\star)}$ [77]	PYTHIA 8.212 [68]	AZNLO [78]	NNLO(QCD) + NLO(EW) [82–88]
$qq \to ZH$ $\to \nu\nu b\bar{b}/\ell\ell b\bar{b}$	POWHEG-BOX v2 + GOSAM + MINLO	NNPDF3.0NLO$^{(\star)}$	PYTHIA 8.212	AZNLO	NNLO(QCD)$^{(\dagger)}$ + NLO(EW)
$gg \to ZH$ $\to \nu\nu b\bar{b}/\ell\ell b\bar{b}$	POWHEG-BOX v2	NNPDF3.0NLO$^{(\star)}$	PYTHIA 8.212	AZNLO	NLO + NLL [89–93]
Top quark, mass set to 172.5 GeV					
$t\bar{t}$	POWHEG-BOX v2 [94]	NNPDF3.0NLO	PYTHIA 8.230	A14 [95]	NNLO+NNLL [96]
s-channel	POWHEG-BOX v2 [97]	NNPDF3.0NLO	PYTHIA 8.230	A14	NLO [98]
t-channel	POWHEG-BOX v2 [97]	NNPDF3.0NLO	PYTHIA 8.230	A14	NLO [99]
Wt	POWHEG-BOX v2 [100]	NNPDF3.0NLO	PYTHIA 8.230	A14	Approximate NNLO [101]
Vector boson + jets					
$W \to \ell\nu$	SHERPA 2.2.1 [71,102,103]	NNPDF3.0NNLO	SHERPA 2.2.1 [104,105]	Default	NNLO [106]
$Z/\gamma^* \to \ell\ell$	SHERPA 2.2.1	NNPDF3.0NNLO	SHERPA 2.2.1	Default	NNLO
$Z \to \nu\nu$	SHERPA 2.2.1	NNPDF3.0NNLO	SHERPA 2.2.1	Default	NNLO
Diboson					
$qq \to WW$	SHERPA 2.2.1	NNPDF3.0NNLO	SHERPA 2.2.1	Default	NLO
$qq \to WZ$	SHERPA 2.2.1	NNPDF3.0NNLO	SHERPA 2.2.1	Default	NLO
$qq \to ZZ$	SHERPA 2.2.1	NNPDF3.0NNLO	SHERPA 2.2.1	Default	NLO
$gg \to VV$	SHERPA 2.2.2	NNPDF3.0NNLO	SHERPA 2.2.2	Default	NLO

those generated using SHERPA [71], the EVTGEN v1.2.0 program [72] was used to describe the decays of bottom and charm hadrons. A summary of all the generators used for the simulation of the signal and background processes is shown in Table 4. Samples produced with alternative generators are used to estimate systematic uncertainties in the event modelling, as described in Section 5.

The background processes involving W or Z boson decays into leptons (including those in which the W boson arises from a top-quark decay) are collectively referred to in the following as electroweak (EW) backgrounds and were simulated as described above. In contrast, the multi-jet background is estimated in all three channels using data-driven methods. In both the 0- and 2-lepton channels, the multi-jet contribution is estimated from template fits to data, using the simulated samples to model the EW backgrounds and a functional form to model the multi-jet background. The template fit is performed using a variable that provides significant discrimination between the multi-jet and EW processes, with any selection on that variable removed. In the 0-lepton channel, $\min[\Delta\phi(\boldsymbol{E}_{\mathrm{T}}^{\mathrm{miss}}, \textbf{jets})]$ is used, and in the 2-lepton channel, the dilepton mass distribution is used for the case where the charges of the lepton candidates have the same sign, assuming the multi-jet contribution is symmetric for opposite- and same-sign lepton charges. In both cases, it is found that the multi-jet contribution is sufficiently small that it can be neglected in the global likelihood fit without having any impact on the extracted signal.

The multi-jet background is found to be non-negligible in the 1-lepton channel and is estimated separately in the electron and muon sub-channels, and in the 2- and 3-jet categories. In each category, a template fit to the transverse mass distribution of the W boson candidate is performed, which offers the clearest discrimination between the multi-jet and EW processes, to extract the multi-jet yield. The template used for the multi-jet contribution is obtained from data in a control region after subtraction of the residual EW contribution, based on MC predictions, while the template for the EW contribution in the signal region is obtained directly from MC predictions. The control region is enriched in multi-jet events that are kinematically close to the corresponding signal region but not overlapping with it, and is defined by applying the nominal selection but inverting the stricter lepton isolation requirements. To increase the statistical precision of the data-driven estimate, the number of required b-tagged jets is reduced from two to one in the multi-jet enriched control region. The template fit applied in the signal region determines the normalisation of the multi-jet contribution, while the shape of the BDT discriminant (or of other relevant observables) is obtained using a control region analogously to the m_{T}^{W} template. Both the normalisation and shape derived for the BDT discriminant are then used in the global likelihood fit. The multi-jet contribution in the 2-jet category is found to be 1.9% (2.8%) of the total background contribution in the electron (muon) sub-channel, while in the 3-jet category it is found to be 0.2% (0.4%). These estimates are subject to sizeable systematic uncertainties, which are described in Section 5.

5. Systematic uncertainties

The sources of systematic uncertainty can be broadly divided into four groups: those of experimental nature, those related to the modelling of the simulated backgrounds, those related to the multi-jet background estimation, and those associated with the Higgs boson signal simulation. The estimation of the uncertainties closely follows the methodology outlined in Ref. [32] and is briefly summarised below.

5.1. Experimental uncertainties

The dominant experimental uncertainties originate from the b-tagging correction factors, determined from the difference between the efficiency measured in data and simulation, from the jet energy scale corrections and from the modelling of the jet energy resolution. The b-tagging correction factors are derived separately

for b-jets, c-jets and light-flavour jets [107–109]. All three correction factors have uncertainties estimated from multiple measurements, which are decomposed into uncorrelated components that are then treated independently, resulting in three uncertainties for b-jets and c-jets, and five for light-flavour jets. The approximate size of the uncertainty in the tagging efficiency is 2% for b-jets, 10% for c-jets and 40% for light-flavour jets. Additional uncertainties are considered in the extrapolation of the b-jet efficiency calibration to jets with $p_{\mathrm{T}} > 300$ GeV and in the misidentification of hadronically decaying τ-leptons as b-jets. The uncertainties in the jet energy scale and resolution are based on their respective measurements [60,110]. The many sources of uncertainty in the correction of the jet energy scale are decomposed into 23 uncorrelated components that are treated as independent. An additional specific uncertainty in the energy calibration of b- and c-jets is considered.

Uncertainties in the reconstruction, identification, isolation and trigger efficiencies of muons [52] and electrons [50], along with the uncertainty in their energy scale and resolution, are estimated using 13 TeV data. These are found to have only a small impact on the result. The uncertainties in the energy scale and resolution of the jets and leptons are propagated to the calculation of $E_{\mathrm{T}}^{\mathrm{miss}}$, which also has additional uncertainties from the scale, resolution and reconstruction efficiency of the tracks used to compute the soft term [61], along with the modelling of the underlying event. An uncertainty is assigned to the $E_{\mathrm{T}}^{\mathrm{miss}}$ trigger correction factors, determined from the difference between the trigger efficiency in data and simulation, to account for the statistical uncertainty in the measured correction factors and for differences between the correction factors determined from $W+$jets, $Z+$jets and $t\bar{t}$ events. The uncertainty in the combined 2015–2017 integrated luminosity is 2.0%. It is derived, following a methodology similar to that detailed in Ref. [64], and using the LUCID-2 detector for the baseline luminosity measurements [65]. The average number of interactions per bunch crossing is rescaled by 1.03 to improve agreement between simulation and data, based on the measurement of the visible cross-section in minimum-bias events [111], and an uncertainty, as large as the correction, is included.

5.2. Simulated sample uncertainties

Modelling uncertainties are derived for the simulated samples and broadly cover three areas: normalisations, acceptance differences that affect the relative normalisations between analysis regions with a common normalisation, and the shapes of the differential distributions of the most important kinematic variables. The overall normalisations and associated uncertainties for the background processes are taken from the currently most accurate calculations as detailed in Table 4, apart from the main backgrounds whose normalisations are left unconstrained (floated) in the global likelihood fit. The additional systematic uncertainties in the acceptance differences and in the shapes are derived either from particle-level comparisons between nominal and alternative simulated samples, or from comparisons with data in control regions. The particle-level comparisons are cross-checked with detector-level simulations whenever these are available, and good agreement is found. The alternative samples were either produced by other generators or by altering the nominal values of generator parameters. When acceptance uncertainties are estimated, the nominal and alternative samples are normalised using the same production cross-section. Shape uncertainties are considered in each of the analysis regions separately, with the samples scaled to have the same normalisation in each region. In this case, the uncertainty is taken from the alternative sample that differs most in shape from the nominal sample. Shape uncertainties are only derived for the m_{bb} and p_{T}^{V} variables, as it was found sufficient to only consider the changes induced in these variables to cover the overall shape variation of the BDT_{VH} discriminant. Full details are provided in Ref. [32].

Table 5
Summary of the systematic uncertainties in the background modelling for $Z+$jets, $W+$jets, $t\bar{t}$, single top-quark and multi-jet production. An 'S' symbol is used when only a shape uncertainty is assessed. The regions for which the normalisations float independently are listed in brackets. Where the size of an acceptance systematic uncertainty varies between regions, a range is displayed.

$Z+$jets	
$Z+ll$ normalisation	18%
$Z+cl$ normalisation	23%
$Z+$HF normalisation	Floating (2-jet, 3-jet)
$Z+bc$-to-$Z+bb$ ratio	30–40%
$Z+cc$-to-$Z+bb$ ratio	13–15%
$Z+bl$-to-$Z+bb$ ratio	20–25%
0-to-2 lepton ratio	7%
m_{bb}, p_{T}^{V}	S
$W+$jets	
$W+ll$ normalisation	32%
$W+cl$ normalisation	37%
$W+$HF normalisation	Floating (2-jet, 3-jet)
$W+bl$-to-$W+bb$ ratio	26% (0-lepton) and 23% (1-lepton)
$W+bc$-to-$W+bb$ ratio	15% (0-lepton) and 30% (1-lepton)
$W+cc$-to-$W+bb$ ratio	10% (0-lepton) and 30% (1-lepton)
0-to-1 lepton ratio	5%
$W+$HF CR to SR ratio	10% (1-lepton)
m_{bb}, p_{T}^{V}	S
$t\bar{t}$ (all are uncorrelated between the $0+1$- and 2-lepton channels)	
$t\bar{t}$ normalisation	Floating ($0+1$-lepton) Floating (2-lepton 2-jet, 2-lepton 3-jet)
0-to-1 lepton ratio	8%
2-to-3-jet ratio	9% (0+1-lepton only)
$W+$HF CR to SR ratio	25%
m_{bb}, p_{T}^{V}	S
Single top-quark	
Cross-section	4.6% (s-channel), 4.4% (t-channel), 6.2% (Wt)
Acceptance 2-jet	17% (t-channel), 55% ($Wt(bb)$), 24% (Wt(other))
Acceptance 3-jet	20% (t-channel), 51% ($Wt(bb)$), 21% (Wt(other))
m_{bb}, p_{T}^{V}	S (t-channel, $Wt(bb)$, Wt(other))
Multi-jet (1-lepton)	
Normalisation	60–100% (2-jet), 90–140% (3-jet)
BDT template	S

5.2.1. Background uncertainties

The systematic uncertainties affecting the modelling of the background samples are summarised in Tables 5 and 6 and key details of the treatment of the backgrounds are reported below.

***V* + jets production** The $V+$jets backgrounds are subdivided into three different components based upon the jet flavour labels of the two b-tagged jets in the event. The main background contributions ($V+bb$, $V+bc$, $V+bl$ and $V+cc$) are jointly considered as the $V+$HF background. Their overall normalisation, separately in the 2- and 3-jet categories, is free to float in the global likelihood fit. The remaining flavour components, $V+cl$ and $V+ll$, constitute less than $\sim 1\%$ of the background in each analysis region, so only uncertainties in the normalisation of these backgrounds are included. Acceptance uncertainties are estimated for the relative normalisations of the different regions that share a common floating normalisation parameter. In the case of the $W+$HF background, this includes the uncertainties in the ratio of the event yield in the 0-lepton channel to that in the 1-lepton channel and, in the 1-lepton channel, in the ratio of the event yield in the $W+$HF control region to that in the signal region. For the $Z+$HF background, there is an uncertainty in the ratio of the event yield in the 0-lepton channel to that in the 2-lepton channel. Uncertain-

Table 6
Summary of the systematic uncertainties in the background modelling for diboson production. An 'S' symbol is used when only a shape uncertainty is assessed and 'PS/UE' indicates parton shower/underlying event. When extracting the $(W/Z)Z$ diboson production signal yield, as the normalisations are unconstrained, the normalisation uncertainties are removed. Where the size of an acceptance systematic uncertainty varies between regions, a range is displayed.

ZZ	
Normalisation	20%
0-to-2 lepton ratio	6%
Acceptance from scale variations	10–18%
Acceptance from PS/UE variations for 2 or more jets	6%
Acceptance from PS/UE variations for 3 jets	7% (0-lepton), 3% (2-lepton)
m_{bb}, p_{T}^{V}, from scale variations	S (correlated with WZ uncertainties)
m_{bb}, p_{T}^{V}, from PS/UE variations	S (correlated with WZ uncertainties)
m_{bb}, from matrix-element variations	S (correlated with WZ uncertainties)
WZ	
Normalisation	26%
0-to-1 lepton ratio	11%
Acceptance from scale variations	13–21%
Acceptance from PS/UE variations for 2 or more jets	4%
Acceptance from PS/UE variations for 3 jets	11%
m_{bb}, p_{T}^{V}, from scale variations	S (correlated with ZZ uncertainties)
m_{bb}, p_{T}^{V}, from PS/UE variations	S (correlated with ZZ uncertainties)
m_{bb}, from matrix-element variations	S (correlated with ZZ uncertainties)
WW	
Normalisation	25%

ties are also estimated in the relative normalisation of the four heavy-flavour components that constitute the $V+\mathrm{HF}$ background. These are taken as uncertainties in the bc, cc and bl yields compared with the dominant bb yield and are estimated separately in each channel in a manner similar to the acceptance systematic uncertainties. Uncertainties are also derived for the shapes of the m_{bb} and p_{T}^{V} distributions, which are evaluated for $W+\mathrm{HF}$ from comparisons with alternative samples and for $Z+\mathrm{HF}$ from comparisons with data in m_{bb} sidebands.

***t*$\bar{t}$ production** Due to the significantly different regions of phase space probed, the $t\bar{t}$ background in the 0- and 1-lepton channels (jointly referred to as 0+1-lepton channel in the following) is considered independently from the $t\bar{t}$ background in the 2-lepton channel; different overall floating normalisation factors are considered, and acceptance uncertainties are derived separately and taken as uncorrelated between the 0+1- and 2-lepton channels. For the 0+1- lepton channels, uncertainties are considered in the normalisation ratios of the 2-jet and 3-jet categories, of the $W+\mathrm{HF}$ control and signal regions, and of the 1-lepton and 0-lepton channels. For the 2-lepton channel, the normalisations in the 2- and 3-jet categories are both left floating, and are effectively determined in their respective $e\mu$ control regions. Uncertainties in the shapes of the p_{T}^{V} and m_{bb} distributions are estimated in the 0+1- and 2-lepton channels separately from comparisons with alternative samples. In addition, the modelling of the $t\bar{t}$ background is validated in the 2-lepton channel by using the data events from the $e\mu$ control region to model this background in the signal region, with good agreement found.

Single top-quark production In the Wt- and t-channels, uncertainties are derived for the normalisation, acceptance and shapes of the m_{bb} and p_{T}^{V} distributions. For the Wt-channel, the estimated modelling uncertainties are based on the flavour of the two b-tagged jets, due to the different regions of phase space being probed when there are two b-jets (bb) present compared with events where there are fewer b-jets present (other). Only a normalisation uncertainty is derived for the s-channel, since its contribution is negligible overall.

Diboson production The diboson backgrounds are composed of three distinct processes: WZ, WW and ZZ production. Given the small contribution from WW production ($< 0.1\%$ of the total background) only a normalisation uncertainty is assigned. The more important contributions from the WZ and ZZ backgrounds have uncertainties derived for the overall normalisation, the relative acceptance between regions and for the m_{bb} and p_{T}^{V} shapes. These are derived following the procedure described in Ref. [32] and are outlined in Table 6.

5.2.2. Signal uncertainties

The systematic uncertainties that affect the modelling of the signal are summarised in Table 7. They are derived following the procedure outlined in Ref. [32], but with updated alternative samples generated with a larger number of events, and using a parameter tune optimized more recently for the evaluation of the parton shower uncertainty. This substantially reduces the parton shower and underlying event (PS/UE) uncertainties. The systematic uncertainties in the calculations of the VH production cross-sections and the $H \to b\bar{b}$ branching fraction[4] are assigned following the recommendations of the LHC Higgs Cross Section Working Group [26,92,93,112,113].

5.3. Multi-jet background uncertainties

Systematic uncertainties can have an impact on the data-driven multi-jet estimate used in the 1-lepton channel in two ways: either changing the m_{T}^{W} distributions used in the multi-jet template fits, thus impacting the extracted multi-jet normalisations, or directly changing the multi-jet BDT distributions used in the global likelihood fit. Several uncertainties are considered, uncorrelated between the electron and muon sub-channels. The respective variations are added in quadrature for the normalisations, or considered as separate shape uncertainties. Variations are obtained by changing the definition of the multi-jet control region (more stringent isolation requirements, a different single-electron trigger to probe a potential trigger bias in the isolation requirements), and varying the normalisation of the contamination from the top ($t\bar{t}$ and

[4] Such systematic uncertainties fully degenerate with the signal yield do not affect the calculation of the significance relative to the background-only prediction.

Table 7
Summary of the systematic uncertainties in the signal modelling. An 'S' symbol is used when only a shape uncertainty is assessed and 'PS/UE' indicates parton shower / underlying event. Where the size of an acceptance systematic uncertainty varies between regions, a range is displayed.

Signal	
Cross-section (scale)	0.7% (qq), 27% (gg)
Cross-section (PDF)	1.9% ($qq \to WH$), 1.6% ($qq \to ZH$), 5% (gg)
$H \to b\bar{b}$ branching fraction	1.7%
Acceptance from scale variations	2.5–8.8%
Acceptance from PS/UE variations for 2 or more jets	2.9–6.2% (depending on lepton channel)
Acceptance from PS/UE variations for 3 jets	1.8–11%
Acceptance from PDF + α_S variations	0.5–1.3%
m_{bb}, p_T^V, from scale variations	S
m_{bb}, p_T^V, from PS/UE variations	S
m_{bb}, p_T^V, from PDF + α_S variations	S
p_T^V from NLO EW correction	S

Wt) and V + jets processes in the multi-jet control region. In addition, the following systematic uncertainties have an impact only on the multi-jet normalisation: use of another discriminant variable instead of m_T^W for the template fit (the azimuthal separation between the directions of the lepton transverse momentum and the vectorial sum of the momenta of the two or three jets) and, for the electron sub-channel only, the inclusion of the $E_T^{miss} < 30$ GeV region, which significantly enhances the multi-jet contribution in the template fit.

6. Statistical analysis

The statistical procedure is based on a likelihood function $\mathcal{L}(\mu, \boldsymbol{\theta})$, constructed as the product of Poisson probability terms over the bins of the input distributions. The parameter of interest, μ, is the signal strength that multiplies the SM Higgs boson production cross-section times the branching fraction into $b\bar{b}$ and is extracted by maximising the likelihood. Systematic uncertainties enter the likelihood as nuisance parameters (NP), $\boldsymbol{\theta}$. Most of the uncertainties discussed in Section 5 are constrained with Gaussian or log-normal probability density functions. The normalisations of the largest backgrounds, $t\bar{t}$, W + HF and Z + HF, can be reliably determined by the fit, so they are left unconstrained in the likelihood. The uncertainties due to the limited number of events in the simulated samples used for the background predictions are included using the Beeston–Barlow technique [114]. As detailed in Ref. [30], systematic variations that are subject to large statistical fluctuations are smoothed, and systematic uncertainties that have a negligible impact on the final results are pruned away region-by-region.

The probability that the background-only hypothesis is compatible with the observed data is determined using the q_0 test statistic constructed from the profile-likelihood ratio with the asymptotic approximation [115].

6.1. Multivariate analysis

As discussed in Section 3.3, the global likelihood fit comprises eight signal regions, defined as the 2- and 3-jet categories in the high-p_T^V region for the three channels, and in the medium-p_T^V region for the 2-lepton channel. The BDT_{VH} multivariate discriminant output distributions in these regions are input to the fit. The event yields are used in the two W + HF control regions of the 1-lepton channel. In the four $e\mu$ control regions of the 2-lepton channel, the m_{bb} distributions are input to the fit, except for the 2-jet category of the high-p_T^V region, where the event yield is used. The post-fit normalisation factors of the unconstrained backgrounds in the global likelihood fit to the 13 TeV data are shown in Table 8.

Table 8
Factors applied to the nominal normalisations of the $t\bar{t}$, W + HF and Z + HF backgrounds, as obtained from the global likelihood fit to the 13 TeV data for the nominal multivariate analysis, used to extract the Higgs boson signal. The errors represent the combined statistical and systematic uncertainties.

Process	Normalisation factor
$t\bar{t}$ 0- and 1-lepton	0.98 ± 0.08
$t\bar{t}$ 2-lepton 2-jet	1.06 ± 0.09
$t\bar{t}$ 2-lepton 3-jet	0.95 ± 0.06
W + HF 2-jet	1.19 ± 0.12
W + HF 3-jet	1.05 ± 0.12
Z + HF 2-jet	1.37 ± 0.11
Z + HF 3-jet	1.09 ± 0.09

The effects of systematic uncertainties on the measurement of the signal strength are displayed in Table 9. The impact of a category of systematic uncertainties is defined as the difference in quadrature between the uncertainty in μ computed when all NPs are fitted and that when the NPs in the category are fixed to their best-fit values. The total statistical uncertainty is defined as the uncertainty in μ when all the NPs are fixed to their best-fit values. The total systematic uncertainty is then defined as the difference in quadrature between the total uncertainty in μ and the total statistical uncertainty. As shown in the table, the systematic uncertainties due to the modelling of the signal play a dominant role, followed by the uncertainty due to the limited size of the simulated samples, the modelling of the backgrounds and the b-tagging uncertainty.

6.2. Dijet-mass analysis

In the dijet-mass analysis, the number of signal regions is increased to fourteen as a consequence of splitting the event regions with $p_T^V > 150$ GeV in two, while the W + HF CRs are merged into the corresponding SR, as outlined in Section 3.4. The m_{bb} distributions are input to the fit in all categories, except for the 2-jet medium- and high-p_T^V categories of the 2-lepton $e\mu$ control region, where the event yield is used.

6.3. Diboson analysis

In the diboson analysis, a measurement of the signal strength of the ZZ and WZ processes is conducted to validate the main multivariate analysis. The method differs from the global likelihood fit only by the use of the BDT_{VZ} output distributions as inputs, instead of BDT_{VH}. The parameter of interest, μ_{VZ}, is the signal strength of the combined WZ and ZZ diboson processes, and the SM Higgs boson is included as a background process normalised to

Table 9
Breakdown of the contributions to the uncertainty in μ. The sum in quadrature of the systematic uncertainties attached to the categories differs from the total systematic uncertainty due to correlations.

Source of uncertainty		σ_μ
Total		0.259
Statistical		0.161
Systematic		0.203
Experimental uncertainties		
Jets		0.035
$E_{\mathrm{T}}^{\mathrm{miss}}$		0.014
Leptons		0.009
b-tagging	b-jets	0.061
	c-jets	0.042
	light-flavour jets	0.009
	extrapolation	0.008
Pile-up		0.007
Luminosity		0.023
Theoretical and modelling uncertainties		
Signal		0.094
Floating normalisations		0.035
$Z+$jets		0.055
$W+$jets		0.060
$t\bar{t}$		0.050
Single top quark		0.028
Diboson		0.054
Multi-jet		0.005
MC statistical		0.070

the predicted SM cross-section with an uncertainty of 50%, which conservatively encompasses the previous measurement and uncertainty [32].

6.4. Combinations

6.4.1. Run 1

The results of the statistical analysis of the 13 TeV data are combined with those from the data recorded at 7 TeV and 8 TeV [30] to improve the precision of the measurement. Detailed studies of the impact of the correlation of systematic uncertainties between the two analyses are reported in Ref. [32]. In most cases, the impact of correlations was found to be negligible. Only a b-jet-specific jet energy scale, and theory uncertainties in the Higgs boson signal (overall cross-section, branching fraction and p_{T}^V-dependent NLO EW corrections) are correlated across the different centre-of-mass energies.

6.4.2. $H \to b\bar{b}$

A second combination is performed with the results of the searches for the $H \to b\bar{b}$ decay in the $t\bar{t}H$ [37,39] and VBF [34,36] production modes carried out with the Run 1 and Run 2 data. As the analysis targeting the VBF production mode has a sizeable contribution from gluon–gluon fusion events, it is referred to as the VBF+ggF analysis in the following. Constraining the cross-sections of the production modes to be as predicted by the SM, the combination measures the ratio of the branching fraction of the Higgs boson into b-quarks to the SM prediction. The only NP correlated across the six analyses is the $H \to b\bar{b}$ branching fraction that affects the SM prediction. A few other NPs are correlated across some of the analyses, following the studies conducted for the combinations of Run 1 results [19], of analyses of the $t\bar{t}H$ production mode [21], and of Run 2 results.

6.4.3. VH

A third combination is also performed combining the Run 2 VH, $H \to b\bar{b}$ result with other results in the VH production mode, but for the case of the Higgs boson decaying into two photons or via ZZ^* into four leptons.

The measurement of VH production in the $H \to \gamma\gamma$ channel, which uses five reconstruction-level categories to target leptonic decays of the vector boson, and two categories targeting hadronic decays of the vector boson, as described in Ref. [9], is updated using 79.8 fb^{-1} of data. Photons are reconstructed from calorimeter energy clusters formed using an enhanced dynamical, topological cell-clustering-based algorithm [49]. The signal yield is extracted in each category using a fit to the diphoton invariant mass distribution in the range 105–160 GeV. Contamination in these categories from non-VH Higgs boson production is constrained using separate categories designed to measure the $t\bar{t}H$ [21], VBF, and ggF production modes.

The measurement of VH production in the four-lepton final state, $H \to ZZ^* \to 4\ell$, where $\ell = e$ or μ, was performed with 36.1 fb^{-1} [10] and has now been extended to 79.8 fb^{-1}. The main enhancements are: improved electron reconstruction [49] and an additional event category targeting vector-boson decays that include missing transverse momentum due to the presence of one or two neutrinos in the final state. This results in three VH categories, targeting the hadronic decays of the vector boson, charged leptonic decays of the vector boson and decays of the vector boson containing one or more neutrinos.

The combination is undertaken as outlined in Ref. [116]. Constraining the branching fractions for the ZZ^*, diphoton and $b\bar{b}$ decays to be as predicted by the SM, this combination measures the signal strength of the VH production mode.

7. Results

7.1. Results of the SM Higgs boson search at $\sqrt{s} = 13$ TeV

Fig. 1 shows the BDT output distributions in the most sensitive, high-p_{T}^V, region. The background prediction in all post-fit distributions is obtained by normalising the backgrounds and setting the nuisance parameters according to the results of the signal extraction fit. The post-fit signal and background yields are shown in Table 10 for all signal regions.

For a Higgs boson mass of 125 GeV, when all lepton channels are combined, the probability p_0 of obtaining a signal at least as strong as the observation from background alone is $5.3 \cdot 10^{-7}$, whilst the expected value is $7.3 \cdot 10^{-6}$. The observation corresponds to an excess with a significance of 4.9 standard deviations, to be compared with an expectation of 4.3 standard deviations. The fitted value of the signal strength is:

$$\mu_{VH}^{bb} = 1.16^{+0.27}_{-0.25} = 1.16 \pm 0.16(\mathrm{stat.})^{+0.21}_{-0.19}(\mathrm{syst.}).$$

Fig. 2 shows the data, background and signal yields, where final-discriminant bins in all regions are combined into bins of $\log_{10}(S/B)$. Here, S and B are the fitted signal and background yields in each analysis bin, respectively.

Table 11 shows the signal strengths, p_0 and significance values from the combined fit with a single signal strength, and from a fit where the lepton channels each have their own signal strength. The probability that the signal strengths measured in the three lepton channels[5] are compatible is 80%.

[5] The probability of compatibility between fits differing only in their number of parameters of interest is evaluated in the asymptotics regime, where the difference

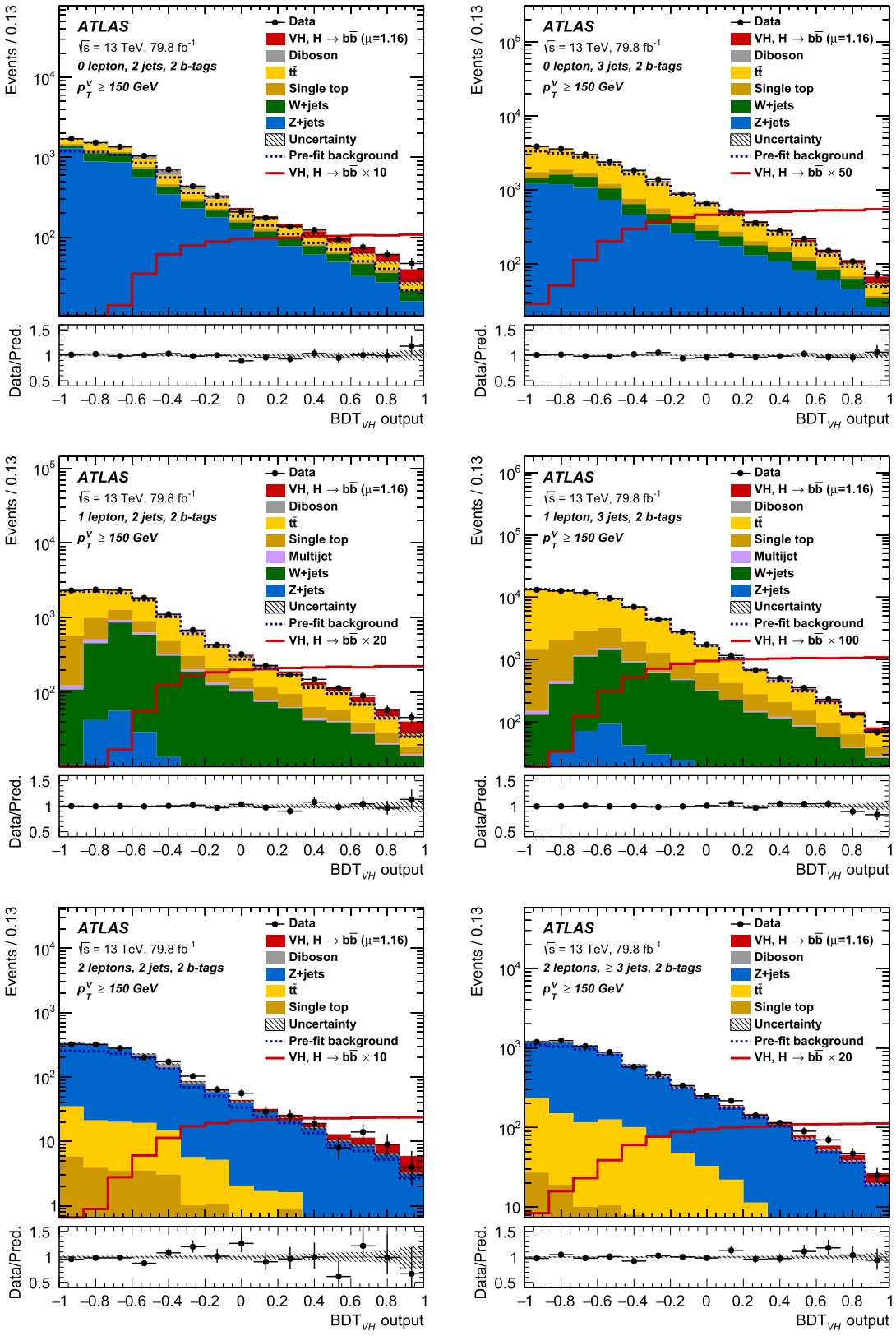

Fig. 1. The BDT_{VH} output post-fit distributions in the 0-lepton (top), 1-lepton (middle) and 2-lepton (bottom) channels for 2-b-tag events, in the 2-jet (left) and exactly 3-jet (or ≥ 3 jets for the 2-lepton case) (right) categories in the high-p_{T}^{V} region. The background contributions after the global likelihood fit are shown as filled histograms. The Higgs boson signal ($m_H = 125$ GeV) is shown as a filled histogram on top of the fitted backgrounds normalised to the signal yield extracted from data ($\mu = 1.16$), and unstacked as an unfilled histogram, scaled by the factor indicated in the legend. The dashed histogram shows the total pre-fit background. The size of the combined statistical and systematic uncertainty for the sum of the fitted signal and background is indicated by the hatched band. The ratio of the data to the sum of the fitted signal ($\mu = 1.16$) and background is shown in the lower panel. The BDT_{VH} output distributions are shown with the binning used in the global likelihood fit.

Table 10
The Higgs boson signal, background and data yields for each signal region category in each channel after the full selection of the multivariate analysis. The signal and background yields are normalised to the results of the global likelihood fit. All systematic uncertainties are included in the indicated uncertainties. An entry of "–" indicates that a specific background component is negligible in a certain region, or that no simulated events are left after the analysis selection.

Process	0-lepton		1-lepton		2-lepton			
	$p_{\mathrm{T}}^{V} > 150$ GeV, 2-b-tag		$p_{\mathrm{T}}^{V} > 150$ GeV, 2-b-tag		75 GeV $< p_{\mathrm{T}}^{V} <$ 150 GeV, 2-b-tag		$p_{\mathrm{T}}^{V} > 150$ GeV, 2-b-tag	
	2-jet	3-jet	2-jet	3-jet	2-jet	≥3-jet	2-jet	≥3-jet
$Z + ll$	17 ± 11	27 ± 18	2 ± 1	3 ± 2	14 ± 9	49 ± 32	4 ± 3	30 ± 19
$Z + cl$	45 ± 18	76 ± 30	3 ± 1	7 ± 3	43 ± 17	170 ± 67	12 ± 5	88 ± 35
$Z +$ HF	4770 ± 140	5940 ± 300	180 ± 9	348 ± 21	7400 ± 120	14160 ± 220	1421 ± 34	5370 ± 100
$W + ll$	20 ± 13	32 ± 22	31 ± 23	65 ± 48	< 1	< 1	< 1	< 1
$W + cl$	43 ± 20	83 ± 38	139 ± 67	250 ± 120	< 1	< 1	< 1	< 1
$W +$ HF	1000 ± 87	1990 ± 200	2660 ± 270	5400 ± 670	2 ± 0	13 ± 2	1 ± 0	4 ± 1
Single top quark	368 ± 53	1410 ± 210	2080 ± 290	9400 ± 1400	188 ± 89	440 ± 200	23 ± 7	93 ± 26
$t\bar{t}$	1333 ± 82	9150 ± 400	6600 ± 320	50200 ± 1400	3170 ± 100	8880 ± 220	104 ± 6	839 ± 40
Diboson	254 ± 49	318 ± 90	178 ± 47	330 ± 110	152 ± 32	355 ± 68	52 ± 11	196 ± 35
Multi-jet e sub-ch.	–	–	100 ± 100	41 ± 35	–	–	–	–
Multi-jet μ sub-ch.	–	–	138 ± 92	260 ± 270	–	–	–	–
Total bkg.	7850 ± 90	19020 ± 140	12110 ± 120	66230 ± 270	10960 ± 100	24070 ± 150	1620 ± 30	6620 ± 80
Signal (post-fit)	128 ± 28	128 ± 29	131 ± 30	125 ± 30	51 ± 11	86 ± 22	28 ± 6	67 ± 17
Data	8003	19143	12242	66348	11014	24197	1626	6686

Table 11
Measured signal strengths with their combined statistical and systematic uncertainties, expected and observed p_0 and significance values (in standard deviations) from the combined fit with a single signal strength, and from a combined fit where each of the lepton channels has its own signal strength, using 13 TeV data.

Signal strength	Signal strength	p_0		Significance	
		Exp.	Obs.	Exp.	Obs.
0-lepton	$1.04^{+0.34}_{-0.32}$	$9.5 \cdot 10^{-4}$	$5.1 \cdot 10^{-4}$	3.1	3.3
1-lepton	$1.09^{+0.46}_{-0.42}$	$8.7 \cdot 10^{-3}$	$4.9 \cdot 10^{-3}$	2.4	2.6
2-lepton	$1.38^{+0.46}_{-0.42}$	$4.0 \cdot 10^{-3}$	$3.3 \cdot 10^{-4}$	2.6	3.4
VH, $H \to b\bar{b}$ combination	$1.16^{+0.27}_{-0.25}$	$7.3 \cdot 10^{-6}$	$5.3 \cdot 10^{-7}$	4.3	4.9

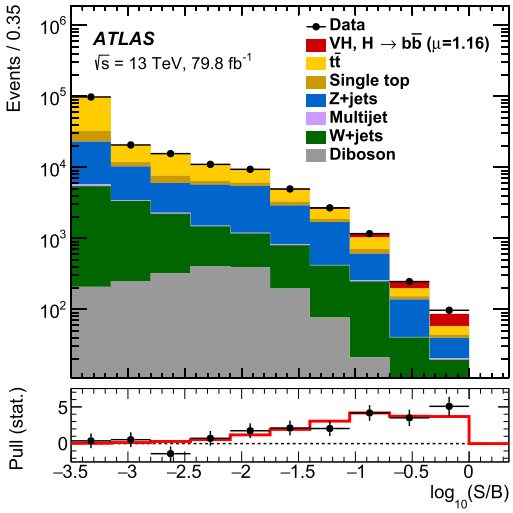

Fig. 2. Event yields as a function of $\log_{10}(S/B)$ for data, background and a Higgs boson signal with $m_H = 125$ GeV. Final-discriminant bins in all regions are combined into bins of $\log_{10}(S/B)$, with S being the fitted signal and B the fitted background yields. The Higgs boson signal contribution is shown after rescaling the SM cross-section according to the value of the signal strength extracted from data ($\mu = 1.16$). In the lower panel, the pull of the data relative to the background (the statistical significance of the difference between data and fitted background) is shown with statistical uncertainties only. The full line indicates the pull expected from the sum of fitted signal and background relative to the fitted background.

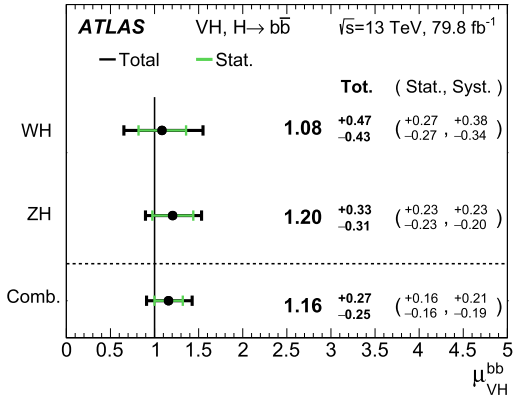

Fig. 3. The fitted values of the Higgs boson signal strength μ_{VH}^{bb} for $m_H = 125$ GeV for the WH and ZH processes and their combination. The individual μ_{VH}^{bb} values for the $(W/Z)H$ processes are obtained from a simultaneous fit with the signal strength for each of the WH and ZH processes floating independently. The probability of compatibility of the individual signal strengths is 84%.

A combined fit is also performed with floating signal strengths separately for the WH and ZH production processes. The results of this fit are shown in Fig. 3. The WH and ZH production modes

between their maximum likelihoods follows a χ^2 distribution with a number of degrees of freedom equal to the difference between the numbers of parameters of interest.

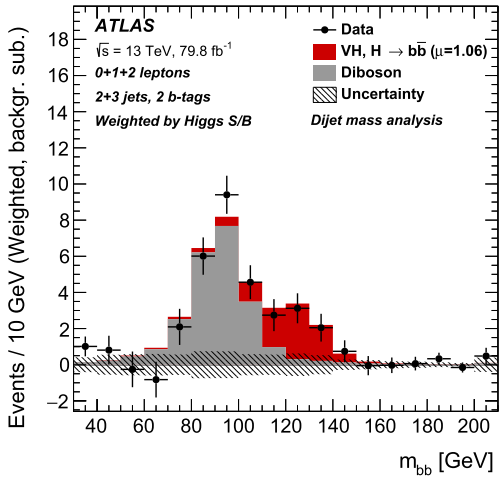

Fig. 4. The distribution of m_{bb} in data after subtraction of all backgrounds except for the WZ and ZZ diboson processes, as obtained with the dijet-mass analysis. The contributions from all lepton channels, p_{T}^{V} regions and number-of-jets categories are summed and weighted by their respective S/B, with S being the total fitted signal and B the total fitted background in each region. The expected contribution of the associated WH and ZH production of a SM Higgs boson with $m_H = 125$ GeV is shown scaled by the measured signal strength ($\mu = 1.06$). The size of the combined statistical and systematic uncertainty for the fitted background is indicated by the hatched band.

have observed (expected) significances of 2.5 (2.3) and 4.0 (3.5) standard deviations, respectively, with a linear correlation between the two signal strengths of −1%.

7.2. Results of the dijet-mass analysis

For all channels combined the fitted value of the signal strength is

$$\mu_{VH}^{bb} = 1.06^{+0.36}_{-0.33} = 1.06 \pm 0.20(\mathrm{stat.})^{+0.30}_{-0.26}(\mathrm{syst.}),$$

in good agreement with the result of the multivariate analysis. The observed excess has a significance of 3.6 standard deviations, compared to an expectation of 3.5 standard deviations. Good agreement is also found when comparing the values of signal strengths in the individual channels from the dijet-mass analysis with those from the multivariate analysis.

The m_{bb} distribution is shown in Fig. 4 summed over all channels and regions, weighted by their respective values of the ratio of fitted Higgs boson signal and background yields and after subtraction of all backgrounds except for the WZ and ZZ diboson processes.

7.3. Results of the diboson analysis

As a validation of the Higgs boson search analysis, the measurement of VZ production based on the multivariate analysis described in Section 6.3 returns a value of signal strength

$$\mu_{VZ}^{bb} = 1.20^{+0.20}_{-0.18} = 1.20 \pm 0.08(\mathrm{stat.})^{+0.19}_{-0.16}(\mathrm{syst.}),$$

in good agreement with the Standard Model prediction. Analogously to the VH signal, fits are also performed with separate signal strengths for the WZ and ZZ production modes, and the results are shown in Fig. 5.

7.4. Results of combinations

7.4.1. Run 1 and Run 2 combination for VH, $H \to b\bar{b}$

The result of the Run 2 analysis is combined with the Run 1 VH, $H \to b\bar{b}$ result following the methodology described in Section 6.4. The observed p_0 value is $5.5 \cdot 10^{-7}$, corresponding to an excess with a significance of 4.9 standard deviations, compared with an expectation of 5.1 standard deviations. The measured signal strength is:

$$\mu_{VH}^{bb} = 0.98^{+0.22}_{-0.21} = 0.98 \pm 0.14(\mathrm{stat.})^{+0.17}_{-0.16}(\mathrm{syst.}).$$

Fits are also performed with the signal strengths floated independently for the WH and ZH production processes. The probability of compatibility of the signal strengths for the WH and ZH production processes is 72%, and the results of this fit are shown in Fig. 6.

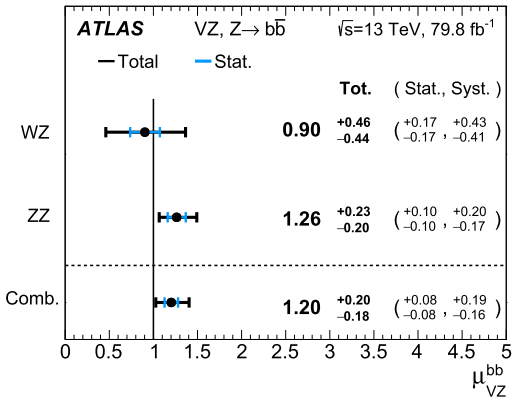

Fig. 5. The fitted values of the VZ signal strength μ_{VZ}^{bb} for the WZ and ZZ processes and their combination. The individual μ_{VZ}^{bb} values for the $(W/Z)Z$ processes are obtained from a simultaneous fit with the signal strengths for each of the WZ and ZZ processes floating independently. The probability of compatibility of the individual signal strengths is 47%.

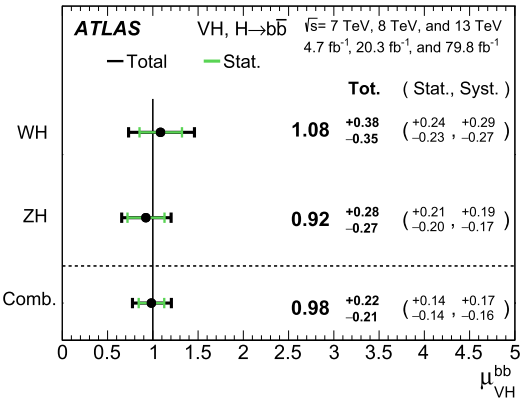

Fig. 6. The fitted values of the Higgs boson signal strength μ_{VH}^{bb} for $m_H = 125$ GeV for the WH and ZH processes and their combination, using the 7 TeV, 8 TeV and 13 TeV data. The individual μ_{VH}^{bb} values for the $(W/Z)H$ processes are obtained from a simultaneous fit with the signal strengths for each of the WH and ZH processes floating independently.

7.4.2. Observation of $H \to b\bar{b}$ decays

The VH result is further combined with results of the searches for the Standard Model Higgs boson decaying into a $b\bar{b}$ pair produced in association with a $t\bar{t}$ pair and in vector-boson fusion for both Run 1 and Run 2, to perform a search for the $H \to b\bar{b}$ decay. For a Higgs boson mass of 125 GeV, and assuming the relative production cross-sections are those predicted by the SM, the observed significance for the $H \to b\bar{b}$ decay is 5.4 standard deviations, to be compared with an expectation of 5.5 standard deviations. With the additional assumption that the production cross-sections are those

Table 12
Expected and observed significance values (in standard deviations) for the $H \to b\bar{b}$ channels fitted independently and their combination using the 7 TeV, 8 TeV and 13 TeV data.

Channel	Significance	
	Exp.	Obs.
VBF+ggF	0.9	1.5
$t\bar{t}H$	1.9	1.9
VH	5.1	4.9
$H \to b\bar{b}$ combination	5.5	5.4

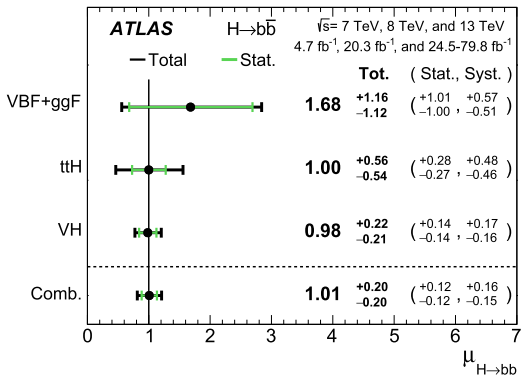

Fig. 7. The fitted values of the Higgs boson signal strength $\mu_{H\to bb}$ for $m_H = 125$ GeV separately for the VH, $t\bar{t}H$ and VBF+ggF analyses along with their combination, using the 7 TeV, 8 TeV and 13 TeV data. The individual $\mu_{H\to bb}$ values for the different production modes are obtained from a simultaneous fit with the signal strengths for each of the processes floating independently. The probability of compatibility of the individual signal strengths is 83%.

predicted by the SM, the fitted value for all channels combined of the signal strength of the branching fraction into b-quark pairs is

$$\mu_{H\to bb} = 1.01 \pm 0.20 = 1.01 \pm 0.12(\text{stat.})^{+0.16}_{-0.15}(\text{syst.}).$$

Table 12 shows the significance values independently for the VBF+ggF, $t\bar{t}H$ and VH channels in the combination of the Run 1 and Run 2 data, and for the combined global likelihood fit. The signal strengths obtained from a fit where individual signal strengths are fitted simultaneously for the three production modes are displayed in Fig. 7. Fits are also performed with the signal strengths floated independently for each of the production processes in both Run 1 and Run 2. The probability of compatibility of the six individual measurements is 54%.

7.4.3. Observation of VH production

The Run 2 VH, $H \to b\bar{b}$ result is further combined with the results of other Run 2 searches for the Higgs boson produced in the VH production mode, but decaying into either two photons or four leptons via ZZ^* decays. For a Higgs boson mass of 125 GeV, and assuming the relative branching fractions of the three decay modes considered to be as predicted by the SM, the observed significance for VH production is 5.3 standard deviations, to be compared with an expectation of 4.8 standard deviations. Table 13 shows the significance values for the combined global likelihood fit, and for a fit where the four-lepton ($H \to ZZ^* \to 4\ell$), diphoton ($H \to \gamma\gamma$) and $H \to b\bar{b}$ decay modes each have their own signal strength for the Run 2 data. Assuming the branching fractions are as predicted by the SM, the fitted value of the VH signal strength for all channels combined is:

$$\mu_{VH} = 1.13^{+0.24}_{-0.23} = 1.13 \pm 0.15(\text{stat.})^{+0.18}_{-0.17}(\text{syst.}).$$

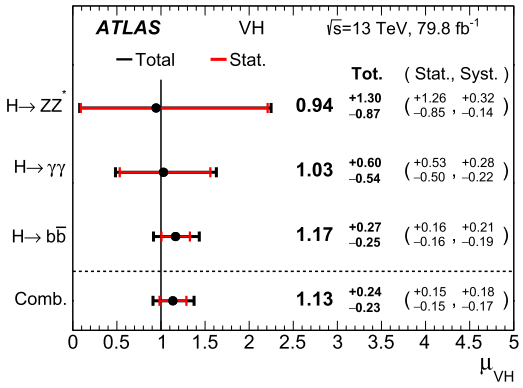

Fig. 8. The fitted values of the Higgs boson signal strength μ_{VH} for $m_H = 125$ GeV separately for the $H \to b\bar{b}$, $H \to \gamma\gamma$ and $H \to ZZ^* \to 4\ell$ decay modes, along with their combination. The individual μ_{VH} values for the different decay modes are obtained from a simultaneous fit with the signal strengths for each of the processes floating independently. The probability of compatibility of the individual signal strengths is 96%.

Table 13
Expected and observed significance values (in standard deviations) for the VH production channels from the combined fit and from a combined fit where each of the lepton channels has its own signal strength, using 13 TeV data.

Channel	Significance	
	Exp.	Obs.
$H \to ZZ^* \to 4\ell$	1.1	1.1
$H \to \gamma\gamma$	1.9	1.9
$H \to b\bar{b}$	4.3	4.9
VH combined	4.8	5.3

The signal strengths obtained from the fit where individual signal strengths are fitted for the three decay modes are displayed in Fig. 8, along with their combination.

8. Conclusion

A search for the Standard Model Higgs boson decaying into a $b\bar{b}$ pair and produced in association with a W or Z boson is presented, using data collected by the ATLAS experiment in proton–proton collisions from Run 2 of the LHC. The data correspond to an integrated luminosity of 79.8 fb^{-1} collected at a centre-of-mass energy of $\sqrt{s}$ =13 TeV. An excess over the expected background is observed, with a significance of 4.9 standard deviations compared with an expectation of 4.3. The measured signal strength relative to the SM prediction for $m_H = 125$ GeV is found to be $\mu^{bb}_{VH} = 1.16 \pm 0.16(\text{stat.})^{+0.21}_{-0.19}(\text{syst.})$.

This result is combined with previous results based on all the Run 1 data collected at centre-of-mass energies of 7 TeV and 8 TeV. An excess over the expected SM background is observed, with a significance of 4.9 standard deviations compared with an expectation of 5.1. The measured signal strength relative to the SM expectation is found to be $\mu^{bb}_{VH} = 0.98 \pm 0.14(\text{stat.})^{+0.17}_{-0.16}(\text{syst.})$.

Results for the SM Higgs boson decaying into a $b\bar{b}$ pair in the VH, $t\bar{t}H$ and VBF+ggF production modes at centre-of-mass energies of 7 TeV, 8 TeV and 13 TeV are also combined, assuming the relative production cross-sections of these processes to be as predicted by the SM. An excess over the expected SM background is observed, with a significance of 5.4 standard deviations compared with an expectation of 5.5, providing an observation of the $H \to b\bar{b}$ decay mode. Assuming the SM production strengths, the measured signal strength relative to the SM expectation is

$\mu_{H\to bb} = 1.01 \pm 0.12(\text{stat.})^{+0.16}_{-0.15}(\text{syst.})$, consistent with the value of the Yukawa coupling to bottom quarks in the SM.

In addition, the Run 2 VH, $H \to b\bar{b}$ result is further combined with the results of other Run 2 searches for the Higgs boson decaying into either four leptons (via ZZ^*) or diphotons in the VH production mode, assuming the relative branching fractions of the three decay modes to be as predicted by the SM. The result is an observed significance of 5.3 standard deviations, to be compared with an expectation of 4.8 standard deviations. Assuming the SM branching fractions, the measured signal strength relative to the SM expectation is $\mu_{VH} = 1.13 \pm 0.15(\text{stat.})^{+0.18}_{-0.17}(\text{syst.})$. This provides a direct observation of the Higgs boson being produced in association with a vector boson.

Acknowledgements

We thank CERN for the very successful operation of the LHC, as well as the support staff from our institutions without whom ATLAS could not be operated efficiently.

We acknowledge the support of ANPCyT, Argentina; YerPhI, Armenia; ARC, Australia; BMWFW and FWF, Austria; ANAS, Azerbaijan; SSTC, Belarus; CNPq and FAPESP, Brazil; NSERC, NRC and CFI, Canada; CERN; CONICYT, Chile; CAS, MOST and NSFC, China; COLCIENCIAS, Colombia; MSMT CR, MPO CR and VSC CR, Czech Republic; DNRF and DNSRC, Denmark; IN2P3-CNRS, CEA-DRF/IRFU, France; SRNSFG, Georgia; BMBF, HGF, and MPG, Germany; GSRT, Greece; RGC, Hong Kong SAR, China; ISF, I-CORE and Benoziyo Center, Israel; INFN, Italy; MEXT and JSPS, Japan; CNRST, Morocco; NWO, Netherlands; RCN, Norway; MNiSW and NCN, Poland; FCT, Portugal; MNE/IFA, Romania; MES of Russia and NRC KI, Russian Federation; JINR; MESTD, Serbia; MSSR, Slovakia; ARRS and MIZŠ, Slovenia; DST/NRF, South Africa; MINECO, Spain; SRC and Wallenberg Foundation, Sweden; SERI, SNSF and Cantons of Bern and Geneva, Switzerland; MOST, Taiwan; TAEK, Turkey; STFC, United Kingdom; DOE and NSF, United States of America. In addition, individual groups and members have received support from BCKDF, the Canada Council, CANARIE, CRC, Compute Canada, FQRNT, and the Ontario Innovation Trust, Canada; EPLANET, ERC, ERDF, FP7, Horizon 2020 and Marie Skłodowska-Curie Actions, European Union; Investissements d'Avenir Labex and Idex, ANR, Région Auvergne and Fondation Partager le Savoir, France; DFG and AvH Foundation, Germany; Herakleitos, Thales and Aristeia programmes co-financed by EU-ESF and the Greek NSRF; BSF, GIF and Minerva, Israel; BRF, Norway; CERCA Programme Generalitat de Catalunya, Generalitat Valenciana, Spain; the Royal Society and Leverhulme Trust, United Kingdom.

The crucial computing support from all WLCG partners is acknowledged gratefully, in particular from CERN, the ATLAS Tier-1 facilities at TRIUMF (Canada), NDGF (Denmark, Norway, Sweden), CC-IN2P3 (France), KIT/GridKA (Germany), INFN-CNAF (Italy), NL-T1 (Netherlands), PIC (Spain), ASGC (Taiwan), RAL (UK) and BNL (USA), the Tier-2 facilities worldwide and large non-WLCG resource providers. Major contributors of computing resources are listed in Ref. [117].

References

[1] F. Englert, R. Brout, Broken symmetry and the mass of gauge vector mesons, Phys. Rev. Lett. 13 (1964) 321.
[2] P.W. Higgs, Broken symmetries, massless particles and gauge fields, Phys. Lett. 12 (1964) 132.
[3] P.W. Higgs, Broken symmetries and the masses of gauge bosons, Phys. Rev. Lett. 13 (1964) 508.
[4] G. Guralnik, C. Hagen, T. Kibble, Global conservation laws and massless particles, Phys. Rev. Lett. 13 (1964) 585.
[5] ATLAS Collaboration, Observation of a new particle in the search for the Standard Model Higgs boson with the ATLAS detector at the LHC, Phys. Lett. B 716 (2012) 1, arXiv:1207.7214 [hep-ex].
[6] CMS Collaboration, Observation of a new boson at a mass of 125 GeV with the CMS experiment at the LHC, Phys. Lett. B 716 (2012) 30, arXiv:1207.7235 [hep-ex].
[7] L. Evans, P. Bryant, LHC machine, J. Instrum. 3 (2008) S08001.
[8] ATLAS, CMS Collaborations, Combined measurement of the Higgs boson mass in pp collisions at $\sqrt{s} = 7$ and 8 TeV with the ATLAS and CMS experiments, Phys. Rev. Lett. 114 (2015) 191803, arXiv:1503.07589 [hep-ex].
[9] ATLAS Collaboration, Measurements of Higgs boson properties in the diphoton decay channel with 36 fb^{-1} of pp collision data at $\sqrt{s} = 13$ TeV with the ATLAS detector, arXiv:1802.04146 [hep-ex], 2018.
[10] ATLAS Collaboration, Measurement of the Higgs boson coupling properties in the $H \to ZZ^* \to 4\ell$ decay channel at $\sqrt{s} = 13$ TeV with the ATLAS detector, J. High Energy Phys. 03 (2018) 095, arXiv:1712.02304 [hep-ex].
[11] ATLAS Collaboration, Measurement of inclusive and differential cross sections in the $H \to ZZ^* \to 4\ell$ decay channel in pp collisions at $\sqrt{s} = 13$ TeV with the ATLAS detector, J. High Energy Phys. 10 (2017) 132, arXiv:1708.02810 [hep-ex].
[12] CMS Collaboration, Measurement of inclusive and differential Higgs boson production cross sections in the diphoton decay channel in proton–proton collisions at $\sqrt{s} = 13$ TeV, CERN-EP-2018-166, arXiv:1807.03825 [hep-ex], 2018.
[13] CMS Collaboration, Measurements of Higgs boson properties in the diphoton decay channel in proton–proton collisions at $\sqrt{s} = 13$ TeV, CERN-EP-2018-060, arXiv:1804.02716, 2018.
[14] CMS Collaboration, Measurements of properties of the Higgs boson decaying into the four-lepton final state in pp collisions at $\sqrt{s} = 13$ TeV, J. High Energy Phys. 11 (2017) 047, arXiv:1706.09936 [hep-ex].
[15] ATLAS Collaboration, Measurement of the Higgs boson mass in the $H \to ZZ^* \to 4\ell$ and $H \to \gamma\gamma$ channels with $\sqrt{s} = 13$ TeV pp collisions using the ATLAS detector, arXiv:1806.00242 [hep-ex], 2018.
[16] ATLAS Collaboration, Combined measurement of differential and total cross sections in the $H \to \gamma\gamma$ and the $H \to ZZ^* \to 4\ell$ decay channels at $\sqrt{s} = 13$ TeV with the ATLAS detector, CERN-EP-2018-080, arXiv:1805.10197 [hep-ex], 2018.
[17] ATLAS Collaboration, Measurements of gluon–gluon fusion and vector-boson fusion Higgs boson production cross-sections in the $H \to WW^* \to e\nu\mu\nu$ decay channel in pp collisions at $\sqrt{s} = 13$ TeV with the ATLAS detector, arXiv:1808.09054 [hep-ex], 2018, CERN-EP-2018-212.
[18] CMS Collaboration, Measurements of properties of the Higgs boson decaying to a W boson pair in pp collisions at $\sqrt{s} = 13$ TeV, CERN-EP-2018-141, arXiv:1806.05246 [hep-ex], 2018.
[19] ATLAS, CMS Collaborations, Measurements of the Higgs boson production and decay rates and constraints on its couplings from a combined ATLAS and CMS analysis of the LHC pp collision data at $\sqrt{s} = 7$ and 8 TeV, J. High Energy Phys. 08 (2016) 045, arXiv:1606.02266 [hep-ex].
[20] CMS Collaboration, Observation of the Higgs boson decay to a pair of τ leptons, Phys. Lett. B 779 (2018) 283, arXiv:1708.00373 [hep-ex].
[21] ATLAS Collaboration, Observation of Higgs boson production in association with a top quark pair at the LHC with the ATLAS detector, arXiv:1806.00425 [hep-ex], 2018.
[22] CMS Collaboration, Observation of $t\bar{t}H$ production, Phys. Rev. Lett. 120 (2018) 231801, arXiv:1804.02610 [hep-ex].
[23] A. Djouadi, J. Kalinowski, M. Spira, HDECAY: a program for Higgs boson decays in the Standard Model and its supersymmetric extension, Comput. Phys. Commun. 108 (1998) 56, arXiv:hep-ph/9704448 [hep-ph].
[24] S. Glashow, D.V. Nanopoulos, A. Yildiz, Associated production of Higgs bosons and Z particles, Phys. Rev. D 18 (1978) 1724.
[25] R. Lafaye, et al., Measuring the Higgs sector, J. High Energy Phys. 08 (2009) 009, arXiv:0904.3866 [hep-ph].
[26] LHC Higgs Cross Section Working Group, in: Handbook of LHC Higgs Cross Sections: 3. Higgs Properties, 2013, CERN-2013-004, arXiv:1307.1347 [hep-ph].
[27] J. Ellis, V. Sanz, T. You, Complete Higgs sector constraints on dimension-6 operators, J. High Energy Phys. 07 (2014) 036, arXiv:1404.3667 [hep-ph].
[28] CDF, D0 Collaborations, Evidence for a particle produced in association with weak bosons and decaying to a bottom-antibottom quark pair in Higgs boson searches at the tevatron, Phys. Rev. Lett. 109 (2012) 071804, arXiv:1207.6436 [hep-ex].
[29] CMS Collaboration, Search for the Standard Model Higgs boson produced in association with a W or a Z boson and decaying to bottom quarks, Phys. Rev. D 89 (2014) 012003, arXiv:1310.3687 [hep-ex].
[30] ATLAS Collaboration, Search for the $b\bar{b}$ decay of the Standard Model Higgs boson in associated $(W/Z)H$ production with the ATLAS detector, J. High Energy Phys. 01 (2015) 069, arXiv:1409.6212 [hep-ex].
[31] CMS Collaboration, Observation of Higgs boson decay to bottom quarks, Phys. Rev. Lett. 121 (2018) 121801, arXiv:1808.08242 [hep-ex].
[32] ATLAS Collaboration, Evidence for the $H \to b\bar{b}$ decay with the ATLAS detector, J. High Energy Phys. 12 (2017) 024, arXiv:1708.03299 [hep-ex].
[33] CMS Collaboration, Evidence for the Higgs boson decay to a bottom quark–antiquark pair, Phys. Lett. B 780 (2018) 501, arXiv:1709.07497 [hep-ex].

[34] ATLAS Collaboration, Search for the Standard Model Higgs boson produced by vector-boson fusion and decaying to bottom quarks in $\sqrt{s} = 8$ TeV pp collisions with the ATLAS detector, J. High Energy Phys. 11 (2016) 112, arXiv:1606.02181 [hep-ex].

[35] CMS Collaboration, Search for the Standard Model Higgs boson produced through vector boson fusion and decaying to $b\bar{b}$, Phys. Rev. D 92 (2015) 032008, arXiv:1506.01010 [hep-ex].

[36] ATLAS Collaboration, Search for Higgs bosons produced via vector-boson fusion and decaying into bottom quark pairs in $\sqrt{s} = 13$ TeV pp collisions with the ATLAS detector, arXiv:1807.08639 [hep-ex], 2018.

[37] ATLAS Collaboration, Search for the Standard Model Higgs boson produced in association with top quarks and decaying into $b\bar{b}$ in pp collisions at $\sqrt{s} = 8$ TeV with the ATLAS detector, Eur. Phys. J. C 75 (2015) 349, arXiv:1503.05066 [hep-ex].

[38] ATLAS Collaboration, Search for the Standard Model Higgs boson decaying into $b\bar{b}$ produced in association with top quarks decaying hadronically in pp collisions at $\sqrt{s} = 8$ TeV with the ATLAS detector, J. High Energy Phys. 05 (2016) 160, arXiv:1604.03812 [hep-ex].

[39] ATLAS Collaboration, Search for the Standard Model Higgs boson produced in association with top quarks and decaying into a $b\bar{b}$ pair in pp collisions at $\sqrt{s} = 13$ TeV with the ATLAS detector, Phys. Rev. D 97 (2018) 072016, arXiv:1712.08895 [hep-ex].

[40] CMS Collaboration, Search for a Standard Model Higgs boson produced in association with a top-quark pair and decaying to bottom quarks using a matrix element method, Eur. Phys. J. C 75 (2015) 251, arXiv:1502.02485 [hep-ex].

[41] CMS Collaboration, Search for $t\bar{t}H$ production in the $H \to b\bar{b}$ decay channel with leptonic $t\bar{t}$ decays in proton–proton collisions at $\sqrt{s} = 13$ TeV, arXiv:1804.03682 [hep-ex], 2018.

[42] CMS Collaboration, Search for $t\bar{t}H$ production in the all-jet final state in proton–proton collisions at $\sqrt{s} = 13$ TeV, J. High Energy Phys. 06 (2018) 101, arXiv:1803.06986 [hep-ex].

[43] CMS Collaboration, Inclusive search for a highly boosted Higgs boson decaying to a bottom quark–antiquark pair, Phys. Rev. Lett. 120 (2018) 071802, arXiv:1709.05543 [hep-ex].

[44] ATLAS Collaboration, The ATLAS experiment at the CERN large hadron collider, J. Instrum. 3 (2008) S08003.

[45] ATLAS Collaboration, ATLAS Insertable B-Layer Technical Design Report, ATLAS-TDR-19, https://cds.cern.ch/record/1291633, 2010;
ATLAS Collaboration, ATLAS Insertable B-Layer Technical Design Report Addendum, ATLAS-TDR-19-ADD-1, https://cds.cern.ch/record/1451888, 2012.

[46] ATLAS IBL Collaboration, Production and integration of the ATLAS insertable B-layer, J. Instrum. 13 (2018) T05008, arXiv:1803.00844 [physics.ins-det].

[47] ATLAS Collaboration, Performance of the ATLAS trigger system in 2015, Eur. Phys. J. C 77 (2017) 317, arXiv:1611.09661 [hep-ex].

[48] ATLAS Collaboration, Reconstruction of primary vertices at the ATLAS experiment in Run 1 proton–proton collisions at the LHC, Eur. Phys. J. C 77 (2017) 332, arXiv:1611.10235 [physics.ins-det].

[49] ATLAS Collaboration, Electron and photon reconstruction and performance in ATLAS using a dynamical, topological cell clustering-based approach, ATL-PHYS-PUB-2017-022, https://cds.cern.ch/record/2298955, 2017.

[50] ATLAS Collaboration, Electron efficiency measurements with the ATLAS detector using the 2015 LHC proton–proton collision data, ATLAS-CONF-2016-024, https://cds.cern.ch/record/2157687, 2016.

[51] ATLAS Collaboration, Electron efficiency measurements with the ATLAS detector using 2012 LHC proton–proton collision data, Eur. Phys. J. C 77 (2017) 195, arXiv:1612.01456 [hep-ex].

[52] ATLAS Collaboration, Muon reconstruction performance of the ATLAS detector in proton–proton collision data at $\sqrt{s} = 13$ TeV, Eur. Phys. J. C 76 (2016) 292, arXiv:1603.05598 [hep-ex].

[53] ATLAS Collaboration, Reconstruction of hadronic decay products of tau leptons with the ATLAS experiment, Eur. Phys. J. C 76 (2016) 295, arXiv:1512.05955 [hep-ex].

[54] ATLAS Collaboration, Measurement of the tau lepton reconstruction and identification performance in the ATLAS experiment using pp collisions at $\sqrt{s} = 13$ TeV, ATLAS-CONF-2017-029, https://cds.cern.ch/record/2261772, 2017.

[55] W. Lampl, et al., Calorimeter clustering algorithms: description and performance, ATL-LARG-PUB-2008-002, https://cds.cern.ch/record/1099735, 2008.

[56] M. Cacciari, G.P. Salam, G. Soyez, The anti-k_t jet clustering algorithm, J. High Energy Phys. 04 (2008) 063, arXiv:0802.1189 [hep-ph].

[57] ATLAS Collaboration, Performance of pile-up mitigation techniques for jets in pp collisions at $\sqrt{s} = 8$ TeV using the ATLAS detector, Eur. Phys. J. C 76 (2016) 581, arXiv:1510.03823 [hep-ex].

[58] ATLAS Collaboration, Selection of jets produced in 13 TeV proton–proton collisions with the ATLAS detector, ATLAS-CONF-2015-029, https://cds.cern.ch/record/2037702, 2015.

[59] ATLAS Collaboration, Optimisation and performance studies of the ATLAS b-tagging algorithms for the 2017–18 LHC run, ATL-PHYS-PUB-2017-013, https://cds.cern.ch/record/2273281, 2017.

[60] ATLAS Collaboration, Jet energy scale measurements and their systematic uncertainties in proton–proton collisions at $\sqrt{s} = 13$ TeV with the ATLAS detector, Phys. Rev. D 96 (2017) 072002, arXiv:1703.09665 [hep-ex].

[61] ATLAS Collaboration, Performance of missing transverse momentum reconstruction with the ATLAS detector using proton–proton collisions at $\sqrt{s} = 13$ TeV, arXiv:1802.08168 [hep-ex], 2018.

[62] J.M. Butterworth, A.R. Davison, M. Rubin, G.P. Salam, Jet substructure as a new Higgs search channel at the LHC, Phys. Rev. Lett. 100 (2008) 242001, arXiv:0802.2470 [hep-ph].

[63] ATLAS Collaboration, ATLAS sensitivity to the Standard Model Higgs in the HW and HZ channels at high transverse momenta, ATL-PHYS-PUB-2009-088, https://cds.cern.ch/record/1201444, 2009.

[64] ATLAS Collaboration, Luminosity determination in pp collisions at $\sqrt{s} = 8$ TeV using the ATLAS detector at the LHC, Eur. Phys. J. C 76 (2016) 653, arXiv:1608.03953 [hep-ex].

[65] ATLAS Collaboration, The new LUCID-2 detector for luminosity measurement and monitoring in ATLAS, J. Instrum. 13 (2018) P07017.

[66] ATLAS Collaboration, The ATLAS simulation infrastructure, Eur. Phys. J. C 70 (2010) 823, arXiv:1005.4568 [physics.ins-det].

[67] S. Agostinelli, et al., GEANT4: a simulation toolkit, Nucl. Instrum. Methods A 506 (2003) 250.

[68] T. Sjöstrand, S. Mrenna, P.Z. Skands, A brief introduction to PYTHIA 8.1, Comput. Phys. Commun. 178 (2008) 852, arXiv:0710.3820 [hep-ph].

[69] ATLAS Collaboration, Summary of ATLAS Pythia 8 tunes, ATL-PHYS-PUB-2012-003, https://cds.cern.ch/record/1474107, 2012.

[70] A. Martin, W. Stirling, R. Thorne, G. Watt, Parton distributions for the LHC, Eur. Phys. J. C 63 (2009) 189, arXiv:0901.0002 [hep-ph].

[71] T. Gleisberg, et al., Event generation with SHERPA 1.1, J. High Energy Phys. 02 (2009) 007, arXiv:0811.4622 [hep-ph].

[72] D. Lange, The EvtGen particle decay simulation package, Nucl. Instrum. Methods A 462 (2001) 152.

[73] J. Butterworth, et al., PDF4LHC recommendations for LHC Run II, J. Phys. G 43 (2016) 023001, arXiv:1510.03865 [hep-ph].

[74] A. Denner, S. Dittmaier, S. Kallweit, A. Mück, Electroweak corrections to Higgs–Strahlung off W/Z bosons at the tevatron and the LHC with hawk, J. High Energy Phys. 03 (2012) 075, arXiv:1112.5142 [hep-ph].

[75] A. Denner, S. Dittmaier, S. Kallweit, A. Mück, HAWK 2.0: a Monte Carlo program for Higgs production in vector-boson fusion and Higgs Strahlung at hadron colliders, Comput. Phys. Commun. 195 (2015) 161, arXiv:1412.5390 [hep-ph].

[76] S. Alioli, P. Nason, C. Oleari, E. Re, A general framework for implementing NLO calculations in shower Monte Carlo programs: the POWHEG BOX, J. High Energy Phys. 06 (2010) 043, arXiv:1002.2581 [hep-ph].

[77] R.D. Ball, et al., Parton distributions for the LHC Run II, J. High Energy Phys. 04 (2015) 040, arXiv:1410.8849 [hep-ph].

[78] ATLAS Collaboration, Measurement of the Z/γ^* boson transverse momentum distribution in pp collisions at $\sqrt{s} = 7$ TeV with the ATLAS detector, J. High Energy Phys. 09 (2014) 145, arXiv:1406.3660 [hep-ex].

[79] G. Cullen, et al., Automated one-loop calculations with GoSam, Eur. Phys. J. C 72 (2012) 1889, arXiv:1111.2034 [hep-ph].

[80] K. Hamilton, P. Nason, G. Zanderighi, MINLO: multi-scale improved NLO, J. High Energy Phys. 10 (2012) 155, arXiv:1206.3572 [hep-ph].

[81] G. Luisoni, P. Nason, C. Oleari, F. Tramontano, $HW^{\pm}/HZ + 0$ and 1 jet at NLO with the POWHEG BOX interfaced to GoSam and their merging within MiNLO, J. High Energy Phys. 10 (2013) 083, arXiv:1306.2542 [hep-ph].

[82] M. Ciccolini, S. Dittmaier, M. Krämer, Electroweak radiative corrections to associated WH and ZH production at hadron colliders, Phys. Rev. D 68 (2003) 073003, arXiv:hep-ph/0306234 [hep-ph].

[83] O. Brein, A. Djouadi, R. Harlander, NNLO QCD corrections to the Higgs–Strahlung processes at hadron colliders, Phys. Lett. B 579 (2004) 149, arXiv:hep-ph/0307206 [hep-ph].

[84] G. Ferrera, M. Grazzini, F. Tramontano, Associated WH production at hadron colliders: a fully exclusive QCD calculation at NNLO, Phys. Rev. Lett. 107 (2011) 152003, arXiv:1107.1164 [hep-ph].

[85] O. Brein, R. Harlander, M. Wiesemann, T. Zirke, Top-quark mediated effects in hadronic Higgs–Strahlung, Eur. Phys. J. C 72 (2012) 1868, arXiv:1111.0761 [hep-ph].

[86] G. Ferrera, M. Grazzini, F. Tramontano, Higher-order QCD effects for associated WH production and decay at the LHC, J. High Energy Phys. 04 (2014) 039, arXiv:1312.1669 [hep-ph].

[87] G. Ferrera, M. Grazzini, F. Tramontano, Associated ZH production at hadron colliders: the fully differential NNLO QCD calculation, Phys. Lett. B 740 (2015) 51, arXiv:1407.4747 [hep-ph].

[88] J.M. Campbell, R.K. Ellis, C. Williams, Associated production of a Higgs boson at NNLO, J. High Energy Phys. 06 (2016) 179, arXiv:1601.00658 [hep-ph].

[89] L. Altenkamp, S. Dittmaier, R.V. Harlander, H. Rzehak, T.J.E. Zirke, Gluon-induced Higgs–Strahlung at next-to-leading order QCD, J. High Energy Phys. 02 (2013) 078, arXiv:1211.5015 [hep-ph].

[90] B. Hespel, F. Maltoni, E. Vryonidou, Higgs and Z boson associated production via gluon fusion in the SM and the 2HDM, J. High Energy Phys. 06 (2015) 065, arXiv:1503.01656 [hep-ph].
[91] R.V. Harlander, A. Kulesza, V. Theeuwes, T. Zirke, Soft gluon resummation for gluon-induced Higgs Strahlung, J. High Energy Phys. 11 (2014) 082, arXiv:1410.0217 [hep-ph].
[92] R.V. Harlander, S. Liebler, T. Zirke, Higgs Strahlung at the large hadron collider in the 2-Higgs-doublet model, J. High Energy Phys. 02 (2014) 023, arXiv:1307.8122 [hep-ph].
[93] O. Brein, R.V. Harlander, T.J.E. Zirke, vh@nnlo – Higgs Strahlung at hadron colliders, Comput. Phys. Commun. 184 (2013) 998, arXiv:1210.5347 [hep-ph].
[94] S. Frixione, P. Nason, G. Ridolfi, A positive-weight next-to-leading-order Monte Carlo for heavy flavour hadroproduction, J. High Energy Phys. 09 (2007) 126, arXiv:0707.3088 [hep-ph].
[95] ATLAS Collaboration, ATLAS Pythia 8 tunes to 7 TeV data, ATL-PHYS-PUB-2014-021, https://cds.cern.ch/record/1966419, 2014.
[96] M. Czakon, A. Mitov, Top++: a program for the calculation of the top-pair cross-section at hadron colliders, Comput. Phys. Commun. 185 (2014) 2930, arXiv:1112.5675 [hep-ph].
[97] S. Alioli, P. Nason, C. Oleari, E. Re, NLO single-top production matched with shower in POWHEG: s- and t-channel contributions, J. High Energy Phys. 09 (2009) 111, Erratum: J. High Energy Phys. 02 (2010) 011, arXiv:0907.4076 [hep-ph].
[98] N. Kidonakis, NNLL resummation for s-channel single top quark production, Phys. Rev. D 81 (2010) 054028, arXiv:1001.5034 [hep-ph].
[99] N. Kidonakis, Next-to-next-to-leading-order collinear and soft gluon corrections for t-channel single top quark production, Phys. Rev. D 83 (2011) 091503, arXiv:1103.2792 [hep-ph].
[100] E. Re, Single-top Wt-channel production matched with parton showers using the POWHEG method, Eur. Phys. J. C 71 (2011) 1547, arXiv:1009.2450 [hep-ph].
[101] N. Kidonakis, Two-loop soft anomalous dimensions for single top quark associated production with a W- or H-, Phys. Rev. D 82 (2010) 054018, arXiv:1005.4451 [hep-ph].
[102] F. Cascioli, P. Maierhofer, S. Pozzorini, Scattering amplitudes with open loops, Phys. Rev. Lett. 108 (2012) 111601, arXiv:1111.5206 [hep-ph].
[103] T. Gleisberg, S. Höche, Comix, a new matrix element generator, J. High Energy Phys. 12 (2008) 039, arXiv:0808.3674 [hep-ph].
[104] S. Schumann, F. Krauss, A parton shower algorithm based on Catani–Seymour dipole factorisation, J. High Energy Phys. 03 (2008) 038, arXiv:0709.1027 [hep-ph].
[105] S. Höche, F. Krauss, M. Schönherr, F. Siegert, QCD matrix elements + parton showers. The NLO case, J. High Energy Phys. 04 (2013) 027, arXiv:1207.5030 [hep-ph].
[106] S. Catani, L. Cieri, G. Ferrera, D. de Florian, M. Grazzini, Vector boson production at hadron colliders: a fully exclusive QCD calculation at next-to-next-to-leading order, Phys. Rev. Lett. 103 (2009) 082001, arXiv:0903.2120 [hep-ph].
[107] ATLAS Collaboration, Measurements of b-jet tagging efficiency with the ATLAS detector using $t\bar{t}$ events at $\sqrt{s} = 13$ TeV, J. High Energy Phys. 08 (2018) 089, arXiv:1805.01845 [hep-ex].
[108] ATLAS Collaboration, Measurement of b-tagging efficiency of c-jets in $t\bar{t}$ events using a likelihood approach with the ATLAS detector, ATLAS-CONF-2018-001, https://cds.cern.ch/record/2306649, 2018.
[109] ATLAS Collaboration, Calibration of light-flavour b-jet mistagging rates using ATLAS proton–proton collision data at $\sqrt{s} = 13$ TeV, ATLAS-CONF-2018-006, https://cds.cern.ch/record/2314418, 2018.
[110] ATLAS Collaboration, Jet energy resolution in proton–proton collisions at $\sqrt{s} = 7$ TeV recorded in 2010 with the ATLAS detector, Eur. Phys. J. C 73 (2013) 2306, arXiv:1210.6210 [hep-ex].
[111] ATLAS Collaboration, Measurement of the inelastic proton–proton cross section at $\sqrt{s} = 13$ TeV with the ATLAS detector at the LHC, Phys. Rev. Lett. 117 (2016) 182002, arXiv:1606.02625 [hep-ex].
[112] LHC Higgs Cross Section Working Group, in: S. Dittmaier, C. Mariotti, G. Passarino, R. Tanaka (Eds.), Handbook of LHC Higgs Cross Sections: 1. Inclusive Observables, 2011, CERN-2011-002, arXiv:1101.0593 [hep-ph].
[113] LHC Higgs Cross Section Working Group, in: S. Dittmaier, C. Mariotti, G. Passarino, R. Tanaka (Eds.), Handbook of LHC Higgs Cross Sections: 2. Differential Distributions, 2012, CERN-2012-002, arXiv:1201.3084 [hep-ph].
[114] R.J. Barlow, C. Beeston, Fitting using finite Monte Carlo samples, Comput. Phys. Commun. 77 (1993) 219.
[115] G. Cowan, K. Cranmer, E. Gross, O. Vitells, Asymptotic formulae for likelihood-based tests of new physics, Eur. Phys. J. C 71 (2011) 1554, Erratum: Eur. Phys. J. C 73 (2013) 2501, arXiv:1007.1727 [physics.data-an].
[116] ATLAS Collaboration, Measurements of the Higgs boson production and decay rates and coupling strengths using pp collision data at $\sqrt{s} = 7$ and 8 TeV in the ATLAS experiment, Eur. Phys. J. C 76 (2016) 6, arXiv:1507.04548 [hep-ex].
[117] ATLAS Collaboration, ATLAS computing acknowledgements, ATL-GEN-PUB-2016-002, https://cds.cern.ch/record/2202407.

The ATLAS Collaboration

M. Aaboud [34d], G. Aad [99], B. Abbott [124], O. Abdinov [13,*], B. Abeloos [128], D.K. Abhayasinghe [91], S.H. Abidi [164], O.S. AbouZeid [39], N.L. Abraham [153], H. Abramowicz [158], H. Abreu [157], Y. Abulaiti [6], B.S. Acharya [64a,64b,o], S. Adachi [160], L. Adam [97], L. Adamczyk [81a], J. Adelman [119], M. Adersberger [112], A. Adiguzel [12c,ag], T. Adye [141], A.A. Affolder [143], Y. Afik [157], C. Agheorghiesei [27c], J.A. Aguilar-Saavedra [136f,136a], F. Ahmadov [77,ae], G. Aielli [71a,71b], S. Akatsuka [83], T.P.A. Åkesson [94], E. Akilli [52], A.V. Akimov [108], G.L. Alberghi [23b,23a], J. Albert [173], P. Albicocco [49], M.J. Alconada Verzini [86], S. Alderweireldt [117], M. Aleksa [35], I.N. Aleksandrov [77], C. Alexa [27b], D. Alexandre [19], T. Alexopoulos [10], M. Alhroob [124], B. Ali [138], G. Alimonti [66a], J. Alison [36], S.P. Alkire [145], C. Allaire [128], B.M.M. Allbrooke [153], B.W. Allen [127], P.P. Allport [21], A. Aloisio [67a,67b], A. Alonso [39], F. Alonso [86], C. Alpigiani [145], A.A. Alshehri [55], M.I. Alstaty [99], B. Alvarez Gonzalez [35], D. Álvarez Piqueras [171], M.G. Alviggi [67a,67b], B.T. Amadio [18], Y. Amaral Coutinho [78b], A. Ambler [101], L. Ambroz [131], C. Amelung [26], D. Amidei [103], S.P. Amor Dos Santos [136a,136c], S. Amoroso [44], C.S. Amrouche [52], F. An [76], C. Anastopoulos [146], L.S. Ancu [52], N. Andari [142], T. Andeen [11], C.F. Anders [59b], J.K. Anders [20], K.J. Anderson [36], A. Andreazza [66a,66b], V. Andrei [59a], C.R. Anelli [173], S. Angelidakis [37], I. Angelozzi [118], A. Angerami [38], A.V. Anisenkov [120b,120a], A. Annovi [69a], C. Antel [59a], M.T. Anthony [146], M. Antonelli [49], D.J.A. Antrim [168], F. Anulli [70a], M. Aoki [79], J.A. Aparisi Pozo [171], L. Aperio Bella [35], G. Arabidze [104], J.P. Araque [136a], V. Araujo Ferraz [78b], R. Araujo Pereira [78b], A.T.H. Arce [47], R.E. Ardell [91], F.A. Arduh [86], J-F. Arguin [107], S. Argyropoulos [75], J.-H. Arling [44], A.J. Armbruster [35], L.J. Armitage [90], A Armstrong [168], O. Arnaez [164], H. Arnold [118], M. Arratia [31], O. Arslan [24], A. Artamonov [109,*], G. Artoni [131], S. Artz [97], S. Asai [160], N. Asbah [57], E.M. Asimakopoulou [169], L. Asquith [153], K. Assamagan [29], R. Astalos [28a], R.J. Atkin [32a], M. Atkinson [170], N.B. Atlay [148], K. Augsten [138], G. Avolio [35], R. Avramidou [58a], M.K. Ayoub [15a], A.M. Azoulay [165b], G. Azuelos [107,at], A.E. Baas [59a], M.J. Baca [21], H. Bachacou [142], K. Bachas [65a,65b], M. Backes [131],

P. Bagnaia [70a,70b], M. Bahmani [82], H. Bahrasemani [149], A.J. Bailey [171], J.T. Baines [141], M. Bajic [39], C. Bakalis [10], O.K. Baker [180], P.J. Bakker [118], D. Bakshi Gupta [8], S. Balaji [154], E.M. Baldin [120b,120a], P. Balek [177], F. Balli [142], W.K. Balunas [133], J. Balz [97], E. Banas [82], A. Bandyopadhyay [24], S. Banerjee [178,k], A.A.E. Bannoura [179], L. Barak [158], W.M. Barbe [37], E.L. Barberio [102], D. Barberis [53b,53a], M. Barbero [99], T. Barillari [113], M-S. Barisits [35], J. Barkeloo [127], T. Barklow [150], R. Barnea [157], S.L. Barnes [58c], B.M. Barnett [141], R.M. Barnett [18], Z. Barnovska-Blenessy [58a], A. Baroncelli [72a], G. Barone [29], A.J. Barr [131], L. Barranco Navarro [171], F. Barreiro [96], J. Barreiro Guimarães da Costa [15a], R. Bartoldus [150], A.E. Barton [87], P. Bartos [28a], A. Basalaev [134], A. Bassalat [128], R.L. Bates [55], S.J. Batista [164], S. Batlamous [34e], J.R. Batley [31], M. Battaglia [143], M. Bauce [70a,70b], F. Bauer [142], K.T. Bauer [168], H.S. Bawa [150,m], J.B. Beacham [122], T. Beau [132], P.H. Beauchemin [167], P. Bechtle [24], H.C. Beck [51], H.P. Beck [20,r], K. Becker [50], M. Becker [97], C. Becot [44], A. Beddall [12d], A.J. Beddall [12a], V.A. Bednyakov [77], M. Bedognetti [118], C.P. Bee [152], T.A. Beermann [74], M. Begalli [78b], M. Begel [29], A. Behera [152], J.K. Behr [44], A.S. Bell [92], G. Bella [158], L. Bellagamba [23b], A. Bellerive [33], M. Bellomo [157], P. Bellos [9], K. Belotskiy [110], N.L. Belyaev [110], O. Benary [158,*], D. Benchekroun [34a], M. Bender [112], N. Benekos [10], Y. Benhammou [158], E. Benhar Noccioli [180], J. Benitez [75], D.P. Benjamin [6], M. Benoit [52], J.R. Bensinger [26], S. Bentvelsen [118], L. Beresford [131], M. Beretta [49], D. Berge [44], E. Bergeaas Kuutmann [169], N. Berger [5], L.J. Bergsten [26], J. Beringer [18], S. Berlendis [7], N.R. Bernard [100], G. Bernardi [132], C. Bernius [150], F.U. Bernlochner [24], T. Berry [91], P. Berta [97], C. Bertella [15a], G. Bertoli [43a,43b], I.A. Bertram [87], G.J. Besjes [39], O. Bessidskaia Bylund [179], M. Bessner [44], N. Besson [142], A. Bethani [98], S. Bethke [113], A. Betti [24], A.J. Bevan [90], J. Beyer [113], R. Bi [135], R.M. Bianchi [135], O. Biebel [112], D. Biedermann [19], R. Bielski [35], K. Bierwagen [97], N.V. Biesuz [69a,69b], M. Biglietti [72a], T.R.V. Billoud [107], M. Bindi [51], A. Bingul [12d], C. Bini [70a,70b], S. Biondi [23b,23a], M. Birman [177], T. Bisanz [51], J.P. Biswal [158], C. Bittrich [46], D.M. Bjergaard [47], J.E. Black [150], K.M. Black [25], T. Blazek [28a], I. Bloch [44], C. Blocker [26], A. Blue [55], U. Blumenschein [90], Dr. Blunier [144a], G.J. Bobbink [118], V.S. Bobrovnikov [120b,120a], S.S. Bocchetta [94], A. Bocci [47], D. Boerner [179], D. Bogavac [112], A.G. Bogdanchikov [120b,120a], C. Bohm [43a], V. Boisvert [91], P. Bokan [169], T. Bold [81a], A.S. Boldyrev [111], A.E. Bolz [59b], M. Bomben [132], M. Bona [90], J.S. Bonilla [127], M. Boonekamp [142], H.M. Borecka-Bielska [88], A. Borisov [140], G. Borissov [87], J. Bortfeldt [35], D. Bortoletto [131], V. Bortolotto [71a,71b], D. Boscherini [23b], M. Bosman [14], J.D. Bossio Sola [30], K. Bouaouda [34a], J. Boudreau [135], E.V. Bouhova-Thacker [87], D. Boumediene [37], C. Bourdarios [128], S.K. Boutle [55], A. Boveia [122], J. Boyd [35], D. Boye [32b], I.R. Boyko [77], A.J. Bozson [91], J. Bracinik [21], N. Brahimi [99], A. Brandt [8], G. Brandt [179], O. Brandt [59a], F. Braren [44], U. Bratzler [161], B. Brau [100], J.E. Brau [127], W.D. Breaden Madden [55], K. Brendlinger [44], L. Brenner [44], R. Brenner [169], S. Bressler [177], B. Brickwedde [97], D.L. Briglin [21], D. Britton [55], D. Britzger [113], I. Brock [24], R. Brock [104], G. Brooijmans [38], T. Brooks [91], W.K. Brooks [144b], E. Brost [119], J.H Broughton [21], P.A. Bruckman de Renstrom [82], D. Bruncko [28b], A. Bruni [23b], G. Bruni [23b], L.S. Bruni [118], S. Bruno [71a,71b], B.H. Brunt [31], M. Bruschi [23b], N. Bruscino [135], P. Bryant [36], L. Bryngemark [94], T. Buanes [17], Q. Buat [35], P. Buchholz [148], A.G. Buckley [55], I.A. Budagov [77], F. Buehrer [50], M.K. Bugge [130], O. Bulekov [110], D. Bullock [8], T.J. Burch [119], S. Burdin [88], C.D. Burgard [118], A.M. Burger [5], B. Burghgrave [119], K. Burka [82], S. Burke [141], I. Burmeister [45], J.T.P. Burr [131], V. Büscher [97], E. Buschmann [51], P. Bussey [55], J.M. Butler [25], C.M. Buttar [55], J.M. Butterworth [92], P. Butti [35], W. Buttinger [35], A. Buzatu [155], A.R. Buzykaev [120b,120a], G. Cabras [23b,23a], S. Cabrera Urbán [171], D. Caforio [138], H. Cai [170], V.M.M. Cairo [2], O. Cakir [4a], N. Calace [52], P. Calafiura [18], A. Calandri [99], G. Calderini [132], P. Calfayan [63], G. Callea [55], L.P. Caloba [78b], S. Calvente Lopez [96], D. Calvet [37], S. Calvet [37], T.P. Calvet [152], M. Calvetti [69a,69b], R. Camacho Toro [132], S. Camarda [35], D. Camarero Munoz [96], P. Camarri [71a,71b], D. Cameron [130], R. Caminal Armadans [100], C. Camincher [35], S. Campana [35], M. Campanelli [92], A. Camplani [39], A. Campoverde [148], V. Canale [67a,67b], M. Cano Bret [58c], J. Cantero [125], T. Cao [158], Y. Cao [170], M.D.M. Capeans Garrido [35], I. Caprini [27b], M. Caprini [27b], M. Capua [40b,40a], R.M. Carbone [38], R. Cardarelli [71a], F.C. Cardillo [146], I. Carli [139], T. Carli [35], G. Carlino [67a], B.T. Carlson [135], L. Carminati [66a,66b], R.M.D. Carney [43a,43b], S. Caron [117], E. Carquin [144b], S. Carrá [66a,66b], J.W.S. Carter [164], D. Casadei [32b], M.P. Casado [14,g], A.F. Casha [164], D.W. Casper [168], R. Castelijn [118], F.L. Castillo [171], V. Castillo Gimenez [171], N.F. Castro [136a,136e], A. Catinaccio [35], J.R. Catmore [130], A. Cattai [35], J. Caudron [24], V. Cavaliere [29], E. Cavallaro [14], D. Cavalli [66a], M. Cavalli-Sforza [14], V. Cavasinni [69a,69b], E. Celebi [12b], F. Ceradini [72a,72b], L. Cerda Alberich [171], A.S. Cerqueira [78a], A. Cerri [153], L. Cerrito [71a,71b], F. Cerutti [18], A. Cervelli [23b,23a], S.A. Cetin [12b], A. Chafaq [34a], D Chakraborty [119], S.K. Chan [57], W.S. Chan [118], Y.L. Chan [61a], J.D. Chapman [31],

B. Chargeishvili [156b], D.G. Charlton [21], C.C. Chau [33], C.A. Chavez Barajas [153], S. Che [122], A. Chegwidden [104], S. Chekanov [6], S.V. Chekulaev [165a], G.A. Chelkov [77,as], M.A. Chelstowska [35], C. Chen [58a], C.H. Chen [76], H. Chen [29], J. Chen [58a], J. Chen [38], S. Chen [133], S.J. Chen [15c], X. Chen [15b,ar], Y. Chen [80], Y-H. Chen [44], H.C. Cheng [103], H.J. Cheng [15d], A. Cheplakov [77], E. Cheremushkina [140], R. Cherkaoui El Moursli [34e], E. Cheu [7], K. Cheung [62], T.J.A. Chevalérias [142], L. Chevalier [142], V. Chiarella [49], G. Chiarelli [69a], G. Chiodini [65a], A.S. Chisholm [35,21], A. Chitan [27b], I. Chiu [160], Y.H. Chiu [173], M.V. Chizhov [77], K. Choi [63], A.R. Chomont [128], S. Chouridou [159], Y.S. Chow [118], V. Christodoulou [92], M.C. Chu [61a], J. Chudoba [137], A.J. Chuinard [101], J.J. Chwastowski [82], L. Chytka [126], D. Cinca [45], V. Cindro [89], I.A. Cioară [24], A. Ciocio [18], F. Cirotto [67a,67b], Z.H. Citron [177], M. Citterio [66a], B.M. Ciungu [164], A. Clark [52], M.R. Clark [38], P.J. Clark [48], C. Clement [43a,43b], Y. Coadou [99], M. Cobal [64a,64c], A. Coccaro [53b,53a], J. Cochran [76], H. Cohen [158], A.E.C. Coimbra [177], L. Colasurdo [117], B. Cole [38], A.P. Colijn [118], J. Collot [56], P. Conde Muiño [136a,136b], E. Coniavitis [50], S.H. Connell [32b], I.A. Connelly [98], S. Constantinescu [27b], F. Conventi [67a,au], A.M. Cooper-Sarkar [131], F. Cormier [172], K.J.R. Cormier [164], L.D. Corpe [92], M. Corradi [70a,70b], E.E. Corrigan [94], F. Corriveau [101,ac], A. Cortes-Gonzalez [35], M.J. Costa [171], F. Costanza [5], D. Costanzo [146], G. Cottin [31], G. Cowan [91], B.E. Cox [98], J. Crane [98], K. Cranmer [121], S.J. Crawley [55], R.A. Creager [133], G. Cree [33], S. Crépé-Renaudin [56], F. Crescioli [132], M. Cristinziani [24], V. Croft [121], G. Crosetti [40b,40a], A. Cueto [96], T. Cuhadar Donszelmann [146], A.R. Cukierman [150], S. Czekierda [82], P. Czodrowski [35], M.J. Da Cunha Sargedas De Sousa [58b,136b], C. Da Via [98], W. Dabrowski [81a], T. Dado [28a,x], S. Dahbi [34e], T. Dai [103], F. Dallaire [107], C. Dallapiccola [100], M. Dam [39], G. D'amen [23b,23a], J. Damp [97], J.R. Dandoy [133], M.F. Daneri [30], N.P. Dang [178,k], N.D Dann [98], M. Danninger [172], V. Dao [35], G. Darbo [53b], S. Darmora [8], O. Dartsi [5], A. Dattagupta [127], T. Daubney [44], S. D'Auria [66a,66b], W. Davey [24], C. David [44], T. Davidek [139], D.R. Davis [47], E. Dawe [102], I. Dawson [146], K. De [8], R. De Asmundis [67a], A. De Benedetti [124], M. De Beurs [118], S. De Castro [23b,23a], S. De Cecco [70a,70b], N. De Groot [117], P. de Jong [118], H. De la Torre [104], F. De Lorenzi [76], A. De Maria [69a,69b], D. De Pedis [70a], A. De Salvo [70a], U. De Sanctis [71a,71b], M. De Santis [71a,71b], A. De Santo [153], K. De Vasconcelos Corga [99], J.B. De Vivie De Regie [128], C. Debenedetti [143], D.V. Dedovich [77], N. Dehghanian [3], M. Del Gaudio [40b,40a], J. Del Peso [96], Y. Delabat Diaz [44], D. Delgove [128], F. Deliot [142], C.M. Delitzsch [7], M. Della Pietra [67a,67b], D. Della Volpe [52], A. Dell'Acqua [35], L. Dell'Asta [25], M. Delmastro [5], C. Delporte [128], P.A. Delsart [56], D.A. DeMarco [164], S. Demers [180], M. Demichev [77], S.P. Denisov [140], D. Denysiuk [118], L. D'Eramo [132], D. Derendarz [82], J.E. Derkaoui [34d], F. Derue [132], P. Dervan [88], K. Desch [24], C. Deterre [44], K. Dette [164], M.R. Devesa [30], P.O. Deviveiros [35], A. Dewhurst [141], S. Dhaliwal [26], F.A. Di Bello [52], A. Di Ciaccio [71a,71b], L. Di Ciaccio [5], W.K. Di Clemente [133], C. Di Donato [67a,67b], A. Di Girolamo [35], G. Di Gregorio [69a,69b], B. Di Micco [72a,72b], R. Di Nardo [100], K.F. Di Petrillo [57], R. Di Sipio [164], D. Di Valentino [33], C. Diaconu [99], M. Diamond [164], F.A. Dias [39], T. Dias Do Vale [136a], M.A. Diaz [144a], J. Dickinson [18], E.B. Diehl [103], J. Dietrich [19], S. Díez Cornell [44], A. Dimitrievska [18], J. Dingfelder [24], F. Dittus [35], F. Djama [99], T. Djobava [156b], J.I. Djuvsland [59a], M.A.B. Do Vale [78c], M. Dobre [27b], D. Dodsworth [26], C. Doglioni [94], J. Dolejsi [139], Z. Dolezal [139], M. Donadelli [78d], J. Donini [37], A. D'onofrio [90], M. D'Onofrio [88], J. Dopke [141], A. Doria [67a], M.T. Dova [86], A.T. Doyle [55], E. Drechsler [51], E. Dreyer [149], T. Dreyer [51], Y. Du [58b], F. Dubinin [108], M. Dubovsky [28a], A. Dubreuil [52], E. Duchovni [177], G. Duckeck [112], A. Ducourthial [132], O.A. Ducu [107,w], D. Duda [113], A. Dudarev [35], A.C. Dudder [97], E.M. Duffield [18], L. Duflot [128], M. Dührssen [35], C. Dülsen [179], M. Dumancic [177], A.E. Dumitriu [27b,e], A.K. Duncan [55], M. Dunford [59a], A. Duperrin [99], H. Duran Yildiz [4a], M. Düren [54], A. Durglishvili [156b], D. Duschinger [46], B. Dutta [44], D. Duvnjak [1], M. Dyndal [44], S. Dysch [98], B.S. Dziedzic [82], C. Eckardt [44], K.M. Ecker [113], R.C. Edgar [103], T. Eifert [35], G. Eigen [17], K. Einsweiler [18], T. Ekelof [169], M. El Kacimi [34c], R. El Kosseifi [99], V. Ellajosyula [99], M. Ellert [169], F. Ellinghaus [179], A.A. Elliot [90], N. Ellis [35], J. Elmsheuser [29], M. Elsing [35], D. Emeliyanov [141], A. Emerman [38], Y. Enari [160], J.S. Ennis [175], M.B. Epland [47], J. Erdmann [45], A. Ereditato [20], S. Errede [170], M. Escalier [128], C. Escobar [171], O. Estrada Pastor [171], A.I. Etienvre [142], E. Etzion [158], H. Evans [63], A. Ezhilov [134], M. Ezzi [34e], F. Fabbri [55], L. Fabbri [23b,23a], V. Fabiani [117], G. Facini [92], R.M. Faisca Rodrigues Pereira [136a], R.M. Fakhrutdinov [140], S. Falciano [70a], P.J. Falke [5], S. Falke [5], J. Faltova [139], Y. Fang [15a], M. Fanti [66a,66b], A. Farbin [8], A. Farilla [72a], E.M. Farina [68a,68b], T. Farooque [104], S. Farrell [18], S.M. Farrington [175], P. Farthouat [35], F. Fassi [34e], P. Fassnacht [35], D. Fassouliotis [9], M. Faucci Giannelli [48], A. Favareto [53b,53a], W.J. Fawcett [31], L. Fayard [128], O.L. Fedin [134,p], W. Fedorko [172], M. Feickert [41], S. Feigl [130], L. Feligioni [99], C. Feng [58b], E.J. Feng [35],

M. Feng [47], M.J. Fenton [55], A.B. Fenyuk [140], L. Feremenga [8], J. Ferrando [44], A. Ferrari [169], P. Ferrari [118], R. Ferrari [68a], D.E. Ferreira de Lima [59b], A. Ferrer [171], D. Ferrere [52], C. Ferretti [103], F. Fiedler [97], A. Filipčič [89], F. Filthaut [117], K.D. Finelli [25], M.C.N. Fiolhais [136a,136c,a], L. Fiorini [171], C. Fischer [14], W.C. Fisher [104], N. Flaschel [44], I. Fleck [148], P. Fleischmann [103], R.R.M. Fletcher [133], T. Flick [179], B.M. Flierl [112], L.M. Flores [133], L.R. Flores Castillo [61a], F.M. Follega [73a,73b], N. Fomin [17], G.T. Forcolin [73a,73b], A. Formica [142], F.A. Förster [14], A.C. Forti [98], A.G. Foster [21], D. Fournier [128], H. Fox [87], S. Fracchia [146], P. Francavilla [69a,69b], M. Franchini [23b,23a], S. Franchino [59a], D. Francis [35], L. Franconi [143], M. Franklin [57], M. Frate [168], M. Fraternali [68a,68b], A.N. Fray [90], D. Freeborn [92], B. Freund [107], W.S. Freund [78b], E.M. Freundlich [45], D.C. Frizzell [124], D. Froidevaux [35], J.A. Frost [131], C. Fukunaga [161], E. Fullana Torregrosa [171], T. Fusayasu [114], J. Fuster [171], O. Gabizon [157], A. Gabrielli [23b,23a], A. Gabrielli [18], G.P. Gach [81a], S. Gadatsch [52], P. Gadow [113], G. Gagliardi [53b,53a], L.G. Gagnon [107], C. Galea [27b], B. Galhardo [136a,136c], E.J. Gallas [131], B.J. Gallop [141], P. Gallus [138], G. Galster [39], R. Gamboa Goni [90], K.K. Gan [122], S. Ganguly [177], J. Gao [58a], Y. Gao [88], Y.S. Gao [150,m], C. García [171], J.E. García Navarro [171], J.A. García Pascual [15a], M. Garcia-Sciveres [18], R.W. Gardner [36], N. Garelli [150], S. Gargiulo [50], V. Garonne [130], K. Gasnikova [44], A. Gaudiello [53b,53a], G. Gaudio [68a], I.L. Gavrilenko [108], A. Gavrilyuk [109], C. Gay [172], G. Gaycken [24], E.N. Gazis [10], C.N.P. Gee [141], J. Geisen [51], M. Geisen [97], M.P. Geisler [59a], C. Gemme [53b], M.H. Genest [56], C. Geng [103], S. Gentile [70a,70b], S. George [91], D. Gerbaudo [14], G. Gessner [45], S. Ghasemi [148], M. Ghasemi Bostanabad [173], M. Ghneimat [24], B. Giacobbe [23b], S. Giagu [70a,70b], N. Giangiacomi [23b,23a], P. Giannetti [69a], A. Giannini [67a,67b], S.M. Gibson [91], M. Gignac [143], D. Gillberg [33], G. Gilles [179], D.M. Gingrich [3,at], M.P. Giordani [64a,64c], F.M. Giorgi [23b], P.F. Giraud [142], P. Giromini [57], G. Giugliarelli [64a,64c], D. Giugni [66a], F. Giuli [131], M. Giulini [59b], S. Gkaitatzis [159], I. Gkialas [9,j], E.L. Gkougkousis [14], P. Gkountoumis [10], L.K. Gladilin [111], C. Glasman [96], J. Glatzer [14], P.C.F. Glaysher [44], A. Glazov [44], M. Goblirsch-Kolb [26], J. Godlewski [82], S. Goldfarb [102], T. Golling [52], D. Golubkov [140], A. Gomes [136a,136b,136d], R. Goncalves Gama [51], R. Gonçalo [136a], G. Gonella [50], L. Gonella [21], A. Gongadze [77], F. Gonnella [21], J.L. Gonski [57], S. González de la Hoz [171], S. Gonzalez-Sevilla [52], L. Goossens [35], P.A. Gorbounov [109], H.A. Gordon [29], B. Gorini [35], E. Gorini [65a,65b], A. Gorišek [89], A.T. Goshaw [47], C. Gössling [45], M.I. Gostkin [77], C.A. Gottardo [24], C.R. Goudet [128], D. Goujdami [34c], A.G. Goussiou [145], N. Govender [32b,c], C. Goy [5], E. Gozani [157], I. Grabowska-Bold [81a], P.O.J. Gradin [169], E.C. Graham [88], J. Gramling [168], E. Gramstad [130], S. Grancagnolo [19], V. Gratchev [134], P.M. Gravila [27f], F.G. Gravili [65a,65b], C. Gray [55], H.M. Gray [18], Z.D. Greenwood [93,aj], C. Grefe [24], K. Gregersen [94], I.M. Gregor [44], P. Grenier [150], K. Grevtsov [44], N.A. Grieser [124], J. Griffiths [8], A.A. Grillo [143], K. Grimm [150,b], S. Grinstein [14,y], Ph. Gris [37], J.-F. Grivaz [128], S. Groh [97], E. Gross [177], J. Grosse-Knetter [51], G.C. Grossi [93], Z.J. Grout [92], C. Grud [103], A. Grummer [116], L. Guan [103], W. Guan [178], J. Guenther [35], A. Guerguichon [128], F. Guescini [165a], D. Guest [168], R. Gugel [50], B. Gui [122], T. Guillemin [5], S. Guindon [35], U. Gul [55], C. Gumpert [35], J. Guo [58c], W. Guo [103], Y. Guo [58a,s], Z. Guo [99], R. Gupta [44], S. Gurbuz [12c], G. Gustavino [124], B.J. Gutelman [157], P. Gutierrez [124], C. Gutschow [92], C. Guyot [142], M.P. Guzik [81a], C. Gwenlan [131], C.B. Gwilliam [88], A. Haas [121], C. Haber [18], H.K. Hadavand [8], N. Haddad [34e], A. Hadef [58a], S. Hageböck [24], M. Hagihara [166], H. Hakobyan [181,*], M. Haleem [174], J. Haley [125], G. Halladjian [104], G.D. Hallewell [99], K. Hamacher [179], P. Hamal [126], K. Hamano [173], A. Hamilton [32a], G.N. Hamity [146], K. Han [58a,ai], L. Han [58a], S. Han [15d], K. Hanagaki [79,u], M. Hance [143], D.M. Handl [112], B. Haney [133], R. Hankache [132], P. Hanke [59a], E. Hansen [94], J.B. Hansen [39], J.D. Hansen [39], M.C. Hansen [24], P.H. Hansen [39], K. Hara [166], A.S. Hard [178], T. Harenberg [179], S. Harkusha [105], P.F. Harrison [175], N.M. Hartmann [112], Y. Hasegawa [147], A. Hasib [48], S. Hassani [142], S. Haug [20], R. Hauser [104], L. Hauswald [46], L.B. Havener [38], M. Havranek [138], C.M. Hawkes [21], R.J. Hawkings [35], D. Hayden [104], C. Hayes [152], C.P. Hays [131], J.M. Hays [90], H.S. Hayward [88], S.J. Haywood [141], M.P. Heath [48], V. Hedberg [94], L. Heelan [8], S. Heer [24], K.K. Heidegger [50], J. Heilman [33], S. Heim [44], T. Heim [18], B. Heinemann [44,ao], J.J. Heinrich [112], L. Heinrich [121], C. Heinz [54], J. Hejbal [137], L. Helary [35], A. Held [172], S. Hellesund [130], C.M. Helling [143], S. Hellman [43a,43b], C. Helsens [35], R.C.W. Henderson [87], Y. Heng [178], S. Henkelmann [172], A.M. Henriques Correia [35], G.H. Herbert [19], H. Herde [26], V. Herget [174], Y. Hernández Jiménez [32c], H. Herr [97], M.G. Herrmann [112], T. Herrmann [46], G. Herten [50], R. Hertenberger [112], L. Hervas [35], T.C. Herwig [133], G.G. Hesketh [92], N.P. Hessey [165a], A. Higashida [160], S. Higashino [79], E. Higón-Rodriguez [171], K. Hildebrand [36], E. Hill [173], J.C. Hill [31], K.K. Hill [29], K.H. Hiller [44], S.J. Hillier [21], M. Hils [46], I. Hinchliffe [18], M. Hirose [129], D. Hirschbuehl [179], B. Hiti [89], O. Hladik [137], D.R. Hlaluku [32c], X. Hoad [48], J. Hobbs [152], N. Hod [165a], M.C. Hodgkinson [146],

A. Hoecker [35], M.R. Hoeferkamp [116], F. Hoenig [112], D. Hohn [50], D. Hohov [128], T.R. Holmes [36], M. Holzbock [112], M. Homann [45], B.H. Hommels [31], S. Honda [166], T. Honda [79], T.M. Hong [135], A. Hönle [113], B.H. Hooberman [170], W.H. Hopkins [127], Y. Horii [115], P. Horn [46], A.J. Horton [149], L.A. Horyn [36], J-Y. Hostachy [56], A. Hostiuc [145], S. Hou [155], A. Hoummada [34a], J. Howarth [98], J. Hoya [86], M. Hrabovsky [126], I. Hristova [19], J. Hrivnac [128], A. Hrynevich [106], T. Hryn'ova [5], P.J. Hsu [62], S.-C. Hsu [145], Q. Hu [29], S. Hu [58c], Y. Huang [15a], Z. Hubacek [138], F. Hubaut [99], M. Huebner [24], F. Huegging [24], T.B. Huffman [131], M. Huhtinen [35], R.F.H. Hunter [33], P. Huo [152], A.M. Hupe [33], N. Huseynov [77,ae], J. Huston [104], J. Huth [57], R. Hyneman [103], G. Iacobucci [52], G. Iakovidis [29], I. Ibragimov [148], L. Iconomidou-Fayard [128], Z. Idrissi [34e], P. Iengo [35], R. Ignazzi [39], O. Igonkina [118,aa], R. Iguchi [160], T. Iizawa [52], Y. Ikegami [79], M. Ikeno [79], D. Iliadis [159], N. Ilic [150], F. Iltzsche [46], G. Introzzi [68a,68b], M. Iodice [72a], K. Iordanidou [38], V. Ippolito [70a,70b], M.F. Isacson [169], N. Ishijima [129], M. Ishino [160], M. Ishitsuka [162], W. Islam [125], C. Issever [131], S. Istin [157], F. Ito [166], J.M. Iturbe Ponce [61a], R. Iuppa [73a,73b], A. Ivina [177], H. Iwasaki [79], J.M. Izen [42], V. Izzo [67a], P. Jacka [137], P. Jackson [1], R.M. Jacobs [24], V. Jain [2], G. Jäkel [179], K.B. Jakobi [97], K. Jakobs [50], S. Jakobsen [74], T. Jakoubek [137], D.O. Jamin [125], R. Jansky [52], J. Janssen [24], M. Janus [51], P.A. Janus [81a], G. Jarlskog [94], N. Javadov [77,ae], T. Javůrek [35], M. Javurkova [50], F. Jeanneau [142], L. Jeanty [18], J. Jejelava [156a,af], A. Jelinskas [175], P. Jenni [50,d], J. Jeong [44], N. Jeong [44], S. Jézéquel [5], H. Ji [178], J. Jia [152], H. Jiang [76], Y. Jiang [58a], Z. Jiang [150,q], S. Jiggins [50], F.A. Jimenez Morales [37], J. Jimenez Pena [171], S. Jin [15c], A. Jinaru [27b], O. Jinnouchi [162], H. Jivan [32c], P. Johansson [146], K.A. Johns [7], C.A. Johnson [63], W.J. Johnson [145], K. Jon-And [43a,43b], R.W.L. Jones [87], S.D. Jones [153], S. Jones [7], T.J. Jones [88], J. Jongmanns [59a], P.M. Jorge [136a,136b], J. Jovicevic [165a], X. Ju [18], J.J. Junggeburth [113], A. Juste Rozas [14,y], A. Kaczmarska [82], M. Kado [128], H. Kagan [122], M. Kagan [150], T. Kaji [176], E. Kajomovitz [157], C.W. Kalderon [94], A. Kaluza [97], S. Kama [41], A. Kamenshchikov [140], L. Kanjir [89], Y. Kano [160], V.A. Kantserov [110], J. Kanzaki [79], L.S. Kaplan [178], D. Kar [32c], M.J. Kareem [165b], E. Karentzos [10], S.N. Karpov [77], Z.M. Karpova [77], V. Kartvelishvili [87], A.N. Karyukhin [140], L. Kashif [178], R.D. Kass [122], A. Kastanas [43a,43b], Y. Kataoka [160], C. Kato [58d,58c], J. Katzy [44], K. Kawade [80], K. Kawagoe [85], T. Kawamoto [160], G. Kawamura [51], E.F. Kay [88], V.F. Kazanin [120b,120a], R. Keeler [173], R. Kehoe [41], J.S. Keller [33], E. Kellermann [94], J.J. Kempster [21], J. Kendrick [21], O. Kepka [137], S. Kersten [179], B.P. Kerševan [89], S. Ketabchi Haghighat [164], R.A. Keyes [101], M. Khader [170], F. Khalil-Zada [13], A. Khanov [125], A.G. Kharlamov [120b,120a], T. Kharlamova [120b,120a], E.E. Khoda [172], A. Khodinov [163], T.J. Khoo [52], E. Khramov [77], J. Khubua [156b], S. Kido [80], M. Kiehn [52], C.R. Kilby [91], Y.K. Kim [36], N. Kimura [64a,64c], O.M. Kind [19], B.T. King [88], D. Kirchmeier [46], J. Kirk [141], A.E. Kiryunin [113], T. Kishimoto [160], D. Kisielewska [81a], V. Kitali [44], O. Kivernyk [5], E. Kladiva [28b,*], T. Klapdor-Kleingrothaus [50], M.H. Klein [103], M. Klein [88], U. Klein [88], K. Kleinknecht [97], P. Klimek [119], A. Klimentov [29], T. Klingl [24], T. Klioutchnikova [35], F.F. Klitzner [112], P. Kluit [118], S. Kluth [113], E. Kneringer [74], E.B.F.G. Knoops [99], A. Knue [50], A. Kobayashi [160], D. Kobayashi [85], T. Kobayashi [160], M. Kobel [46], M. Kocian [150], P. Kodys [139], P.T. Koenig [24], T. Koffas [33], E. Koffeman [118], N.M. Köhler [113], T. Koi [150], M. Kolb [59b], I. Koletsou [5], T. Kondo [79], N. Kondrashova [58c], K. Köneke [50], A.C. König [117], T. Kono [79], R. Konoplich [121,al], V. Konstantinides [92], N. Konstantinidis [92], B. Konya [94], R. Kopeliansky [63], S. Koperny [81a], K. Korcyl [82], K. Kordas [159], G. Koren [158], A. Korn [92], I. Korolkov [14], E.V. Korolkova [146], N. Korotkova [111], O. Kortner [113], S. Kortner [113], T. Kosek [139], V.V. Kostyukhin [24], A. Kotwal [47], A. Koulouris [10], A. Kourkoumeli-Charalampidi [68a,68b], C. Kourkoumelis [9], E. Kourlitis [146], V. Kouskoura [29], A.B. Kowalewska [82], R. Kowalewski [173], T.Z. Kowalski [81a], C. Kozakai [160], W. Kozanecki [142], A.S. Kozhin [140], V.A. Kramarenko [111], G. Kramberger [89], D. Krasnopevtsev [58a], M.W. Krasny [132], A. Krasznahorkay [35], D. Krauss [113], J.A. Kremer [81a], J. Kretzschmar [88], P. Krieger [164], K. Krizka [18], K. Kroeninger [45], H. Kroha [113], J. Kroll [137], J. Kroll [133], J. Krstic [16], U. Kruchonak [77], H. Krüger [24], N. Krumnack [76], M.C. Kruse [47], T. Kubota [102], S. Kuday [4b], J.T. Kuechler [179], S. Kuehn [35], A. Kugel [59a], T. Kuhl [44], V. Kukhtin [77], R. Kukla [99], Y. Kulchitsky [105,ah], S. Kuleshov [144b], Y.P. Kulinich [170], M. Kuna [56], T. Kunigo [83], A. Kupco [137], T. Kupfer [45], O. Kuprash [158], H. Kurashige [80], L.L. Kurchaninov [165a], Y.A. Kurochkin [105], A. Kurova [110], M.G. Kurth [15d], E.S. Kuwertz [35], M. Kuze [162], J. Kvita [126], T. Kwan [101], A. La Rosa [113], J.L. La Rosa Navarro [78d], L. La Rotonda [40b,40a], F. La Ruffa [40b,40a], C. Lacasta [171], F. Lacava [70a,70b], J. Lacey [44], D.P.J. Lack [98], H. Lacker [19], D. Lacour [132], E. Ladygin [77], R. Lafaye [5], B. Laforge [132], T. Lagouri [32c], S. Lai [51], S. Lammers [63], W. Lampl [7], E. Lançon [29], U. Landgraf [50], M.P.J. Landon [90], M.C. Lanfermann [52], V.S. Lang [44], J.C. Lange [51], R.J. Langenberg [35], A.J. Lankford [168], F. Lanni [29], K. Lantzsch [24], A. Lanza [68a], A. Lapertosa [53b,53a],

S. Laplace [132], J.F. Laporte [142], T. Lari [66a], F. Lasagni Manghi [23b,23a], M. Lassnig [35], T.S. Lau [61a], A. Laudrain [128], M. Lavorgna [67a,67b], M. Lazzaroni [66a,66b], B. Le [102], O. Le Dortz [132], E. Le Guirriec [99], E.P. Le Quilleuc [142], M. LeBlanc [7], T. LeCompte [6], F. Ledroit-Guillon [56], C.A. Lee [29], G.R. Lee [144a], L. Lee [57], S.C. Lee [155], B. Lefebvre [101], M. Lefebvre [173], F. Legger [112], C. Leggett [18], K. Lehmann [149], N. Lehmann [179], G. Lehmann Miotto [35], W.A. Leight [44], A. Leisos [159,v], M.A.L. Leite [78d], R. Leitner [139], D. Lellouch [177], K.J.C. Leney [92], T. Lenz [24], B. Lenzi [35], R. Leone [7], S. Leone [69a], C. Leonidopoulos [48], G. Lerner [153], C. Leroy [107], R. Les [164], A.A.J. Lesage [142], C.G. Lester [31], M. Levchenko [134], J. Levêque [5], D. Levin [103], L.J. Levinson [177], D. Lewis [90], B. Li [15b], B. Li [103], C-Q. Li [58a,ak], H. Li [58a], H. Li [58b], L. Li [58c], M. Li [15a], Q. Li [15d], Q.Y. Li [58a], S. Li [58d,58c], X. Li [58c], Y. Li [148], Z. Liang [15a], B. Liberti [71a], A. Liblong [164], K. Lie [61c], S. Liem [118], A. Limosani [154], C.Y. Lin [31], K. Lin [104], T.H. Lin [97], R.A. Linck [63], J.H. Lindon [21], B.E. Lindquist [152], A.L. Lionti [52], E. Lipeles [133], A. Lipniacka [17], M. Lisovyi [59b], T.M. Liss [170,aq], A. Lister [172], A.M. Litke [143], J.D. Little [8], B. Liu [76], B.L Liu [6], H.B. Liu [29], H. Liu [103], J.B. Liu [58a], J.K.K. Liu [131], K. Liu [132], M. Liu [58a], P. Liu [18], Y. Liu [15a], Y.L. Liu [58a], Y.W. Liu [58a], M. Livan [68a,68b], A. Lleres [56], J. Llorente Merino [15a], S.L. Lloyd [90], C.Y. Lo [61b], F. Lo Sterzo [41], E.M. Lobodzinska [44], P. Loch [7], T. Lohse [19], K. Lohwasser [146], M. Lokajicek [137], J.D. Long [170], R.E. Long [87], L. Longo [65a,65b], K.A. Looper [122], J.A. Lopez [144b], I. Lopez Paz [98], A. Lopez Solis [146], J. Lorenz [112], N. Lorenzo Martinez [5], M. Losada [22], P.J. Lösel [112], A. Lösle [50], X. Lou [44], X. Lou [15a], A. Lounis [128], J. Love [6], P.A. Love [87], J.J. Lozano Bahilo [171], H. Lu [61a], M. Lu [58a], Y.J. Lu [62], H.J. Lubatti [145], C. Luci [70a,70b], A. Lucotte [56], C. Luedtke [50], F. Luehring [63], I. Luise [132], L. Luminari [70a], B. Lund-Jensen [151], M.S. Lutz [100], P.M. Luzi [132], D. Lynn [29], R. Lysak [137], E. Lytken [94], F. Lyu [15a], V. Lyubushkin [77], T. Lyubushkina [77], H. Ma [29], L.L. Ma [58b], Y. Ma [58b], G. Maccarrone [49], A. Macchiolo [113], C.M. Macdonald [146], J. Machado Miguens [133,136b], D. Madaffari [171], R. Madar [37], W.F. Mader [46], A. Madsen [44], N. Madysa [46], J. Maeda [80], K. Maekawa [160], S. Maeland [17], T. Maeno [29], M. Maerker [46], A.S. Maevskiy [111], V. Magerl [50], D.J. Mahon [38], C. Maidantchik [78b], T. Maier [112], A. Maio [136a,136b,136d], O. Majersky [28a], S. Majewski [127], Y. Makida [79], N. Makovec [128], B. Malaescu [132], Pa. Malecki [82], V.P. Maleev [134], F. Malek [56], U. Mallik [75], D. Malon [6], C. Malone [31], S. Maltezos [10], S. Malyukov [35], J. Mamuzic [171], G. Mancini [49], I. Mandić [89], J. Maneira [136a], L. Manhaes de Andrade Filho [78a], J. Manjarres Ramos [46], K.H. Mankinen [94], A. Mann [112], A. Manousos [74], B. Mansoulie [142], J.D. Mansour [15a], S. Manzoni [66a,66b], A. Marantis [159], G. Marceca [30], L. March [52], L. Marchese [131], G. Marchiori [132], M. Marcisovsky [137], C. Marcon [94], C.A. Marin Tobon [35], M. Marjanovic [37], F. Marroquim [78b], Z. Marshall [18], M.U.F Martensson [169], S. Marti-Garcia [171], C.B. Martin [122], T.A. Martin [175], V.J. Martin [48], B. Martin dit Latour [17], M. Martinez [14,y], V.I. Martinez Outschoorn [100], S. Martin-Haugh [141], V.S. Martoiu [27b], A.C. Martyniuk [92], A. Marzin [35], L. Masetti [97], T. Mashimo [160], R. Mashinistov [108], J. Masik [98], A.L. Maslennikov [120b,120a], L.H. Mason [102], L. Massa [71a,71b], P. Massarotti [67a,67b], P. Mastrandrea [152], A. Mastroberardino [40b,40a], T. Masubuchi [160], P. Mättig [179], J. Maurer [27b], B. Maček [89], S.J. Maxfield [88], D.A. Maximov [120b,120a], R. Mazini [155], I. Maznas [159], S.M. Mazza [143], G. Mc Goldrick [164], S.P. Mc Kee [103], A. McCarn [41], T.G. McCarthy [113], L.I. McClymont [92], W.P. McCormack [18], E.F. McDonald [102], J.A. Mcfayden [35], G. Mchedlidze [51], M.A. McKay [41], K.D. McLean [173], S.J. McMahon [141], P.C. McNamara [102], C.J. McNicol [175], R.A. McPherson [173,ac], J.E. Mdhluli [32c], Z.A. Meadows [100], S. Meehan [145], T.M. Megy [50], S. Mehlhase [112], A. Mehta [88], T. Meideck [56], B. Meirose [42], D. Melini [171,h], B.R. Mellado Garcia [32c], J.D. Mellenthin [51], M. Melo [28a], F. Meloni [44], A. Melzer [24], S.B. Menary [98], E.D. Mendes Gouveia [136a], L. Meng [88], X.T. Meng [103], S. Menke [113], E. Meoni [40b,40a], S. Mergelmeyer [19], S.A.M. Merkt [135], C. Merlassino [20], P. Mermod [52], L. Merola [67a,67b], C. Meroni [66a], F.S. Merritt [36], A. Messina [70a,70b], J. Metcalfe [6], A.S. Mete [168], C. Meyer [133], J. Meyer [157], J-P. Meyer [142], H. Meyer Zu Theenhausen [59a], F. Miano [153], R.P. Middleton [141], L. Mijović [48], G. Mikenberg [177], M. Mikestikova [137], M. Mikuž [89], M. Milesi [102], A. Milic [164], D.A. Millar [90], D.W. Miller [36], A. Milov [177], D.A. Milstead [43a,43b], R.A. Mina [150,q], A.A. Minaenko [140], M. Miñano Moya [171], I.A. Minashvili [156b], A.I. Mincer [121], B. Mindur [81a], M. Mineev [77], Y. Minegishi [160], Y. Ming [178], L.M. Mir [14], A. Mirto [65a,65b], K.P. Mistry [133], T. Mitani [176], J. Mitrevski [112], V.A. Mitsou [171], M. Mittal [58c], A. Miucci [20], P.S. Miyagawa [146], A. Mizukami [79], J.U. Mjörnmark [94], T. Mkrtchyan [181], M. Mlynarikova [139], T. Moa [43a,43b], K. Mochizuki [107], P. Mogg [50], S. Mohapatra [38], S. Molander [43a,43b], R. Moles-Valls [24], M.C. Mondragon [104], K. Mönig [44], J. Monk [39], E. Monnier [99], A. Montalbano [149], J. Montejo Berlingen [35], F. Monticelli [86], S. Monzani [66a], N. Morange [128], D. Moreno [22], M. Moreno Llácer [35], P. Morettini [53b], M. Morgenstern [118], S. Morgenstern [46], D. Mori [149], M. Morii [57],

M. Morinaga [176], V. Morisbak [130], A.K. Morley [35], G. Mornacchi [35], A.P. Morris [92], J.D. Morris [90], L. Morvaj [152], P. Moschovakos [10], M. Mosidze [156b], H.J. Moss [146], J. Moss [150,n], K. Motohashi [162], R. Mount [150], E. Mountricha [35], E.J.W. Moyse [100], S. Muanza [99], F. Mueller [113], J. Mueller [135], R.S.P. Mueller [112], D. Muenstermann [87], G.A. Mullier [94], F.J. Munoz Sanchez [98], P. Murin [28b], W.J. Murray [175,141], A. Murrone [66a,66b], M. Muškinja [89], C. Mwewa [32a], A.G. Myagkov [140,am], J. Myers [127], M. Myska [138], B.P. Nachman [18], O. Nackenhorst [45], K. Nagai [131], K. Nagano [79], Y. Nagasaka [60], M. Nagel [50], E. Nagy [99], A.M. Nairz [35], Y. Nakahama [115], K. Nakamura [79], T. Nakamura [160], I. Nakano [123], H. Nanjo [129], F. Napolitano [59a], R.F. Naranjo Garcia [44], R. Narayan [11], D.I. Narrias Villar [59a], I. Naryshkin [134], T. Naumann [44], G. Navarro [22], R. Nayyar [7], H.A. Neal [103,*], P.Y. Nechaeva [108], T.J. Neep [142], A. Negri [68a,68b], M. Negrini [23b], S. Nektarijevic [117], C. Nellist [51], M.E. Nelson [131], S. Nemecek [137], P. Nemethy [121], M. Nessi [35,f], M.S. Neubauer [170], M. Neumann [179], P.R. Newman [21], T.Y. Ng [61c], Y.S. Ng [19], Y.W.Y. Ng [168], H.D.N. Nguyen [99], T. Nguyen Manh [107], E. Nibigira [37], R.B. Nickerson [131], R. Nicolaidou [142], D.S. Nielsen [39], J. Nielsen [143], N. Nikiforou [11], V. Nikolaenko [140,am], I. Nikolic-Audit [132], K. Nikolopoulos [21], P. Nilsson [29], Y. Ninomiya [79], A. Nisati [70a], N. Nishu [58c], R. Nisius [113], I. Nitsche [45], T. Nitta [176], T. Nobe [160], Y. Noguchi [83], M. Nomachi [129], I. Nomidis [132], M.A. Nomura [29], T. Nooney [90], M. Nordberg [35], N. Norjoharuddeen [131], T. Novak [89], O. Novgorodova [46], R. Novotny [138], L. Nozka [126], K. Ntekas [168], E. Nurse [92], F. Nuti [102], F.G. Oakham [33,at], H. Oberlack [113], J. Ocariz [132], A. Ochi [80], I. Ochoa [38], J.P. Ochoa-Ricoux [144a], K. O'Connor [26], S. Oda [85], S. Odaka [79], S. Oerdek [51], A. Oh [98], S.H. Oh [47], C.C. Ohm [151], H. Oide [53b,53a], M.L. Ojeda [164], H. Okawa [166], Y. Okazaki [83], Y. Okumura [160], T. Okuyama [79], A. Olariu [27b], L.F. Oleiro Seabra [136a], S.A. Olivares Pino [144a], D. Oliveira Damazio [29], J.L. Oliver [1], M.J.R. Olsson [36], A. Olszewski [82], J. Olszowska [82], D.C. O'Neil [149], A. Onofre [136a,136e], K. Onogi [115], P.U.E. Onyisi [11], H. Oppen [130], M.J. Oreglia [36], G.E. Orellana [86], Y. Oren [158], D. Orestano [72a,72b], E.C. Orgill [98], N. Orlando [61b], A.A. O'Rourke [44], R.S. Orr [164], B. Osculati [53b,53a,*], V. O'Shea [55], R. Ospanov [58a], G. Otero y Garzon [30], H. Otono [85], M. Ouchrif [34d], F. Ould-Saada [130], A. Ouraou [142], Q. Ouyang [15a], M. Owen [55], R.E. Owen [21], V.E. Ozcan [12c], N. Ozturk [8], J. Pacalt [126], H.A. Pacey [31], K. Pachal [149], A. Pacheco Pages [14], L. Pacheco Rodriguez [142], C. Padilla Aranda [14], S. Pagan Griso [18], M. Paganini [180], G. Palacino [63], S. Palazzo [48], S. Palestini [35], M. Palka [81b], D. Pallin [37], I. Panagoulias [10], C.E. Pandini [35], J.G. Panduro Vazquez [91], P. Pani [35], G. Panizzo [64a,64c], L. Paolozzi [52], T.D. Papadopoulou [10], K. Papageorgiou [9,j], A. Paramonov [6], D. Paredes Hernandez [61b], S.R. Paredes Saenz [131], B. Parida [163], A.J. Parker [87], K.A. Parker [44], M.A. Parker [31], F. Parodi [53b,53a], J.A. Parsons [38], U. Parzefall [50], V.R. Pascuzzi [164], J.M.P. Pasner [143], E. Pasqualucci [70a], S. Passaggio [53b], F. Pastore [91], P. Pasuwan [43a,43b], S. Pataraia [97], J.R. Pater [98], A. Pathak [178,k], T. Pauly [35], B. Pearson [113], M. Pedersen [130], L. Pedraza Diaz [117], R. Pedro [136a,136b], S.V. Peleganchuk [120b,120a], O. Penc [137], C. Peng [15d], H. Peng [58a], B.S. Peralva [78a], M.M. Perego [128], A.P. Pereira Peixoto [136a], D.V. Perepelitsa [29], F. Peri [19], L. Perini [66a,66b], H. Pernegger [35], S. Perrella [67a,67b], V.D. Peshekhonov [77,*], K. Peters [44], R.F.Y. Peters [98], B.A. Petersen [35], T.C. Petersen [39], E. Petit [56], A. Petridis [1], C. Petridou [159], P. Petroff [128], M. Petrov [131], F. Petrucci [72a,72b], M. Pettee [180], N.E. Pettersson [100], A. Peyaud [142], R. Pezoa [144b], T. Pham [102], F.H. Phillips [104], P.W. Phillips [141], M.W. Phipps [170], G. Piacquadio [152], E. Pianori [18], A. Picazio [100], M.A. Pickering [131], R.H. Pickles [98], R. Piegaia [30], J.E. Pilcher [36], A.D. Pilkington [98], M. Pinamonti [71a,71b], J.L. Pinfold [3], M. Pitt [177], L. Pizzimento [71a,71b], M-A. Pleier [29], V. Pleskot [139], E. Plotnikova [77], D. Pluth [76], P. Podberezko [120b,120a], R. Poettgen [94], R. Poggi [52], L. Poggioli [128], I. Pogrebnyak [104], D. Pohl [24], I. Pokharel [51], G. Polesello [68a], A. Poley [18], A. Policicchio [70a,70b], R. Polifka [35], A. Polini [23b], C.S. Pollard [44], V. Polychronakos [29], D. Ponomarenko [110], L. Pontecorvo [70a], G.A. Popeneciu [27d], D.M. Portillo Quintero [132], S. Pospisil [138], K. Potamianos [44], I.N. Potrap [77], C.J. Potter [31], H. Potti [11], T. Poulsen [94], J. Poveda [35], T.D. Powell [146], M.E. Pozo Astigarraga [35], P. Pralavorio [99], S. Prell [76], D. Price [98], M. Primavera [65a], S. Prince [101], N. Proklova [110], K. Prokofiev [61c], F. Prokoshin [144b], S. Protopopescu [29], J. Proudfoot [6], M. Przybycien [81a], A. Puri [170], P. Puzo [128], J. Qian [103], Y. Qin [98], A. Quadt [51], M. Queitsch-Maitland [44], A. Qureshi [1], P. Rados [102], F. Ragusa [66a,66b], G. Rahal [95], J.A. Raine [52], S. Rajagopalan [29], A. Ramirez Morales [90], T. Rashid [128], S. Raspopov [5], M.G. Ratti [66a,66b], D.M. Rauch [44], F. Rauscher [112], S. Rave [97], B. Ravina [146], I. Ravinovich [177], J.H. Rawling [98], M. Raymond [35], A.L. Read [130], N.P. Readioff [56], M. Reale [65a,65b], D.M. Rebuzzi [68a,68b], A. Redelbach [174], G. Redlinger [29], R. Reece [143], R.G. Reed [32c], K. Reeves [42], L. Rehnisch [19], J. Reichert [133], D. Reikher [158], A. Reiss [97], C. Rembser [35], H. Ren [15d], M. Rescigno [70a],

S. Resconi [66a], E.D. Resseguie [133], S. Rettie [172], E. Reynolds [21], O.L. Rezanova [120b,120a], P. Reznicek [139], E. Ricci [73a,73b], R. Richter [113], S. Richter [44], E. Richter-Was [81b], O. Ricken [24], M. Ridel [132], P. Rieck [113], C.J. Riegel [179], O. Rifki [44], M. Rijssenbeek [152], A. Rimoldi [68a,68b], M. Rimoldi [20], L. Rinaldi [23b], G. Ripellino [151], B. Ristić [87], E. Ritsch [35], I. Riu [14], J.C. Rivera Vergara [144a], F. Rizatdinova [125], E. Rizvi [90], C. Rizzi [14], R.T. Roberts [98], S.H. Robertson [101,ac], D. Robinson [31], J.E.M. Robinson [44], A. Robson [55], E. Rocco [97], C. Roda [69a,69b], Y. Rodina [99], S. Rodriguez Bosca [171], A. Rodriguez Perez [14], D. Rodriguez Rodriguez [171], A.M. Rodríguez Vera [165b], S. Roe [35], C.S. Rogan [57], O. Røhne [130], R. Röhrig [113], C.P.A. Roland [63], J. Roloff [57], A. Romaniouk [110], M. Romano [23b,23a], N. Rompotis [88], M. Ronzani [121], L. Roos [132], S. Rosati [70a], K. Rosbach [50], N-A. Rosien [51], B.J. Rosser [133], E. Rossi [44], E. Rossi [72a,72b], E. Rossi [67a,67b], L.P. Rossi [53b], L. Rossini [66a,66b], J.H.N. Rosten [31], R. Rosten [14], M. Rotaru [27b], J. Rothberg [145], D. Rousseau [128], D. Roy [32c], A. Rozanov [99], Y. Rozen [157], X. Ruan [32c], F. Rubbo [150], F. Rühr [50], A. Ruiz-Martinez [171], Z. Rurikova [50], N.A. Rusakovich [77], H.L. Russell [101], J.P. Rutherfoord [7], E.M. Rüttinger [44,l], Y.F. Ryabov [134], M. Rybar [170], G. Rybkin [128], S. Ryu [6], A. Ryzhov [140], G.F. Rzehorz [51], P. Sabatini [51], G. Sabato [118], S. Sacerdoti [128], H.F-W. Sadrozinski [143], R. Sadykov [77], F. Safai Tehrani [70a], P. Saha [119], M. Sahinsoy [59a], A. Sahu [179], M. Saimpert [44], M. Saito [160], T. Saito [160], H. Sakamoto [160], A. Sakharov [121,al], D. Salamani [52], G. Salamanna [72a,72b], J.E. Salazar Loyola [144b], P.H. Sales De Bruin [169], D. Salihagic [113], A. Salnikov [150], J. Salt [171], D. Salvatore [40b,40a], F. Salvatore [153], A. Salvucci [61a,61b,61c], A. Salzburger [35], J. Samarati [35], D. Sammel [50], D. Sampsonidis [159], D. Sampsonidou [159], J. Sánchez [171], A. Sanchez Pineda [64a,64c], H. Sandaker [130], C.O. Sander [44], M. Sandhoff [179], C. Sandoval [22], D.P.C. Sankey [141], M. Sannino [53b,53a], Y. Sano [115], A. Sansoni [49], C. Santoni [37], H. Santos [136a], I. Santoyo Castillo [153], A. Santra [171], A. Sapronov [77], J.G. Saraiva [136a,136d], O. Sasaki [79], K. Sato [166], E. Sauvan [5], P. Savard [164,at], N. Savic [113], R. Sawada [160], C. Sawyer [141], L. Sawyer [93,aj], C. Sbarra [23b], A. Sbrizzi [23b,23a], T. Scanlon [92], J. Schaarschmidt [145], P. Schacht [113], B.M. Schachtner [112], D. Schaefer [36], L. Schaefer [133], J. Schaeffer [97], S. Schaepe [35], U. Schäfer [97], A.C. Schaffer [128], D. Schaile [112], R.D. Schamberger [152], N. Scharmberg [98], V.A. Schegelsky [134], D. Scheirich [139], F. Schenck [19], M. Schernau [168], C. Schiavi [53b,53a], S. Schier [143], L.K. Schildgen [24], Z.M. Schillaci [26], E.J. Schioppa [35], M. Schioppa [40b,40a], K.E. Schleicher [50], S. Schlenker [35], K.R. Schmidt-Sommerfeld [113], K. Schmieden [35], C. Schmitt [97], S. Schmitt [44], S. Schmitz [97], J.C. Schmoeckel [44], U. Schnoor [50], L. Schoeffel [142], A. Schoening [59b], E. Schopf [131], M. Schott [97], J.F.P. Schouwenberg [117], J. Schovancova [35], S. Schramm [52], A. Schulte [97], H-C. Schultz-Coulon [59a], M. Schumacher [50], B.A. Schumm [143], Ph. Schune [142], A. Schwartzman [150], T.A. Schwarz [103], Ph. Schwemling [142], R. Schwienhorst [104], A. Sciandra [24], G. Sciolla [26], M. Scornajenghi [40b,40a], F. Scuri [69a], F. Scutti [102], L.M. Scyboz [113], C.D. Sebastiani [70a,70b], P. Seema [19], S.C. Seidel [116], A. Seiden [143], T. Seiss [36], J.M. Seixas [78b], G. Sekhniaidze [67a], K. Sekhon [103], S.J. Sekula [41], N. Semprini-Cesari [23b,23a], S. Sen [47], S. Senkin [37], C. Serfon [130], L. Serin [128], L. Serkin [64a,64b], M. Sessa [58a], H. Severini [124], F. Sforza [167], A. Sfyrla [52], E. Shabalina [51], J.D. Shahinian [143], N.W. Shaikh [43a,43b], D. Shaked Renous [177], L.Y. Shan [15a], R. Shang [170], J.T. Shank [25], M. Shapiro [18], A.S. Sharma [1], A. Sharma [131], P.B. Shatalov [109], K. Shaw [153], S.M. Shaw [98], A. Shcherbakova [134], Y. Shen [124], N. Sherafati [33], A.D. Sherman [25], P. Sherwood [92], L. Shi [155,ap], S. Shimizu [79], C.O. Shimmin [180], Y. Shimogama [176], M. Shimojima [114], I.P.J. Shipsey [131], S. Shirabe [85], M. Shiyakova [77], J. Shlomi [177], A. Shmeleva [108], D. Shoaleh Saadi [107], M.J. Shochet [36], S. Shojaii [102], D.R. Shope [124], S. Shrestha [122], E. Shulga [110], P. Sicho [137], A.M. Sickles [170], P.E. Sidebo [151], E. Sideras Haddad [32c], O. Sidiropoulou [35], A. Sidoti [23b,23a], F. Siegert [46], Dj. Sijacki [16], J. Silva [136a], M. Silva Jr. [178], M.V. Silva Oliveira [78a], S.B. Silverstein [43a], S. Simion [128], E. Simioni [97], M. Simon [97], R. Simoniello [97], P. Sinervo [164], N.B. Sinev [127], M. Sioli [23b,23a], I. Siral [103], S.Yu. Sivoklokov [111], J. Sjölin [43a,43b], P. Skubic [124], M. Slater [21], T. Slavicek [138], M. Slawinska [82], K. Sliwa [167], R. Slovak [139], V. Smakhtin [177], B.H. Smart [5], J. Smiesko [28a], N. Smirnov [110], S.Yu. Smirnov [110], Y. Smirnov [110], L.N. Smirnova [111], O. Smirnova [94], J.W. Smith [51], M. Smizanska [87], K. Smolek [138], A. Smykiewicz [82], A.A. Snesarev [108], I.M. Snyder [127], S. Snyder [29], R. Sobie [173,ac], A.M. Soffa [168], A. Soffer [158], A. Søgaard [48], D.A. Soh [155], G. Sokhrannyi [89], C.A. Solans Sanchez [35], M. Solar [138], E.Yu. Soldatov [110], U. Soldevila [171], A.A. Solodkov [140], A. Soloshenko [77], O.V. Solovyanov [140], V. Solovyev [134], P. Sommer [146], H. Son [167], W. Song [141], W.Y. Song [165b], A. Sopczak [138], F. Sopkova [28b], C.L. Sotiropoulou [69a,69b], S. Sottocornola [68a,68b], R. Soualah [64a,64c,i], A.M. Soukharev [120b,120a], D. South [44], B.C. Sowden [91], S. Spagnolo [65a,65b], M. Spalla [113], M. Spangenberg [175], F. Spanò [91], D. Sperlich [19],

T.M. Spieker [59a], R. Spighi [23b], G. Spigo [35], L.A. Spiller [102], D.P. Spiteri [55], M. Spousta [139], A. Stabile [66a,66b], R. Stamen [59a], S. Stamm [19], E. Stanecka [82], R.W. Stanek [6], C. Stanescu [72a], B. Stanislaus [131], M.M. Stanitzki [44], B. Stapf [118], S. Stapnes [130], E.A. Starchenko [140], G.H. Stark [36], J. Stark [56], S.H Stark [39], P. Staroba [137], P. Starovoitov [59a], S. Stärz [35], R. Staszewski [82], M. Stegler [44], P. Steinberg [29], B. Stelzer [149], H.J. Stelzer [35], O. Stelzer-Chilton [165a], H. Stenzel [54], T.J. Stevenson [90], G.A. Stewart [55], M.C. Stockton [35], G. Stoicea [27b], P. Stolte [51], S. Stonjek [113], A. Straessner [46], J. Strandberg [151], S. Strandberg [43a,43b], M. Strauss [124], P. Strizenec [28b], R. Ströhmer [174], D.M. Strom [127], R. Stroynowski [41], A. Strubig [48], S.A. Stucci [29], B. Stugu [17], J. Stupak [124], N.A. Styles [44], D. Su [150], J. Su [135], S. Suchek [59a], Y. Sugaya [129], M. Suk [138], V.V. Sulin [108], M.J. Sullivan [88], D.M.S. Sultan [52], S. Sultansoy [4c], T. Sumida [83], S. Sun [103], X. Sun [3], K. Suruliz [153], C.J.E. Suster [154], M.R. Sutton [153], S. Suzuki [79], M. Svatos [137], M. Swiatlowski [36], S.P. Swift [2], A. Sydorenko [97], I. Sykora [28a], T. Sykora [139], D. Ta [97], K. Tackmann [44,z], J. Taenzer [158], A. Taffard [168], R. Tafirout [165a], E. Tahirovic [90], N. Taiblum [158], H. Takai [29], R. Takashima [84], E.H. Takasugi [113], K. Takeda [80], T. Takeshita [147], Y. Takubo [79], M. Talby [99], A.A. Talyshev [120b,120a], J. Tanaka [160], M. Tanaka [162], R. Tanaka [128], B.B. Tannenwald [122], S. Tapia Araya [144b], S. Tapprogge [97], A. Tarek Abouelfadl Mohamed [132], S. Tarem [157], G. Tarna [27b,e], G.F. Tartarelli [66a], P. Tas [139], M. Tasevsky [137], T. Tashiro [83], E. Tassi [40b,40a], A. Tavares Delgado [136a,136b], Y. Tayalati [34e], A.C. Taylor [116], A.J. Taylor [48], G.N. Taylor [102], P.T.E. Taylor [102], W. Taylor [165b], A.S. Tee [87], P. Teixeira-Dias [91], H. Ten Kate [35], J.J. Teoh [118], S. Terada [79], K. Terashi [160], J. Terron [96], S. Terzo [14], M. Testa [49], R.J. Teuscher [164,ac], S.J. Thais [180], T. Theveneaux-Pelzer [44], F. Thiele [39], D.W. Thomas [91], J.P. Thomas [21], A.S. Thompson [55], P.D. Thompson [21], L.A. Thomsen [180], E. Thomson [133], Y. Tian [38], R.E. Ticse Torres [51], V.O. Tikhomirov [108,an], Yu.A. Tikhonov [120b,120a], S. Timoshenko [110], P. Tipton [180], S. Tisserant [99], K. Todome [162], S. Todorova-Nova [5], S. Todt [46], J. Tojo [85], S. Tokár [28a], K. Tokushuku [79], E. Tolley [122], K.G. Tomiwa [32c], M. Tomoto [115], L. Tompkins [150,q], K. Toms [116], B. Tong [57], P. Tornambe [50], E. Torrence [127], H. Torres [46], E. Torró Pastor [145], C. Tosciri [131], J. Toth [99,ab], F. Touchard [99], D.R. Tovey [146], C.J. Treado [121], T. Trefzger [174], F. Tresoldi [153], A. Tricoli [29], I.M. Trigger [165a], S. Trincaz-Duvoid [132], M.F. Tripiana [14], W. Trischuk [164], B. Trocmé [56], A. Trofymov [128], C. Troncon [66a], M. Trovatelli [173], F. Trovato [153], L. Truong [32b], M. Trzebinski [82], A. Trzupek [82], F. Tsai [44], J.C-L. Tseng [131], P.V. Tsiareshka [105,ah], A. Tsirigotis [159], N. Tsirintanis [9], V. Tsiskaridze [152], E.G. Tskhadadze [156a], I.I. Tsukerman [109], V. Tsulaia [18], S. Tsuno [79], D. Tsybychev [152,163], Y. Tu [61b], A. Tudorache [27b], V. Tudorache [27b], T.T. Tulbure [27a], A.N. Tuna [57], S. Turchikhin [77], D. Turgeman [177], I. Turk Cakir [4b,t], R. Turra [66a], P.M. Tuts [38], E. Tzovara [97], G. Ucchielli [45], I. Ueda [79], M. Ughetto [43a,43b], F. Ukegawa [166], G. Unal [35], A. Undrus [29], G. Unel [168], F.C. Ungaro [102], Y. Unno [79], K. Uno [160], J. Urban [28b], P. Urquijo [102], P. Urrejola [97], G. Usai [8], J. Usui [79], L. Vacavant [99], V. Vacek [138], B. Vachon [101], K.O.H. Vadla [130], A. Vaidya [92], C. Valderanis [112], E. Valdes Santurio [43a,43b], M. Valente [52], S. Valentinetti [23b,23a], A. Valero [171], L. Valéry [44], R.A. Vallance [21], A. Vallier [5], J.A. Valls Ferrer [171], T.R. Van Daalen [14], H. Van der Graaf [118], P. Van Gemmeren [6], I. Van Vulpen [118], M. Vanadia [71a,71b], W. Vandelli [35], A. Vaniachine [163], P. Vankov [118], R. Vari [70a], E.W. Varnes [7], C. Varni [53b,53a], T. Varol [41], D. Varouchas [128], K.E. Varvell [154], G.A. Vasquez [144b], J.G. Vasquez [180], F. Vazeille [37], D. Vazquez Furelos [14], T. Vazquez Schroeder [35], J. Veatch [51], V. Vecchio [72a,72b], L.M. Veloce [164], F. Veloso [136a,136c], S. Veneziano [70a], A. Ventura [65a,65b], N. Venturi [35], V. Vercesi [68a], M. Verducci [72a,72b], C.M. Vergel Infante [76], C. Vergis [24], W. Verkerke [118], A.T. Vermeulen [118], J.C. Vermeulen [118], M.C. Vetterli [149,at], N. Viaux Maira [144b], M. Vicente Barreto Pinto [52], I. Vichou [170,*], T. Vickey [146], O.E. Vickey Boeriu [146], G.H.A. Viehhauser [131], S. Viel [18], L. Vigani [131], M. Villa [23b,23a], M. Villaplana Perez [66a,66b], E. Vilucchi [49], M.G. Vincter [33], V.B. Vinogradov [77], A. Vishwakarma [44], C. Vittori [23b,23a], I. Vivarelli [153], S. Vlachos [10], M. Vogel [179], P. Vokac [138], G. Volpi [14], S.E. von Buddenbrock [32c], E. Von Toerne [24], V. Vorobel [139], K. Vorobev [110], M. Vos [171], J.H. Vossebeld [88], N. Vranjes [16], M. Vranjes Milosavljevic [16], V. Vrba [138], M. Vreeswijk [118], T. Šfiligoj [89], R. Vuillermet [35], I. Vukotic [36], T. Ženiš [28a], L. Živković [16], P. Wagner [24], W. Wagner [179], J. Wagner-Kuhr [112], H. Wahlberg [86], S. Wahrmund [46], K. Wakamiya [80], V.M. Walbrecht [113], J. Walder [87], R. Walker [112], S.D. Walker [91], W. Walkowiak [148], V. Wallangen [43a,43b], A.M. Wang [57], C. Wang [58b], F. Wang [178], H. Wang [18], H. Wang [3], J. Wang [154], J. Wang [59b], P. Wang [41], Q. Wang [124], R.-J. Wang [132], R. Wang [58a], R. Wang [6], S.M. Wang [155], W.T. Wang [58a], W. Wang [15c,ad], W.X. Wang [58a,ad], Y. Wang [58a,ak], Z. Wang [58c], C. Wanotayaroj [44], A. Warburton [101], C.P. Ward [31], D.R. Wardrope [92], A. Washbrook [48], P.M. Watkins [21], A.T. Watson [21], M.F. Watson [21], G. Watts [145], S. Watts [98], B.M. Waugh [92], A.F. Webb [11], S. Webb [97], C. Weber [180],

M.S. Weber [20], S.A. Weber [33], S.M. Weber [59a], A.R. Weidberg [131], J. Weingarten [45], M. Weirich [97], C. Weiser [50], P.S. Wells [35], T. Wenaus [29], T. Wengler [35], S. Wenig [35], N. Wermes [24], M.D. Werner [76], P. Werner [35], M. Wessels [59a], T.D. Weston [20], K. Whalen [127], N.L. Whallon [145], A.M. Wharton [87], A.S. White [103], A. White [8], M.J. White [1], R. White [144b], D. Whiteson [168], B.W. Whitmore [87], F.J. Wickens [141], W. Wiedenmann [178], M. Wielers [141], C. Wiglesworth [39], L.A.M. Wiik-Fuchs [50], F. Wilk [98], H.G. Wilkens [35], L.J. Wilkins [91], H.H. Williams [133], S. Williams [31], C. Willis [104], S. Willocq [100], J.A. Wilson [21], I. Wingerter-Seez [5], E. Winkels [153], F. Winklmeier [127], O.J. Winston [153], B.T. Winter [50], M. Wittgen [150], M. Wobisch [93], A. Wolf [97], T.M.H. Wolf [118], R. Wolff [99], M.W. Wolter [82], H. Wolters [136a,136c], V.W.S. Wong [172], N.L. Woods [143], S.D. Worm [21], B.K. Wosiek [82], K.W. Woźniak [82], K. Wraight [55], M. Wu [36], S.L. Wu [178], X. Wu [52], Y. Wu [58a], T.R. Wyatt [98], B.M. Wynne [48], S. Xella [39], Z. Xi [103], L. Xia [175], D. Xu [15a], H. Xu [58a,e], L. Xu [29], T. Xu [142], W. Xu [103], B. Yabsley [154], S. Yacoob [32a], K. Yajima [129], D.P. Yallup [92], D. Yamaguchi [162], Y. Yamaguchi [162], A. Yamamoto [79], T. Yamanaka [160], F. Yamane [80], M. Yamatani [160], T. Yamazaki [160], Y. Yamazaki [80], Z. Yan [25], H.J. Yang [58c,58d], H.T. Yang [18], S. Yang [75], Y. Yang [160], Z. Yang [17], W-M. Yao [18], Y.C. Yap [44], Y. Yasu [79], E. Yatsenko [58c,58d], J. Ye [41], S. Ye [29], I. Yeletskikh [77], E. Yigitbasi [25], E. Yildirim [97], K. Yorita [176], K. Yoshihara [133], C.J.S. Young [35], C. Young [150], J. Yu [8], J. Yu [76], X. Yue [59a], S.P.Y. Yuen [24], B. Zabinski [82], G. Zacharis [10], E. Zaffaroni [52], R. Zaidan [14], A.M. Zaitsev [140,am], T. Zakareishvili [156b], N. Zakharchuk [33], J. Zalieckas [17], S. Zambito [57], D. Zanzi [35], D.R. Zaripovas [55], S.V. Zeißner [45], C. Zeitnitz [179], G. Zemaityte [131], J.C. Zeng [170], Q. Zeng [150], O. Zenin [140], D. Zerwas [128], M. Zgubič [131], D.F. Zhang [58b], D. Zhang [103], F. Zhang [178], G. Zhang [58a], G. Zhang [15b], H. Zhang [15c], J. Zhang [6], L. Zhang [15c], L. Zhang [58a], M. Zhang [170], P. Zhang [15c], R. Zhang [58a], R. Zhang [24], X. Zhang [58b], Y. Zhang [15d], Z. Zhang [128], P. Zhao [47], Y. Zhao [58b,128,ai], Z. Zhao [58a], A. Zhemchugov [77], Z. Zheng [103], D. Zhong [170], B. Zhou [103], C. Zhou [178], L. Zhou [41], M.S. Zhou [15d], M. Zhou [152], N. Zhou [58c], Y. Zhou [7], C.G. Zhu [58b], H.L. Zhu [58a], H. Zhu [15a], J. Zhu [103], Y. Zhu [58a], X. Zhuang [15a], K. Zhukov [108], V. Zhulanov [120b,120a], A. Zibell [174], D. Zieminska [63], N.I. Zimine [77], S. Zimmermann [50], Z. Zinonos [113], M. Ziolkowski [148], G. Zobernig [178], A. Zoccoli [23b,23a], K. Zoch [51], T.G. Zorbas [146], R. Zou [36], M. Zur Nedden [19], L. Zwalinski [35]

[1] *Department of Physics, University of Adelaide, Adelaide, Australia*
[2] *Physics Department, SUNY Albany, Albany, NY, United States of America*
[3] *Department of Physics, University of Alberta, Edmonton, AB, Canada*
[4] [(a)] *Department of Physics, Ankara University, Ankara;* [(b)] *Istanbul Aydin University, Istanbul;* [(c)] *Division of Physics, TOBB University of Economics and Technology, Ankara, Turkey*
[5] *LAPP, Université Grenoble Alpes, Université Savoie Mont Blanc, CNRS/IN2P3, Annecy, France*
[6] *High Energy Physics Division, Argonne National Laboratory, Argonne, IL, United States of America*
[7] *Department of Physics, University of Arizona, Tucson, AZ, United States of America*
[8] *Department of Physics, University of Texas at Arlington, Arlington, TX, United States of America*
[9] *Physics Department, National and Kapodistrian University of Athens, Athens, Greece*
[10] *Physics Department, National Technical University of Athens, Zografou, Greece*
[11] *Department of Physics, University of Texas at Austin, Austin, TX, United States of America*
[12] [(a)] *Bahcesehir University, Faculty of Engineering and Natural Sciences, Istanbul;* [(b)] *Istanbul Bilgi University, Faculty of Engineering and Natural Sciences, Istanbul;* [(c)] *Department of Physics, Bogazici University, Istanbul;* [(d)] *Department of Physics Engineering, Gaziantep University, Gaziantep, Turkey*
[13] *Institute of Physics, Azerbaijan Academy of Sciences, Baku, Azerbaijan*
[14] *Institut de Física d'Altes Energies (IFAE), Barcelona Institute of Science and Technology, Barcelona, Spain*
[15] [(a)] *Institute of High Energy Physics, Chinese Academy of Sciences, Beijing;* [(b)] *Physics Department, Tsinghua University, Beijing;* [(c)] *Department of Physics, Nanjing University, Nanjing;* [(d)] *University of Chinese Academy of Science (UCAS), Beijing, China*
[16] *Institute of Physics, University of Belgrade, Belgrade, Serbia*
[17] *Department for Physics and Technology, University of Bergen, Bergen, Norway*
[18] *Physics Division, Lawrence Berkeley National Laboratory and University of California, Berkeley, CA, United States of America*
[19] *Institut für Physik, Humboldt Universität zu Berlin, Berlin, Germany*
[20] *Albert Einstein Center for Fundamental Physics and Laboratory for High Energy Physics, University of Bern, Bern, Switzerland*
[21] *School of Physics and Astronomy, University of Birmingham, Birmingham, United Kingdom*
[22] *Centro de Investigaciónes, Universidad Antonio Nariño, Bogota, Colombia*
[23] [(a)] *Dipartimento di Fisica e Astronomia, Università di Bologna, Bologna;* [(b)] *INFN Sezione di Bologna, Italy*
[24] *Physikalisches Institut, Universität Bonn, Bonn, Germany*
[25] *Department of Physics, Boston University, Boston, MA, United States of America*
[26] *Department of Physics, Brandeis University, Waltham, MA, United States of America*
[27] [(a)] *Transilvania University of Brasov, Brasov;* [(b)] *Horia Hulubei National Institute of Physics and Nuclear Engineering, Bucharest;* [(c)] *Department of Physics, Alexandru Ioan Cuza University of Iasi, Iasi;* [(d)] *National Institute for Research and Development of Isotopic and Molecular Technologies, Physics Department, Cluj-Napoca;* [(e)] *University Politehnica Bucharest, Bucharest;* [(f)] *West University in Timisoara, Timisoara, Romania*
[28] [(a)] *Faculty of Mathematics, Physics and Informatics, Comenius University, Bratislava;* [(b)] *Department of Subnuclear Physics, Institute of Experimental Physics of the Slovak Academy of Sciences, Kosice, Slovak Republic*
[29] *Physics Department, Brookhaven National Laboratory, Upton, NY, United States of America*
[30] *Departamento de Física, Universidad de Buenos Aires, Buenos Aires, Argentina*
[31] *Cavendish Laboratory, University of Cambridge, Cambridge, United Kingdom*
[32] [(a)] *Department of Physics, University of Cape Town, Cape Town;* [(b)] *Department of Mechanical Engineering Science, University of Johannesburg, Johannesburg;* [(c)] *School of Physics, University of the Witwatersrand, Johannesburg, South Africa*
[33] *Department of Physics, Carleton University, Ottawa, ON, Canada*

[34] [(a)] Faculté des Sciences Ain Chock, Réseau Universitaire de Physique des Hautes Energies – Université Hassan II, Casablanca; [(b)] Centre National de l'Energie des Sciences Techniques Nucleaires (CNESTEN), Rabat; [(c)] Faculté des Sciences Semlalia, Université Cadi Ayyad, LPHEA, Marrakech; [(d)] Faculté des Sciences, Université Mohamed Premier and LPTPM, Oujda; [(e)] Faculté des sciences, Université Mohammed V, Rabat, Morocco
[35] CERN, Geneva, Switzerland
[36] Enrico Fermi Institute, University of Chicago, Chicago, IL, United States of America
[37] LPC, Université Clermont Auvergne, CNRS/IN2P3, Clermont-Ferrand, France
[38] Nevis Laboratory, Columbia University, Irvington, NY, United States of America
[39] Niels Bohr Institute, University of Copenhagen, Copenhagen, Denmark
[40] [(a)] Dipartimento di Fisica, Università della Calabria, Rende; [(b)] INFN Gruppo Collegato di Cosenza, Laboratori Nazionali di Frascati, Italy
[41] Physics Department, Southern Methodist University, Dallas, TX, United States of America
[42] Physics Department, University of Texas at Dallas, Richardson, TX, United States of America
[43] [(a)] Department of Physics, Stockholm University; [(b)] Oskar Klein Centre, Stockholm, Sweden
[44] Deutsches Elektronen-Synchrotron DESY, Hamburg and Zeuthen, Germany
[45] Lehrstuhl für Experimentelle Physik IV, Technische Universität Dortmund, Dortmund, Germany
[46] Institut für Kern- und Teilchenphysik, Technische Universität Dresden, Dresden, Germany
[47] Department of Physics, Duke University, Durham, NC, United States of America
[48] SUPA – School of Physics and Astronomy, University of Edinburgh, Edinburgh, United Kingdom
[49] INFN e Laboratori Nazionali di Frascati, Frascati, Italy
[50] Physikalisches Institut, Albert-Ludwigs-Universität Freiburg, Freiburg, Germany
[51] II. Physikalisches Institut, Georg-August-Universität Göttingen, Göttingen, Germany
[52] Département de Physique Nucléaire et Corpusculaire, Université de Genève, Genève, Switzerland
[53] [(a)] Dipartimento di Fisica, Università di Genova, Genova; [(b)] INFN Sezione di Genova, Italy
[54] II. Physikalisches Institut, Justus-Liebig-Universität Giessen, Giessen, Germany
[55] SUPA – School of Physics and Astronomy, University of Glasgow, Glasgow, United Kingdom
[56] LPSC, Université Grenoble Alpes, CNRS/IN2P3, Grenoble INP, Grenoble, France
[57] Laboratory for Particle Physics and Cosmology, Harvard University, Cambridge, MA, United States of America
[58] [(a)] Department of Modern Physics and State Key Laboratory of Particle Detection and Electronics, University of Science and Technology of China, Hefei; [(b)] Institute of Frontier and Interdisciplinary Science and Key Laboratory of Particle Physics and Particle Irradiation (MOE), Shandong University, Qingdao; [(c)] School of Physics and Astronomy, Shanghai Jiao Tong University, KLPPAC-MoE, SKLPPC, Shanghai; [(d)] Tsung-Dao Lee Institute, Shanghai, China
[59] [(a)] Kirchhoff-Institut für Physik, Ruprecht-Karls-Universität Heidelberg, Heidelberg; [(b)] Physikalisches Institut, Ruprecht-Karls-Universität Heidelberg, Heidelberg, Germany
[60] Faculty of Applied Information Science, Hiroshima Institute of Technology, Hiroshima, Japan
[61] [(a)] Department of Physics, Chinese University of Hong Kong, Shatin, N.T., Hong Kong; [(b)] Department of Physics, University of Hong Kong, Hong Kong; [(c)] Department of Physics and Institute for Advanced Study, Hong Kong University of Science and Technology, Clear Water Bay, Kowloon, Hong Kong, China
[62] Department of Physics, National Tsing Hua University, Hsinchu, Taiwan
[63] Department of Physics, Indiana University, Bloomington, IN, United States of America
[64] [(a)] INFN Gruppo Collegato di Udine, Sezione di Trieste, Udine; [(b)] ICTP, Trieste; [(c)] Dipartimento di Chimica, Fisica e Ambiente, Università di Udine, Udine, Italy
[65] [(a)] INFN Sezione di Lecce; [(b)] Dipartimento di Matematica e Fisica, Università del Salento, Lecce, Italy
[66] [(a)] INFN Sezione di Milano; [(b)] Dipartimento di Fisica, Università di Milano, Milano, Italy
[67] [(a)] INFN Sezione di Napoli; [(b)] Dipartimento di Fisica, Università di Napoli, Napoli, Italy
[68] [(a)] INFN Sezione di Pavia; [(b)] Dipartimento di Fisica, Università di Pavia, Pavia, Italy
[69] [(a)] INFN Sezione di Pisa; [(b)] Dipartimento di Fisica E. Fermi, Università di Pisa, Pisa, Italy
[70] [(a)] INFN Sezione di Roma; [(b)] Dipartimento di Fisica, Sapienza Università di Roma, Roma, Italy
[71] [(a)] INFN Sezione di Roma Tor Vergata; [(b)] Dipartimento di Fisica, Università di Roma Tor Vergata, Roma, Italy
[72] [(a)] INFN Sezione di Roma Tre; [(b)] Dipartimento di Matematica e Fisica, Università Roma Tre, Roma, Italy
[73] [(a)] INFN-TIFPA; [(b)] Università degli Studi di Trento, Trento, Italy
[74] Institut für Astro- und Teilchenphysik, Leopold-Franzens-Universität, Innsbruck, Austria
[75] University of Iowa, Iowa City, IA, United States of America
[76] Department of Physics and Astronomy, Iowa State University, Ames, IA, United States of America
[77] Joint Institute for Nuclear Research, Dubna, Russia
[78] [(a)] Departamento de Engenharia Elétrica, Universidade Federal de Juiz de Fora (UFJF), Juiz de Fora; [(b)] Universidade Federal do Rio De Janeiro COPPE/EE/IF, Rio de Janeiro; [(c)] Universidade Federal de São João del Rei (UFSJ), São João del Rei; [(d)] Instituto de Física, Universidade de São Paulo, São Paulo, Brazil
[79] KEK, High Energy Accelerator Research Organization, Tsukuba, Japan
[80] Graduate School of Science, Kobe University, Kobe, Japan
[81] [(a)] AGH University of Science and Technology, Faculty of Physics and Applied Computer Science, Krakow; [(b)] Marian Smoluchowski Institute of Physics, Jagiellonian University, Krakow, Poland
[82] Institute of Nuclear Physics Polish Academy of Sciences, Krakow, Poland
[83] Faculty of Science, Kyoto University, Kyoto, Japan
[84] Kyoto University of Education, Kyoto, Japan
[85] Research Center for Advanced Particle Physics and Department of Physics, Kyushu University, Fukuoka, Japan
[86] Instituto de Física La Plata, Universidad Nacional de La Plata and CONICET, La Plata, Argentina
[87] Physics Department, Lancaster University, Lancaster, United Kingdom
[88] Oliver Lodge Laboratory, University of Liverpool, Liverpool, United Kingdom
[89] Department of Experimental Particle Physics, Jožef Stefan Institute and Department of Physics, University of Ljubljana, Ljubljana, Slovenia
[90] School of Physics and Astronomy, Queen Mary University of London, London, United Kingdom
[91] Department of Physics, Royal Holloway University of London, Egham, United Kingdom
[92] Department of Physics and Astronomy, University College London, London, United Kingdom
[93] Louisiana Tech University, Ruston, LA, United States of America
[94] Fysiska institutionen, Lunds universitet, Lund, Sweden
[95] Centre de Calcul de l'Institut National de Physique Nucléaire et de Physique des Particules (IN2P3), Villeurbanne, France
[96] Departamento de Física Teorica C-15 and CIAFF, Universidad Autónoma de Madrid, Madrid, Spain
[97] Institut für Physik, Universität Mainz, Mainz, Germany
[98] School of Physics and Astronomy, University of Manchester, Manchester, United Kingdom
[99] CPPM, Aix-Marseille Université, CNRS/IN2P3, Marseille, France
[100] Department of Physics, University of Massachusetts, Amherst, MA, United States of America
[101] Department of Physics, McGill University, Montreal, QC, Canada
[102] School of Physics, University of Melbourne, Victoria, Australia
[103] Department of Physics, University of Michigan, Ann Arbor, MI, United States of America
[104] Department of Physics and Astronomy, Michigan State University, East Lansing, MI, United States of America
[105] B.I. Stepanov Institute of Physics, National Academy of Sciences of Belarus, Minsk, Belarus

[106] Research Institute for Nuclear Problems of Byelorussian State University, Minsk, Belarus
[107] Group of Particle Physics, University of Montreal, Montreal, QC, Canada
[108] P.N. Lebedev Physical Institute of the Russian Academy of Sciences, Moscow, Russia
[109] Institute for Theoretical and Experimental Physics (ITEP), Moscow, Russia
[110] National Research Nuclear University MEPhI, Moscow, Russia
[111] D.V. Skobeltsyn Institute of Nuclear Physics, M.V. Lomonosov Moscow State University, Moscow, Russia
[112] Fakultät für Physik, Ludwig-Maximilians-Universität München, München, Germany
[113] Max-Planck-Institut für Physik (Werner-Heisenberg-Institut), München, Germany
[114] Nagasaki Institute of Applied Science, Nagasaki, Japan
[115] Graduate School of Science and Kobayashi–Maskawa Institute, Nagoya University, Nagoya, Japan
[116] Department of Physics and Astronomy, University of New Mexico, Albuquerque, NM, United States of America
[117] Institute for Mathematics, Astrophysics and Particle Physics, Radboud University Nijmegen/Nikhef, Nijmegen, Netherlands
[118] Nikhef National Institute for Subatomic Physics and University of Amsterdam, Amsterdam, Netherlands
[119] Department of Physics, Northern Illinois University, DeKalb, IL, United States of America
[120] [(a)] Budker Institute of Nuclear Physics, SB RAS, Novosibirsk; [(b)] Novosibirsk State University, Novosibirsk, Russia
[121] Department of Physics, New York University, New York, NY, United States of America
[122] Ohio State University, Columbus, OH, United States of America
[123] Faculty of Science, Okayama University, Okayama, Japan
[124] Homer L. Dodge Department of Physics and Astronomy, University of Oklahoma, Norman, OK, United States of America
[125] Department of Physics, Oklahoma State University, Stillwater, OK, United States of America
[126] Palacký University, RCPTM, Joint Laboratory of Optics, Olomouc, Czech Republic
[127] Center for High Energy Physics, University of Oregon, Eugene, OR, United States of America
[128] LAL, Université Paris-Sud, CNRS/IN2P3, Université Paris-Saclay, Orsay, France
[129] Graduate School of Science, Osaka University, Osaka, Japan
[130] Department of Physics, University of Oslo, Oslo, Norway
[131] Department of Physics, Oxford University, Oxford, United Kingdom
[132] LPNHE, Sorbonne Université, Paris Diderot Sorbonne Paris Cité, CNRS/IN2P3, Paris, France
[133] Department of Physics, University of Pennsylvania, Philadelphia, PA, United States of America
[134] Konstantinov Nuclear Physics Institute of National Research Centre "Kurchatov Institute", PNPI, St. Petersburg, Russia
[135] Department of Physics and Astronomy, University of Pittsburgh, Pittsburgh, PA, United States of America
[136] [(a)] Laboratório de Instrumentação e Física Experimental de Partículas – LIP; [(b)] Departamento de Física, Faculdade de Ciências, Universidade de Lisboa, Lisboa; [(c)] Departamento de Física, Universidade de Coimbra, Coimbra; [(d)] Centro de Física Nuclear da Universidade de Lisboa, Lisboa; [(e)] Departamento de Física, Universidade do Minho, Braga; [(f)] Departamento de Física Teorica y del Cosmos, Universidad de Granada, Granada (Spain); [(g)] Dep Física and CEFITEC of Faculdade de Ciências e Tecnologia, Universidade Nova de Lisboa, Caparica, Portugal
[137] Institute of Physics, Academy of Sciences of the Czech Republic, Prague, Czech Republic
[138] Czech Technical University in Prague, Prague, Czech Republic
[139] Charles University, Faculty of Mathematics and Physics, Prague, Czech Republic
[140] State Research Center Institute for High Energy Physics, NRC KI, Protvino, Russia
[141] Particle Physics Department, Rutherford Appleton Laboratory, Didcot, United Kingdom
[142] IRFU, CEA, Université Paris-Saclay, Gif-sur-Yvette, France
[143] Santa Cruz Institute for Particle Physics, University of California Santa Cruz, Santa Cruz, CA, United States of America
[144] [(a)] Departamento de Física, Pontificia Universidad Católica de Chile, Santiago; [(b)] Departamento de Física, Universidad Técnica Federico Santa María, Valparaíso, Chile
[145] Department of Physics, University of Washington, Seattle, WA, United States of America
[146] Department of Physics and Astronomy, University of Sheffield, Sheffield, United Kingdom
[147] Department of Physics, Shinshu University, Nagano, Japan
[148] Department Physik, Universität Siegen, Siegen, Germany
[149] Department of Physics, Simon Fraser University, Burnaby, BC, Canada
[150] SLAC National Accelerator Laboratory, Stanford, CA, United States of America
[151] Physics Department, Royal Institute of Technology, Stockholm, Sweden
[152] Departments of Physics and Astronomy, Stony Brook University, Stony Brook, NY, United States of America
[153] Department of Physics and Astronomy, University of Sussex, Brighton, United Kingdom
[154] School of Physics, University of Sydney, Sydney, Australia
[155] Institute of Physics, Academia Sinica, Taipei, Taiwan
[156] [(a)] E. Andronikashvili Institute of Physics, Iv. Javakhishvili Tbilisi State University, Tbilisi; [(b)] High Energy Physics Institute, Tbilisi State University, Tbilisi, Georgia
[157] Department of Physics, Technion, Israel Institute of Technology, Haifa, Israel
[158] Raymond and Beverly Sackler School of Physics and Astronomy, Tel Aviv University, Tel Aviv, Israel
[159] Department of Physics, Aristotle University of Thessaloniki, Thessaloniki, Greece
[160] International Center for Elementary Particle Physics and Department of Physics, University of Tokyo, Tokyo, Japan
[161] Graduate School of Science and Technology, Tokyo Metropolitan University, Tokyo, Japan
[162] Department of Physics, Tokyo Institute of Technology, Tokyo, Japan
[163] Tomsk State University, Tomsk, Russia
[164] Department of Physics, University of Toronto, Toronto, ON, Canada
[165] [(a)] TRIUMF, Vancouver, BC; [(b)] Department of Physics and Astronomy, York University, Toronto, ON, Canada
[166] Division of Physics and Tomonaga Center for the History of the Universe, Faculty of Pure and Applied Sciences, University of Tsukuba, Tsukuba, Japan
[167] Department of Physics and Astronomy, Tufts University, Medford, MA, United States of America
[168] Department of Physics and Astronomy, University of California Irvine, Irvine, CA, United States of America
[169] Department of Physics and Astronomy, University of Uppsala, Uppsala, Sweden
[170] Department of Physics, University of Illinois, Urbana, IL, United States of America
[171] Instituto de Física Corpuscular (IFIC), Centro Mixto Universidad de Valencia – CSIC, Valencia, Spain
[172] Department of Physics, University of British Columbia, Vancouver, BC, Canada
[173] Department of Physics and Astronomy, University of Victoria, Victoria, BC, Canada
[174] Fakultät für Physik und Astronomie, Julius-Maximilians-Universität Würzburg, Würzburg, Germany
[175] Department of Physics, University of Warwick, Coventry, United Kingdom
[176] Waseda University, Tokyo, Japan
[177] Department of Particle Physics, Weizmann Institute of Science, Rehovot, Israel
[178] Department of Physics, University of Wisconsin, Madison, WI, United States of America
[179] Fakultät für Mathematik und Naturwissenschaften, Fachgruppe Physik, Bergische Universität Wuppertal, Wuppertal, Germany
[180] Department of Physics, Yale University, New Haven, CT, United States of America
[181] Yerevan Physics Institute, Yerevan, Armenia

[a] Also at Borough of Manhattan Community College, City University of New York, NY, United States of America.
[b] Also at California State University, East Bay, United States of America.
[c] Also at Centre for High Performance Computing, CSIR Campus, Rosebank, Cape Town, South Africa.
[d] Also at CERN, Geneva, Switzerland.
[e] Also at CPPM, Aix-Marseille Université, CNRS/IN2P3, Marseille, France.
[f] Also at Département de Physique Nucléaire et Corpusculaire, Université de Genève, Genève, Switzerland.
[g] Also at Departament de Fisica de la Universitat Autonoma de Barcelona, Barcelona, Spain.
[h] Also at Departamento de Física Teorica y del Cosmos, Universidad de Granada, Granada (Spain), Spain.
[i] Also at Department of Applied Physics and Astronomy, University of Sharjah, Sharjah, United Arab Emirates.
[j] Also at Department of Financial and Management Engineering, University of the Aegean, Chios, Greece.
[k] Also at Department of Physics and Astronomy, University of Louisville, Louisville, KY, United States of America.
[l] Also at Department of Physics and Astronomy, University of Sheffield, Sheffield, United Kingdom.
[m] Also at Department of Physics, California State University, Fresno, CA, United States of America.
[n] Also at Department of Physics, California State University, Sacramento, CA, United States of America.
[o] Also at Department of Physics, King's College London, London, United Kingdom.
[p] Also at Department of Physics, St. Petersburg State Polytechnical University, St. Petersburg, Russia.
[q] Also at Department of Physics, Stanford University, United States of America.
[r] Also at Department of Physics, University of Fribourg, Fribourg, Switzerland.
[s] Also at Department of Physics, University of Michigan, Ann Arbor, MI, United States of America.
[t] Also at Giresun University, Faculty of Engineering, Giresun, Turkey.
[u] Also at Graduate School of Science, Osaka University, Osaka, Japan.
[v] Also at Hellenic Open University, Patras, Greece.
[w] Also at Horia Hulubei National Institute of Physics and Nuclear Engineering, Bucharest, Romania.
[x] Also at II. Physikalisches Institut, Georg-August-Universität Göttingen, Göttingen, Germany.
[y] Also at Institucio Catalana de Recerca i Estudis Avancats, ICREA, Barcelona, Spain.
[z] Also at Institut für Experimentalphysik, Universität Hamburg, Hamburg, Germany.
[aa] Also at Institute for Mathematics, Astrophysics and Particle Physics, Radboud University Nijmegen/Nikhef, Nijmegen, Netherlands.
[ab] Also at Institute for Particle and Nuclear Physics, Wigner Research Centre for Physics, Budapest, Hungary.
[ac] Also at Institute of Particle Physics (IPP), Canada.
[ad] Also at Institute of Physics, Academia Sinica, Taipei, Taiwan.
[ae] Also at Institute of Physics, Azerbaijan Academy of Sciences, Baku, Azerbaijan.
[af] Also at Institute of Theoretical Physics, Ilia State University, Tbilisi, Georgia.
[ag] Also at Istanbul University, Dept. of Physics, Istanbul, Turkey.
[ah] Also at Joint Institute for Nuclear Research, Dubna, Russia.
[ai] Also at LAL, Université Paris-Sud, CNRS/IN2P3, Université Paris-Saclay, Orsay, France.
[aj] Also at Louisiana Tech University, Ruston, LA, United States of America.
[ak] Also at LPNHE, Sorbonne Université, Paris Diderot Sorbonne Paris Cité, CNRS/IN2P3, Paris, France.
[al] Also at Manhattan College, New York, NY, United States of America.
[am] Also at Moscow Institute of Physics and Technology State University, Dolgoprudny, Russia.
[an] Also at National Research Nuclear University MEPhI, Moscow, Russia.
[ao] Also at Physikalisches Institut, Albert-Ludwigs-Universität Freiburg, Freiburg, Germany.
[ap] Also at School of Physics, Sun Yat-sen University, Guangzhou, China.
[aq] Also at The City College of New York, New York, NY, United States of America.
[ar] Also at The Collaborative Innovation Center of Quantum Matter (CICQM), Beijing, China.
[as] Also at Tomsk State University, Tomsk, and Moscow Institute of Physics and Technology State University, Dolgoprudny, Russia.
[at] Also at TRIUMF, Vancouver, BC, Canada.
[au] Also at Universita di Napoli Parthenope, Napoli, Italy.
* Deceased.